

Design, Fabrication, and Characterization of Three Dimensional Complete Scaffolds for Bone Tissue Engineering

Tea Andric

Dissertation submitted to the faculty of the Virginia Polytechnic Institute and State University in
partial fulfillment of the requirements for the degree of

Doctor of Philosophy

In

Biomedical Engineering

Joseph W. Freeman, Chair

Abby R. Whittington

M. Nicole Rylander

Linda A. Dahlgren

Aaron S. Goldstein

March 27, 2012

Blacksburg, VA

Keywords: Bone, Electrospinning, Calcium Phosphate, Tissue Engineering

Copyright 2012, Tea Andric

Design, Fabrication, and Characterization of Three Dimensional Complete Scaffolds for Bone Tissue Engineering

Tea Andric

ABSTRACT

Skeletal loss and bone deficiencies are major worldwide problem that is only expected to increase due to increase in aging population. As current standards in treatment autografts and allografts are not without drawbacks, there is a need for alternative bone grafts substitutes. The goal of this project was to utilize electrospinning and heat sintering techniques to create biodegradable full thickness three dimensional biomimetic polymeric scaffolds with macro and nano architecture similar to natural bone for bone tissue engineering.

First we have investigated pretreatment with 0.1M NaOH and electrospinning gelatin/PLLA blends as means to increase overall mineral precipitation and distribution throughout the scaffolds when incubated in concentrated simulated body fluid (SBF)10XSBF. Mixture of 10% gelatin and PLLA resulted in the significantly higher degree of mineralization, increased mechanical properties, and scaffolds that supported cellular adhesion and proliferation. In the next step we applied heat sintering technique to fabricate 3D electrospun scaffolds that were used to evaluate effects of mineralization and fiber orientation on scaffold strength. Fiber orientation can make a slight difference in nanofibrous scaffold compressive mechanical properties, but this difference is not as profound as the difference seen with increased mineralization. We also developed a technique to fabricate scaffolds that mimic the organization of an osteon, the structural unit of cortical bone. Resulting scaffolds consisted of concentric layers of electrospun

gelatin/PLLA nanofibers wrapped around microfiber core with diameters that ranged from 200-600 μ m. Individual osteon-like scaffolds were heat sintered to fabricate three dimensional scaffolds contained a system of channels running parallel to the length of the scaffolds, as found naturally in bone tissue.

Finally we combined two previously fabricated structures, sintered electrospun sheets and individual osteon-like scaffolds, to create novel scaffolds that mimic dual structural organization of natural bone with cortical and trabecular regions. Mineralization for 24 hr significantly increased mechanical properties of the scaffolds, both yield stress and compressive modulus under physiological conditions. Both nonmineralized and mineralized scaffolds were found to support cellular attachment and proliferation over 28 days in culture, but scaffolds mineralized for 24hr were found to better support osteoblastic differentiation and mineral deposition.

ACKNOWLEDGMENTS

There are a few people that I would like to thank for their help and guidance during my journey as a graduate student. First I would like to thank my advisor, Dr. Joseph Freeman, for his support, guidance, and always being there for me during these five years. I would also like to thank Dr. Abby Whittington for her support and welcoming me into her lab this last year. I am also grateful to the rest of my committee members, Dr. Linda Dahlgren, Dr. Aaron Goldstein, and Dr. Nicole Rylander for serving on my committee, their expertise advice, support and use of their lab equipment.

I would also like to thank all the members of the Musculoskeletal Tissue Regeneration (MTR) Laboratory, especially Dr. Lee D. Wright, Dr. Kristin Fischer, Albert Kwansa, Cara Buchanan and Chris Szot. They were always there to help me solve the problems along the way, offering insight and advice. We have all become such close friends over these five years and they have made this experience much more fun.

Also I would like to thank my family, who I am very fortunate to have, for their immense support and belief in me during all these years. I would like to especially thank my parents for everything they have done for me and always being there for me. Most importantly I would like to thank Oliver, my future husband. Thank you for supporting me and always finding a way to make me laugh, I am not sure I could have done it without your love and support.

ATTRIBUTION

Several colleagues aided in the research presented in this document and a brief description is located below.

Chapter 2:

2.1. Rapid Mineralization of Electrospun Scaffolds for Bone Tissue Engineering

Lee D. Wright was a fellow graduate student and a co-author on this paper. He helped with electrospinning process, scaffold fabrication and he also contributed to the editorial process. He was a graduate student at Virginia Tech.

Joseph W. Freeman is a co-author on this paper and is also the principal investigator for this project. He contributed to the experimental process and provided editorial comments. He was an assistant professor at Virginia Tech.

2.2. Biological Evaluation of Electrospun Cross-linked PLLA/gelatin Scaffolds

Joseph W. Freeman is a co-author on this paper and is also the principal investigator for this project. He contributed to the experimental process and provided editorial comments. He was an assistant professor at Virginia Tech.

3. Fabrication and Characterization of Three Dimensional Electrospun Scaffolds for Bone Tissue Engineering

Lee D. Wright was a fellow graduate student and a co-author on this paper. He helped with heat sintering process in the scaffolds fabrication and he also contributed to the editorial process. He was a graduate student at Virginia Tech.

Joseph W. Freeman is a co-author on this paper and is also the principal investigator for this project. He contributed to the experimental process and provided editorial comments. He was an assistant professor at Virginia Tech.

Chapter 4: Fabrication and Characterization of Electrospun Osteon Mimicking Scaffolds for Bone Tissue Engineering

Alana C. Sampson was an undergraduate student and a co-author that conducted research with the author on this study. She fabricated the scaffolds that were used in the

studies and also performed the degradation study. She was an undergraduate student at Virginia Tech.

Joseph W. Freeman is a co-author on this paper and is also the principal investigator for this project. He contributed to the experimental process and provided editorial comments. He was an assistant professor at Virginia Tech.

Chapter 5: Fabrication and Characterization of Three Dimensional Electrospun

Cortical Bone Scaffolds

Katherine E. Degen was an undergraduate student that conducted the research with the author of this study. She fabricated scaffolds and helped with mechanical testing of the scaffolds. She was an undergraduate student at University of Virginia that did summer research program at Virginia Tech.

Joseph W. Freeman is a co-author on this paper and is also the principal investigator for this project. He contributed to the experimental process and provided editorial comments. He was an assistant professor at Virginia Tech.

Chapter 6: Fabrication and Characterization of Complete Electrospun Scaffolds for Bone Tissue Engineering

Abby R. Whittington is a co-author on this paper as she contributed to both the experimental and editorial processes. She is an assistant professor at Virginia Tech.

Joseph W. Freeman is a co-author on this paper and is also the principal investigator for this project. He contributed to the experimental process and provided editorial comments. He was an assistant professor at Virginia Tech.

TABLE OF CONTENTS

Abstract	ii
Acknowledgments.....	iv
Attribution.....	v
Table of Contents	vii
List of Figures	xiii
List of Tables	xvii
Chapter 1: Introduction	1
1.1. Objective.....	1
1.2. Bone Biology	1
1.2.1. Bone Structure	1
1.2.2. Bone Composition	3
1.3. Current Treatments	5
1.4. Tissue Engineering of Bone.....	7
1.4.1. Materials	8
1.4.1.1.Synthetic Biodegradable Polymers	8
1.4.1.2.Natural Polymers	10
1.4.1.3.Ceramics	11
1.4.1.4.Composite Scaffolds.....	11
1.4.2. Scaffold Fabrication Techniques	12
1.4.2.1.Electrospinning.....	13
1.4.2.2.Electrospinning for Bone Tissue Engineering.....	14
1.4.3. Mineralization of Scaffolds	15
1.5. Project Description	16
1.6. References.....	18
Chapter 2:	23
2.1. Rapid Mineralization of Electrospun Scaffolds for Bone Tissue Engineering....	23
2.1.1. Abstract	23
2.1.2. Introduction.....	24

2.1.3. Materials and Methods.....	25
2.1.3.1.Fabrication of Scaffolds by Electrospinning.....	25
2.1.3.2.Mineralization of Scaffolds.....	26
2.1.3.3.Mineral Ash Weight.....	27
2.1.3.4.Characterization of the Scaffolds.....	28
2.1.3.5.Mechanical Testing.....	28
2.1.3.6.Cell Culture.....	29
2.1.3.7.Statistical Analysis.....	30
2.1.4. Results	30
2.1.4.1.Mineral Ash Weight	31
2.1.4.2.Mineralization of the Scaffolds	31
2.1.4.3.Mechanical Properties.....	34
2.1.4.4. Cell Culture.....	35
2.1.5. Discussion.....	37
2.1.6. Conclusions.....	40
2.1.7. References.....	41
2.2. Biological Evaluation of Electrospun Cross-linked PLLA/gelatin Scaffolds.....	43
2.2.1. Introduction.....	43
2.2.2. Materials and Methods	44
2.2.2.1.Scaffold Fabrication by Electrospinning	44
2.2.2.2.Mineralization of Scaffolds.....	44
2.2.2.3.Scaffold Characterization.....	45
2.2.2.4.Cell Study.....	45
2.2.2.4.1. Cellular Proliferation	45
2.2.2.4.2. Alkaline Phosphatase Activity.....	46
2.2.2.4.3. Alizarin Red and Fluorescence Stain.....	46
2.2.2.5.Statistical Analysis.....	47
2.2.3. Results	47

2.2.3.1.Scaffold Characterization.....	47
2.2.3.2.Cellular Proliferation	48
2.2.3.3.Alkaline Phosphatase Activity	49
2.2.3.4.Alizarin Red and Fluorescence Stain	51
2.2.4. Discussion.....	53
2.2.5. Conclusions.....	55
2.2.6. References.....	56

Chapter 3: Fabrication and Characterization of Three Dimensional Electrospun Scaffolds for Bone Tissue Engineering57

3.1. Abstract	57
3.2. Introduction	57
3.3. Materials and Methods	60
3.3.1. Fabrication of Scaffolds by Electrospinning.....	60
3.3.2. Heat Sintering	61
3.3.3. Variation of the Angles	61
3.3.4. Addition of Hydroxyapatite	61
3.3.5. Mineralization of the Scaffolds.....	61
3.3.6. Scaffold Characterization.....	62
3.3.7. Mechanical Properties.....	62
3.3.8. Mineral Ash Weights	62
3.3.9. Alizarin Red Stains	62
3.3.10. Statistical Analysis.....	63
3.4. Results	63
3.4.1. Variation of the Angles	63
3.4.2. Addition of Hydroxyapatite and Mineralization.....	64
3.4.3. Mechanical Properties.....	66
3.4.4. Ash Weights.....	67
3.4.5. Alizarin Red Stains	68
3.5. Discussion.....	68
3.6. Conclusion	71

3.7. Acknowledgments	72
3.8. References	73

Chapter 4: Fabrication and Characterization of Electrospun Osteon Mimicking

Scaffolds for Bone Tissue Engineering74

4.1. Abstract	74
4.2. Introduction.....	75
4.3. Materials and Methods.....	76
4.3.1. Scaffold Fabrication by Electrospinning	76
4.3.2. Mineralization of Scaffolds.....	77
4.3.3. Mineral Ash Weight.....	78
4.3.4. Scaffold Characterization.....	78
4.3.5. Degradation Study	79
4.3.6. Cell Study.....	79
4.3.6.1. Cellular Proliferation	79
4.3.6.2. Alkaline Phosphatase Activity	80
4.3.6.3. Alizarin Red and Fluorescence Stain	80
4.3.7. Statistical Analysis.....	81
4.4. Results	81
4.4.1. Mineralization of Scaffolds.....	82
4.4.2. Degradation Study	83
4.4.3. Cell Study.....	85
4.4.3.1. Cellular Proliferation	85
4.4.3.2. Alkaline Phosphatase Activity	86
4.4.3.3. Alizarin Red Stain.....	87
4.5. Discussion.....	88
4.6. Conclusions.....	90
4.7. Acknowledgements.....	91
4.8. References.....	92

Chapter 5: Fabrication and Characterization of Three Dimensional Electrospun

Cortical Bone Scaffolds97

5.1. Abstract97

5.2. Introduction97

5.3. Materials and Methods.....98

 5.3.1. Scaffold Fabrication by Electrospinning98

 5.3.2. Heat sintering of the Scaffolds100

 5.3.3. Mineralization of the Scaffolds100

 5.3.4. Alizarin Red Staining100

 5.3.5. Mechanical Testing.....101

 5.3.6. Mineral Ash Weights101

 5.3.7. Statistical Analysis.....101

5.4. Results102

 5.4.1. Alizarin Red Staining.....102

 5.4.2. Mechanical Testing103

 5.4.3. Mineral Ash Weights105

5.5. Discussion106

5.6. Conclusions.....107

5.7. References108

Chapter 6: Fabrication and Characterization of Complete Electrospun Scaffolds for Bone Tissue Engineering110

6.1. Abstract110

6.2. Introduction.....110

6.3. Materials and Methods.....113

 6.3.1. Electrospinning113

 6.3.2. Heat Sintering of Scaffolds.....114

 6.3.3. Mineralization of Scaffolds114

 6.3.4. Alizarin Red Staining115

 6.3.5. Mechanical Properties115

 6.3.6. Mineral Ash Weights115

 6.3.7. Cell Study115

6.3.7.1.Osteocalcin ELISA Assay	116
6.3.7.2.Alizarin Red and Fluorescence Stain	117
6.4. Results.....	117
6.4.1. Alizarin Red Staining.....	117
6.4.2. Mineral Ash Weights	118
6.4.3. Mechanical Properties	119
6.4.4. Cell Study	120
6.4.3.1.Osteocalcin ELISA Assay	120
6.4.3.2.Alizarin Red and Fluorescence Stain	121
6.5. Discussion.....	123
6.6. Conclusion	126
6.7. References.....	127
Chapter 7: Conclusions and Future Directions	129
7.1. Project Conclusions	129
7.2. Future Directions	131
7.2.1. Flow Mineralization	131
7.2.2. Bioreactors	131
7.2.3. Vascularization of Scaffolds	132
7.2.4. Improving Mechanical Properties.....	133
7.3.References	134

LIST OF FIGURES

Figure 1.1. Structural organization of the bone tissue	2
Figure 1.2. Detailed structure of an osteon	2
Figure 1.3. Organization of the collagen fibril.....	3
Figure 1.4. A schematic diagram of the organization of collagen and mineral at different structural levels	4
Figure 1.5. Ring-opening polymerization of cyclic diesters (A) and hydrolytic cleavage of ester bonds (B).....	8
Figure 1.6. D and L isomers of lactide.....	9
Figure 1.7. SEM images of scaffolds fabricated by various fabrication techniques: A) thermally induced phase separation B) solvent casting/particulate leaching, and C) heat sintering of microspheres	12
Figure 1.8. Schematic diagram of set up for electrospinning and SEM of electrospun fibers	14
Figure 2.1.1. SEM images of electrospun PLLA (A) and 10%Gel/PLLA (B).....	30
Figure 2.1.2. SEM images of mineralized scaffolds: A) PLLA_MIN - Mineralized PLLA no vacuum, larger crystals can be seen of surface, B) PLLA_V_MIN - mineralized PLLA in vacuum, combination of large crystals with smaller crystals grain can be seen, C) PLLA_NaOH_V_MIN – mineralized PLLA in vacuum, pretreated with NaOH, small mineral crystals cover surface, but fiber morphology is preserved, D) 10% gel/PLLA_V_MIN – 10% gelatin/PLLA mineralized, surface is covered with small grain mineral crystals and fiber morphology is still visible	32
Figure 2.1.3. EDS map of mineralized scaffolds cross-sections where calcium is tagged with red, and phosphorus is tagged with green: A) PLLA no vacuum, presence of Ca and P on surfaces, scale bar shown 30µm , B) PLLA vacuum, no pretreatment (PLLA_MIN), presence of Ca and P on the surfaces with very little present in the center, scale bar shown 40 µm , C) PLLA pretreated with 0.1M NaOH (PLLA_T_MIN), presence of Ca and P can be seen across the cross-section, scale bar shown 60µm , D) 10% gelatin/PLLA mineralized, presence of Ca and P can be seen across the cross-section, scale bar shown 30µm	33

Figure 2.1.4. X-ray diffraction pattern of PLLA_NaOH_V_MIN (top) and 10%gel/PLLA_V_MIN (bottom) scaffolds mineralized by incubation in 10X SBF for 2 h in vacuum.....	34
Figure 2.1.5. Mechanical testing data graphs include yield stress (top) and elastic moduli (bottom) averages as bars, and standard deviations as error bars	35
Figure 2.1.6. Cellular attachment and ECM after 21 days of MC3T3 cells culture on following electrospun scaffolds (note the scale bars as the pictures are at different magnifications): A) PLLA, scale bar shown 100µm, B) PLLA_V_MIN, scale bar shown 50µm, C) 10%gel/PLLA, scale bar shown 200µm, and D) 10%gel/PLLA_V_MIN, scale bar shown 100µm.....	36
Figure 2.1.7. Average absorbences of MTS assay with standard deviations as error bars of MCT3T3 –E1 cells	37
Figure 2.2.1. SEM images of electrospun PLLA gelatin mixtures, not cross-linked (left) and cross-linked (right)	47
Figure 2.2.2. MTS assay absorbances of cell viability	48
Figure 2.2.3. Fluorescent stains of actin (green) and nuclei (blue) on scaffolds after 28 days in culture. A) PLLAgel, B) PLLAgelCL and C) PLLAgelCL_MIN	49
Figure 2.2.4. ALP expression as a function of total protein	50
Figure 2.2.5. Average total protein concentration on the scaffolds over the 4 week period	51
Figure 2.2.6. Alizarin red stains of the following scaffolds PLLAgel (A, B), PLLAgelCL(C, D) and PLLAgelCL_MIN(E, F).....	52
Figure 2.2.7. Alizarin red stain absorbances over the period of 4 weeks.	53
Figure 3.1. Schematic representation of cutting 1 cm strips at angles: 0°, 45°, and 90° ..	61
Figure 3.2. Effects of fiber alignment on compressive mechanical properties of the scaffolds.	64
Figure 3.3. SEM images of electrospun PLLAgelatin cross-linked scaffolds (A) and scaffolds with hydroxyapatite (HA) microparticles on the surface (B, C).....	65
Figure 3.4. SEM images of the following scaffolds: NoHA (A, B, C), 50wt%HA (D, E), and 100wt%HA (F,G, H)	66

Figure 3.5. Mechanical properties of the scaffolds in compression after mineralization up to 48 hrs.....	67
Figure 3.6. Alizarin red cross-sections stains of the following scaffolds: NoHA (A, B, C), 50wt%HA (D, E), and 100wt%HA (F, G, H).....	69
Figure 4.1. Set up that was used for rotation of PGA fibers and scaffolds fabrication	79
Figure 4.2. ESEM of scaffold cross-section, where PGA fibers are visible in the core surrounded by concentric layers of PLLA fibers.....	83
Figure 4.3. ESEM pictures of PLLA_MIN (A), 5% gel/PLLA_MIN (B), and 10% gel/PLLA_MIN(C) scaffolds and corresponding EDS maps (D,E,F)	85
Figure 4.4. Diffraction pattern of the 10% gel/PLLA_MIN scaffolds with brushite and hydroxyapatite peaks labeled	85
Figure 4.5. Average weight percent loss over the 4 week degradation study.....	86
Figure 4.6. ESEM of scaffold cross-section on day 28 of degradation study.....	87
Figure 4.7. MTS assay absorbances over the period of 4 week cell study	88
Figure 4.8. Fluorescently labeled scaffolds after 28 days of cell culture, actin filaments are stained green and the cell's nuclei stained blue for the following scaffolds: A) PLLA , B) PLLA_MIN, C) 10% gel/PLLA, and D) 10% gel/PLLA_MIN (scale bar 75µm).....	89
Figure 4.9. ALP expression as the fraction of the total cell protein	90
Figure 4.10. Alizarin red stains of scaffolds: PLLA (A, E), PLLA_MIN (B, F), 10% gel/PLLA(C, G), and 10% gel/PLLA_MIN (D, H) after 7 (A-D) and 28(E-H) days of cell culture.....	91
Figure 5.1. Picture of the electrospinning set for rotating PEO fibers.....	99
Figure 5.2. Alizarin red stain of cross-sections after 6 hr of mineralization: A) Min6h, B) Premin1h_Min6h, C) CL_Min6h, and D) CL_premin1h_Min6h	103
Figure 5.3. Compressive moduli of scaffolds.	104
Figure 5.4. Compressive yield stress of scaffolds.....	105
Figure 6.1. Alizarin red staining after 6hr (A, D), 24hr (B, E) and 48 hr(C, F) of mineralization.	118
Figure 6.2. Mechanical testing data.	120
Figure 6.3. MTS absorbances over the 4 week cell study (left) and cell numbers determined from MTS curve (right)	120

Figure 6.4. Secreted OCN protein in cell culture media121

Figure 6.5. Alizarin red stain pictures of scaffolds Min0 (top) and Min24 (bottom) over period of 28 days.....122

Figure 6.6. Fluorescence stain of actin(green) and nuclei (blue) after 21 days (A, B) and 28 days (C,D) on scaffolds Min0 (A,C) and Min24(B,D)123

Figure 6.7. SEM image of scaffolds sectioned using cryostat where fiber fusion is visible on the surface126

Figure 7.1. Electrospun scaffolds with channels loaded with fluorescent microbeads..132

LIST OF TABLES

Table 1.1. List of possible and commercially available candidates for bone grafts	6
Table 2.1.1. List of group names and descriptions	27
Table 2.1.2. Average mineral ash weight percent.	31
Table 3.1. Average mineral ash weight percents	68
Table 4.1. Average mineral ash weight percentages.	84
Table 5.1. Mineral ash weight percentages	105
Table 6.1. Mineral ash weight percentages	119

Chapter 1

Introduction

1.1. OBJECTIVE

After uncomplicated fractures bone has an ability to regenerate itself. However in cases of traumatic injury, tumor removal, or disease, when the bone mass loss is significant, reconstructive surgery is required. Bone grafts are used in the orthopaedic reconstructive procedures to provide mechanical support and promote bone regeneration. It is estimated that 600,000 bone grafting procedures are performed annually, making bone one of the most transplanted tissue, second to blood only [2]. The bone grafting market has an estimated value at over \$1 billion globally, and this number is expected to increase due to a projected annual increase of 2-3% in the population of over 65. Unfortunately, current standards in treatment are not without drawbacks, such as donor site morbidity for autografts and high failure rates for allografts [3]; there is a need for alternative bone grafts substitutes.

1.2. BONE BIOLOGY

Bone is a living, dynamic, vascular, mineralized, connective tissue. It is characterized by its hardness, resistance and ability to remodel and repair itself [2]. It has many functions in the body: provides structural support for movement, support and protection for the body and vital organs, serves as a mineral (calcium), growth factor, and blood cell reservoir for the body [1].

1.2.1. *Bone Structure*

Structurally bone is organized in two major types: compact or cortical bone and cancellous or trabecular bone [1, 2, 4, 5]. Two types are easily distinguished by density and location. Cortical bone is dense and usually found on the outside, while cancellous bone is highly porous and found within the confines of the cortical bone, as shown in Figure 1.1.

Cancellous bone, also called trabecular bone, is composed of short struts of bone material called trabeculae (Latin for little beam) that surround interconnected spaces or cancelli, as shown in Figure 1.1 [1, 2]. Trabecular bone is often referred to as spongy, with porosities as high as 90% [1, 4, 6]. Trabecular bone is anisotropic due to the orientation of the trabeculae along the lines of principal stresses.

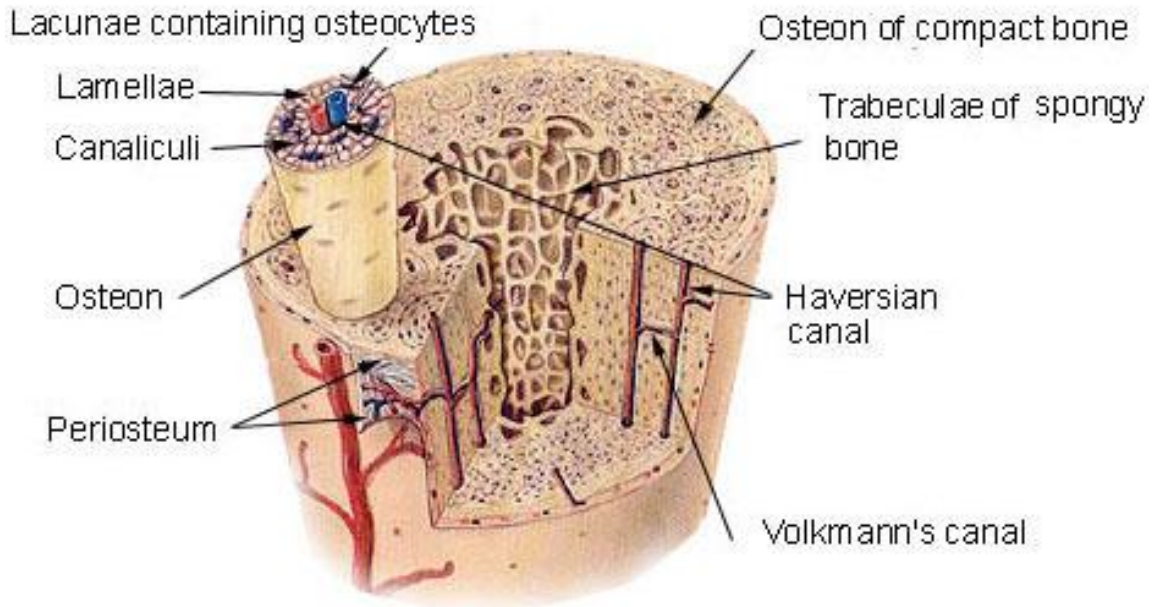


Figure 1.1. Structural organization of the bone tissue [7]

Cortical bone is highly organized, dense and compact. It has low porosity, ranging from 5 to 30% [6], is usually found on the outside of the bone, as illustrated in Figure 1.1. There are three types of cortical bone: lamellar, woven and osteonal. Lamellar bone is composed of 200µm thick laminae that are concentrically arranged. Woven bone is less organized, and is replaced with lamellar bone by maturation process. Osteonal bone is composed of tightly packed units, called osteons, oriented parallel along the axis of the bone, Figure 1.1. Each osteon is a cylindrical unit with a diameter of 200-300 µm, composed of concentric layers of mineralized collagen fibers (lamella) and a Haversian canal in the center, as illustrated in Figure 1.2. Blood vessels are housed in the Haversian canals, and bone cells are usually housed in lacunae, small openings in between

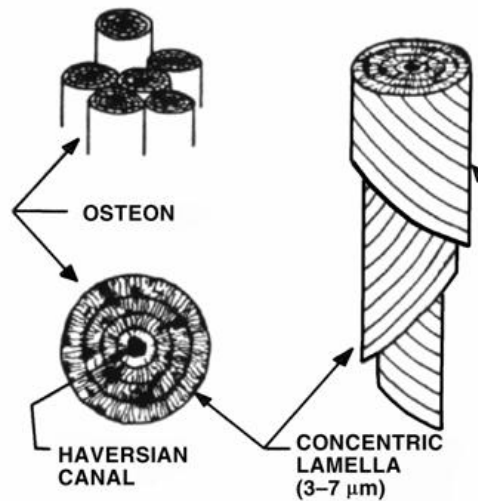


Figure 1.2. Detailed structure of an osteon. Springer, Tissue Mechanics, 2007,XVI, Bone Tissue, p.341-384, Stephen C. Cowin, Stephen B. Doty Copyright (2012) with kind permission from Springer Science and Business Media [1]

lamellar layers, as shown in Figure 1.1 [1, 4, 6]. Their high organization and compact nature provide excellent micro-crack propagation prevention and high tensile and compressive mechanical properties.

Due to differences in organizations and porosities, mechanical properties of each structure vary accordingly. Cortical bone has compressive and tensile strengths in the range of 167-215 MPa and 107-140 MPa respectively, and Young's modulus of 10-20 GPa [2, 8]. Trabecular bone has compressive strength in the range of 3- 9 MPa, and Young's modulus in 0.01 – 0.9 GPa [2, 8].

1.2.2. Bone Composition

While the structure of the bone varies greatly in organization, porosity and mechanical properties, all the types of bone have the same composition. Bone is composed of an organic matrix of collagen fibers (20-30 wt%) and inorganic calcium phosphate mineral crystals (60-70 wt%) and water (10 wt%) [2, 5, 9]. Each of these plays an important role in contributing to bones' very strong mechanical properties; mineral content contributes to the stiffness of the tissue and the collagen matrix contributes to the toughness of the tissue [5].

Bone's matrix is mostly composed of collagen type I, a fibril forming collagen. Collagen

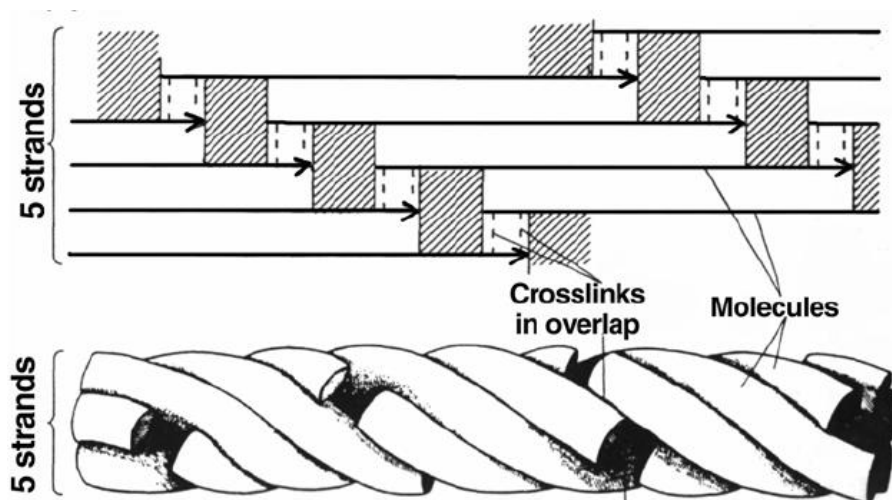


Figure 1.3. Organization of the collagen fibril. Periodic pattern that consists of gap (shaded) and overlap (crosslink) region. Springer, *Tissue Mechanics*, 2007, XVI, Collagen, p.289-339, Stephen C. Cowin, Stephen B. Doty Copyright (2012) with kind permission from Springer Science and Business Media [1]

is the most abundant protein found in the body. Collagen consists of arrays of tropocollagen molecules, which are 300 nm long and 1.5 nm wide and are composed of three left-handed helical peptides, two identical ($\alpha 1$) and one dissimilar ($\alpha 2$) chains, that are bound together into a right-handed triple helix [2, 9]. Tropocollagen molecules are then assembled into $\frac{3}{4}$ stagger, parallel array to form collagen fibrils, as shown in Figure 1.3 [2, 9]. Due to this orientation, fibers exhibit a characteristic banding pattern that repeats every 67nm, that consists of gap region and overlap region, as shown if Figure 1.3.

The majority of mineral phase of bone is composed of hydrated calcium phosphate mineral also referred to as hydroxyapatite (HA). It has a chemical formula $\text{Ca}_{10}(\text{PO}_4)_6(\text{OH})_2$ and Ca:P ratio of 1.66. Bone crystals are plate-shaped 2-6 nm thick, 25-50 nm wide, and 50-100 nm long [1, 4]. Apatite crystals form within the spaces between the collagen fibrils (Figure 1.4 A) and grow in length along fibers and in width through the gap spaces, as depicted in Figure 1.4 B-D. As the collagen microfibrils grow, crystals fuse into larger and thicker plates, still oriented parallel to one another [1, 9].

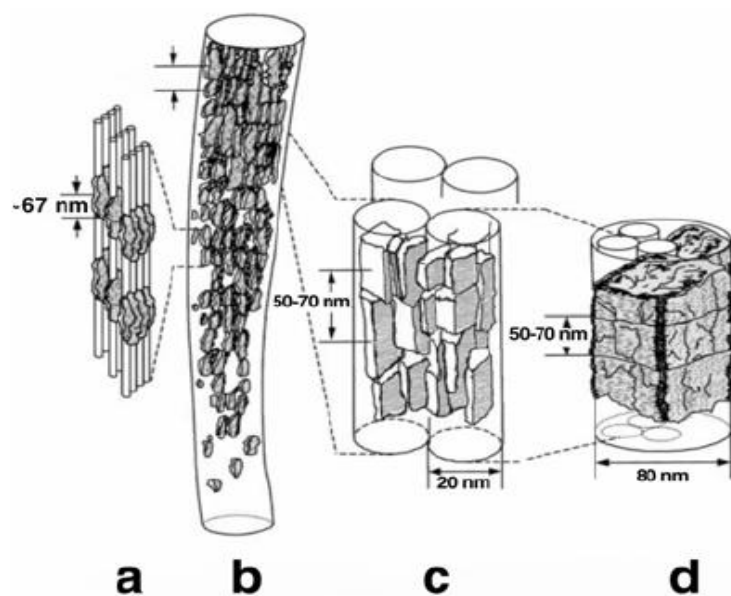


Figure 1.4. A schematic diagram of the organization of collagen and mineral at different structural levels. **A)** Crystal plates nucleate in the gaps **B)** Crystals grow in length along fibers **C)** and **D)** crystals fuse into larger plates while still maintaining parallel orientation [1]. Springer, Tissue Mechanics, 2007,XVI, Bone Tissue, p.341-384, Stephen C. Cowin, Stephen B. Doty Copyright (2012) with kind permission from Springer Science and Business Media

Three cells types are responsible for the production, maintenance and resorption of the bone, and they are osteoblasts, osteocytes, and osteoclasts [1, 2]. Osteoblasts are bone forming cells. They produce the unmineralized collagen matrix and also participate in the calcification of the matrix. Osteocytes are derived from the osteoblasts, are found in the lacunae, and maintain surrounding bone tissue. Osteoclasts are derived from monocytes and are multinucleated giant cells responsible for resorption of the bone [1, 2].

1.3. CURRENT TREATMENTS

Bone has a unique ability to heal when damaged without the formation of the scar tissue [10]. When this normal physiological response fails due to significant bone mass loss, a reconstructive surgery is required. Bone grafts are used in the orthopaedic reconstructive procedures to provide mechanical support and promote bone regeneration. It is estimated that 600,000 bone grafting procedures are performed annually, making bone one of the most transplanted tissues, second only to blood [2]. The current treatment or “gold standard” for bone grafting procedures is an autograft, an autologous bone tissue harvested from the patient. Although autografts have a very high success rates, they do have drawbacks, namely donor site morbidity and limited supply. Incidences of donor site morbidity are reported to be as high as 44% [11]. The amount of viable tissue that can be harvested can be very limited or nonexistent, in cases of bone disease. The current alternative to autografts is allografts. Although the use of allografts eliminates the potential drawbacks of the autografts, they do have the limitations of their own. Whenever a donor tissue is transplanted, there is a chance of disease transmission. In addition the harsh sterilization techniques denature the bone matrix and decrease its mechanical properties. Recent reports on long term use of allografts *in vivo* state that they exhibit decreases in mechanical strength and have failure rates of 30-60% over a period of ten years [3].

Due to the limitations of the autografts and allografts, various bone graft substitutes have become commercially available. Some attributes that should be considered when discussing bone grafts are: *biocompatibility* – performing with an appropriate host response [12]; *osteoconductivity* - allowing and promoting cell attachment, proliferation, and migration throughout the scaffold; *osteoinductivity* – possessing necessary bioactive molecules that can induce differentiation of progenitor cells toward osteoblastic lineage; *osteogenicity* – allowing osteoblasts that are on site to produce minerals and calcify surrounding matrix [2, 13].

Some of the commercially available bone graft substitutes include derivatives of biological material such as collagen and demineralized bone matrix (DBM), ceramics such as tricalcium phosphate, hydroxyapatite, and calcium phosphate cements, synthetic polymers and growth factors [10, 14-18]; these are shown in Table 1.1. and will be discussed in more detail in the next section. While a majority of the grafts listed are osteoconductive, with highly porous matrices, a small number of them have osteoinductive capacities. Recent attempts to enhance the osteoinductive properties of graft substitutes include the use of bone marrow aspirate and the use of bone morphogenetic proteins. Bone marrow aspirate can be used in conjunction with various matrices, and can be easily available and harvested from the patient. This technique has shown some success in clinical applications, however the concentration of the osteoprogenitor cells can be low [17, 19]. Another alternative, recently approved by the FDA, are two types of bone morphogenetic proteins (BMP), type 2 and 7 [13, 20]. BMPs are groups of growth factors that are derived from the transforming growth factor β (TGF- β) family; BMP-2 and BMP-7 promote bone morphogenesis [21, 22]. For clinical applications, they are delivered in absorbable bovine collagen sponges for treatment of long bone non-unions (BMP-7/OP-1) and fusion of spinal vertebrae (BMP-2) [13, 20-24]. Current research is investigating delivery of these factors from mechanically stronger scaffolds that contain an inorganic calcium phosphate phase [21, 23, 25, 26].

Table 1.1. List of possible and commercially available candidates for bone grafts. Reprinted from Injury, 36, Giannoudis, P.V., H. Dinopoulos, and E. Tsiridis, Bone substitutes: an update, p. S20-7, Copyright (2012), with permission from Elsevier [17]

Type	Graft	Osteoconduction	Osteoinduction	Osteogenesis	Advantages
Bone	Autograft	3	2	2	"Gold standard"
	Allograft	3	1	0	Availability in many forms
Biomaterials	DBM	1	2	0	Supplies osteoinductive BMPs, bone graft extender
	Collagen	2	0	0	Good as delivery vehicle system
Ceramics	TCP, hydroxyapatite	1	0	0	Biocompatible
	Calcium phosphate cement (CPC)	1	0	0	Some initial structural support
Composite grafts	β -TCP/BMA composite	3	2	2	Ample supply
	BMP/synthetic composite	—	3	—	Potentially limitless supply

Score: 0 (none) to 3 (excellent). DBM: demineralised bone matrix, TCP: tricalcium phosphate, BMA: bone marrow aspirate, BMP: bone morphogenetic protein.

1.4. TISSUE ENGINEERING OF BONE

The field of tissue engineering has emerged with a goal to bridge the gap between the need and lack of an ideal bone graft. Tissue engineering is defined as “an interdisciplinary field that applies the principles of engineering and life sciences toward the development of biological substitutes that restore, maintain, or improve tissue function or a whole organ” [27]. It combines the use of cells, bioactive molecules, and engineered scaffolds to improve tissue regeneration. Some of the properties that should be considered in scaffold design are biocompatibility, porosity, degradation rate, and mechanical properties. Porosity and pore interconnectivity of the scaffolds is essential to allow infiltration of the cells and new tissue growth. The degradation rate of the scaffolds should be comparable to the tissue growth rate, as the implant needs to maintain mechanical properties initially to bear loads, but over time the load bearing should transfer onto the new forming tissue. Mechanical properties of the scaffold should match the properties of the surrounding tissue. Various materials and scaffolds fabrication techniques have been investigated for bone tissue engineering applications.

1.4.1. *Materials*

Due to the complexity in organization of the natural bone tissue, various materials are being investigated as potential scaffolds for applications in bone tissue engineering. The materials investigated include synthetic polymers, natural polymers, calcium phosphate ceramics, and composites of two or more of these materials.

1.4.1.1. *Synthetic Biodegradable Polymers*

Synthetic polymers offer unique benefits for fabrication techniques, as they are produced under controlled conditions giving them predictable and reproducible mechanical and degradation properties [28]. While many biodegradable synthetic polymers are available, poly(α -hydroxy acid)s, a subgroup of polyesters, are most commonly used due to their ease of processing, biocompatibility, wide range of degradation rates, good mechanical properties, and are also FDA approved [12, 28-32]. Poly (α -hydroxy acid)s include poly(glycolic acid) and stereoisomeric forms of poly(lactic acid). They are formed by ring opening polymerization of cyclic diester (Figure 1.5), where methyl R-group would be poly(lactide) and hydrogen R-group would be poly(glycolide) [29].

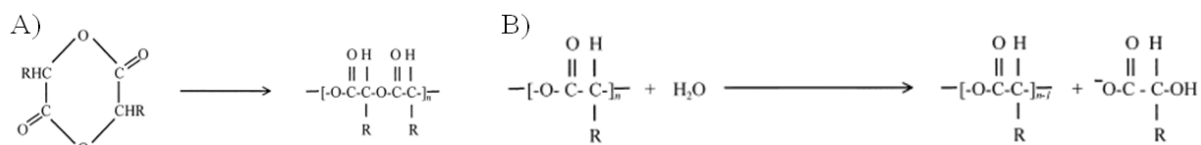


Figure 1.5. Ring-opening polymerization of cyclic diesters (A) and hydrolytic cleavage of ester bonds (B). Reprinted from *Biomaterials*, 21(24), An, Y.H., S.K. Woolf, and R.J. Friedman, Pre-clinical in vivo evaluation of orthopaedic bioabsorbable devices, p. 2635-2652, Copyright (2012) with permission from Elsevier [29]

Poly(glycolic acid) (PGA) is a hard polymer characterized by high crystallinity (45-55%), high melting point (220-225 °C) and glass transition temperature of 35°C [31, 33]. PGA has the following mechanical properties: tensile strength 60-80 MPa, Young's modulus 5-7 GPa [34]. PGA and its products are biodegradable and they degrade by hydrolysis and degradation *in vivo* is enhanced by the degradation by enzymes [29, 33]. The hydrolytic degradation results in the breakage of ester bonds producing glycolic acid monomers, which are converted into glycine and then converted into pyruvate. The pyruvate enters the tricarboxylic acid (TCA) cycle which yields CO_2 and water [33]. Degradation time of the PGA products has been reported as 6 – 12 months, but they lose their strength after 1-2 months [6, 12, 28, 29, 31, 33, 34].

Poly(lactide) (PLA) is synthesized from lactide, a cyclic dimer of lactic acid which exists in two optical isomers D and L (Figure 1.6). The polymerization of lactide is similar to the PGA polymerization as it is ring-opening polymerization; however due to two isomers the final polymer can be L-, D-, or DL- lactide isomer. Poly(L-lactide) (PLLA) is a semi-crystalline polymer (37% crystallinity) with a glass transition temperature of 60-65 °C and a melting temperature of 175°C. It has high tensile strength, 60-70 MPa, and a high tensile modulus, 3 GPa [31, 34, 35]. Poly (DL-lactide) (PDLLA) is an amorphous polymer that has random distribution of D and L isomers. It is characterized by lower mechanical properties (tensile strength of 40-50 MPa and tensile modulus of 2 GPa) than PLLA, higher elongation, and faster degradation [31, 34]. PLA degrades by the hydrolysis mechanism. The ester bonds are cleaved creating lactic acid. Lactic acid is converted to pyruvic acid which can enter the TCA cycle, and be excreted as water and carbon dioxide [29]. Besides the normal factors that affect the degradation times, the degradation of PLA depends on what type of isomer is present, which is correlated to the

crystallinity of the polymer. PLLA is the more crystalline and has the highest degradation time (> 24 months) and PDLA which is amorphous (less crystalline) and has a degradation time of 12-15 months [12, 28, 29, 31, 34].

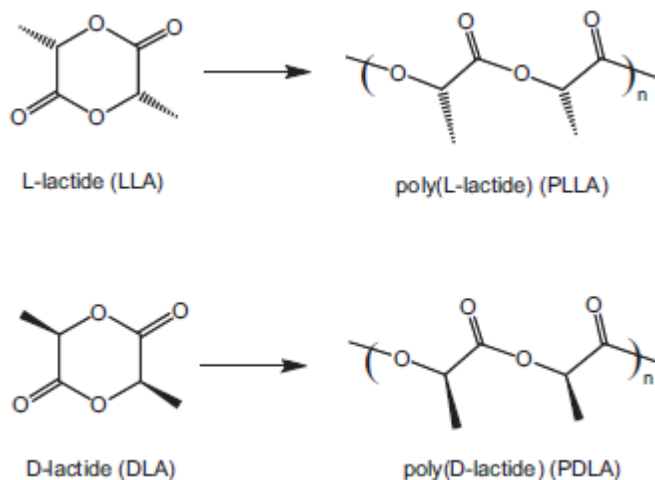


Figure 1.6. D and L isomers of lactide. Used with permission of John Wiley and Sons, 2012 [36]

Poly (lactide-co-glycolide) (PLGA) is the copolymer composed of the two monomers, glycolide and lactide. PLGA degrades by hydrolysis, following the same degradation cycle as PGA and PLA. It is an amorphous polymer with a glass transition temperature of 45-55°C, tensile strength of 40-50 MPa, and tensile modulus of 2GPa [31, 34]. Combining the two monomers allows one to tailor the properties of the copolymer synthesized simply by changing the ratio of PLA to the PGA. However the relationship between the polymer composition and mechanical properties is not linear [31].

1.4.1.2. Natural Polymers

Proteins are natural polymers, as they are essentially amino acid polymers arranged into three-dimensional structures. The most commonly used proteins are collagen, gelatin, elastin, albumin, and fibrin [12, 37].

Collagen is the most abundant protein in the human body, and is naturally found in the extracellular matrices of many tissues, including bone. This makes it a desirable candidate for applications in tissue engineering. It degrades by enzymatic degradation via natural enzymes,

collagenases and metalloproteinases. The drawbacks of the use of collagen for tissue engineering are the high cost of pure collagen, variable physio-chemical and degradation properties, and mild immunogenicity because the collagen for biomedical applications is derived from bovine or porcine skin and bovine and equine tendons [12, 37].

Gelatin is a natural protein derived from denaturing the collagen triple helical structure. As it is derived from collagen, it resembles collagen, but it eliminates the high cost associated with use of collagen. It is very abundant and often used in many industries, including food, pharmaceuticals and cosmetics; it is biocompatible and commercially available at low cost [38-43]. All of these characteristics make it an attractive candidate for tissue engineering applications. However, gelatin is water soluble and cannot retain 3D structures in aqueous environments, and as a result it is either cross-linked [40, 42, 43] or mixed with polymer to stabilize it [40, 44]. Electrospun gelatin is commonly cross-linked in glutaraldehyde vapor, which is also a commonly used cross-linking method for electrospun collagen. The cross-linking by glutaraldehyde occurs between the carboxyl groups on the glutaraldehyde and the amine groups of the gelatin [43].

1.4.1.3. *Ceramics*

Since over 60 wt% of bone is composed of inorganic calcium phosphate mineral, inorganic ceramics have been intensely investigated and used for applications in bone grafts. Some of the ceramics materials investigated are bioactive glass, hydroxyapatite, and tricalcium phosphate [13, 19, 20, 28, 45]. Bioactive glasses are characterized by their bioactive nature, namely the ability to form bonds with surrounding natural tissue by formation of the carbonated hydroxyapatite layer [13, 20, 28]. They can have very high compressive mechanical properties, compressive strength ~500MPa and compressive modulus ~35GPa, but are very brittle and have low fracture toughness [13, 20, 28]. Hydroxyapatite (HA) ($\text{Ca}_{10}(\text{PO}_4)_6(\text{OH})_2$) and tricalcium phosphate (TCP) ($\text{Ca}_3(\text{PO}_4)_2$) are attractive candidates as natural bone tissue is also composed of HA. Because HA is more crystalline, it has higher mechanical properties (compressive strength of >400 MPa and compressive modulus ~100 GPa [28]), and degrades very slowly, TCP is more amorphous, and as a result has lower mechanical properties (compressive strength of 400-600 MPa and compressive modulus 30-90 GPa [46]) but is reabsorbed easily and faster, and can be converted to HA in the body. Calcium phosphate ceramics possess excellent osteoconductive

properties and are bioactive, but their applications are hindered by their highly brittle nature which can lead to catastrophic failures [13, 17, 19, 20, 28].

1.4.1.4. *Composite Scaffolds*

Bone is a composite tissue, composed of collagenous matrix and calcium phosphate mineral, and each material contributes to the high mechanical properties of the bone. While the mineral content contributes to the stiffness of the bone, the collagenous network contributes to the toughness of the tissue [5]. As result, a single material cannot replicate bone properties, and composites of materials are used as they mimic composition of the bone more closely. Synthetic polymers and natural materials are used to mimic the organic collagen matrix, contributing to the ductility of the scaffolds. Calcium phosphates increase mechanical properties, are naturally found in the bone, and certain types can be remodeled by cells. By combining synthetic and natural polymers with ceramics, the goal is to maximize the benefits of each while reducing the drawbacks. The approaches that are being investigated for creating polymer/ceramic composite scaffolds will be discussed in Section 1.4.3.

1.4.2. *Scaffold Fabrication Techniques*

A large number of scaffold fabrications techniques are being investigated for applications in tissue engineering of bone [13, 28, 30, 32, 47, 48]. Some important properties of the scaffolds should be noted when comparing different techniques, namely average pore size, porosity, pore interconnectivity and mechanical properties. Porosity and interconnectivity play an important role in tissue regeneration, as it is necessary for migration and proliferation of the cells and tissue formation within the scaffolds. Higher porosities and larger pore sizes enhance bone ingrowth and osteointegration; optimal pores sizes for scaffolds have been reported to range from 100-300 μm [13, 48-51]. While macroporosity is important for tissue integration, microporosity and surface roughness also play a role in cellular attachment, proliferation, and differentiation [13, 48-51]. Some of the techniques for scaffold fabrication that will be reviewed are thermally induced phase separation, solvent casting/particulate leaching, heat sintering microspheres, and electrospinning.

Thermally induced phase separation (TIPS) is a technique used to create highly porous 3-D scaffolds by dissolving polymer in a solvent at a higher temperature and then inducing liquid-

liquid or liquid-solid phase separation by lowering the temperature. The porosity is achieved by sublimation of solidified, solvent rich phase. Porosity, pore size and pore orientation is controlled by controlling polymer concentration and temperature gradient [30, 52, 53]. Resulting scaffolds have very high porosities (Figure 1.7 A), 80-97%, with average pore sizes of 10-100 μ m, and low mechanical properties, compressive moduli in the range of 4-15 MPa for PLLA, PDLA and PLGA polymers [30, 52, 53].

Solvent casting/particulate leaching is a scaffold fabrication technique where water soluble particles or paraffin are used as space holders for future pore networks, while polymer solution is cast around them. After the solvent is evaporated and polymer set, the porogens are leached out leaving a pore network behind. Porogens can be sintered together to ensure pore interconnectivity. Porosity and pore size is controlled by controlling porogen size. Resulting scaffolds (Figure 1.7 B) have high porosities, 70-95%, and a wide range of pore sizes 100-500 μ m [54-56]. While the use of porogens provides the control of pore size and porosity,

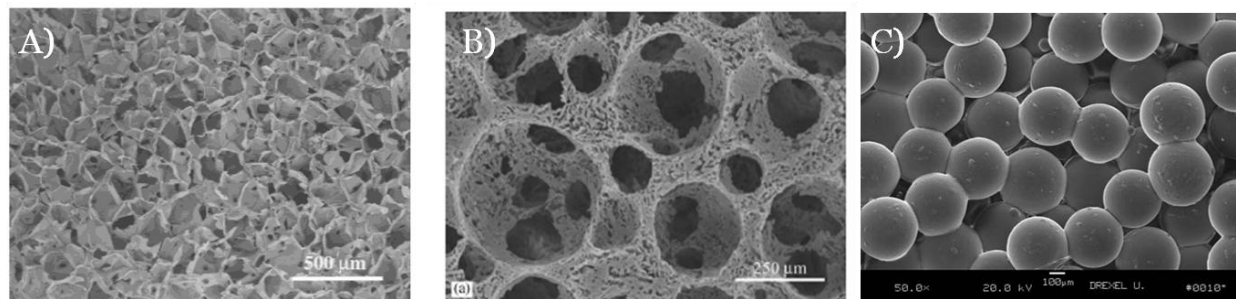


Figure 1.7. SEM images of scaffolds fabricated by various fabrication techniques: A) thermally induced phase separation (Reprinted from *Biomaterials*, 25(19), Wei, G. and P.X. Ma, Structure and properties of nano-hydroxyapatite/polymer composite scaffolds for bone tissue engineering, p. 4749-57, Copyright (2012), with permission from Elsevier) [60], B) solvent casting/particulate leaching (Reprinted from *Biomaterials*, 25(11), Chen, V.J. and P.X. Ma, Nano-fibrous poly(L-lactic acid) scaffolds with interconnected spherical macropores, p. 2065-73, Copyright (2012), with permission from Elsevier) [54], and C) heat sintering of microspheres (Reprinted from *Biomaterials*, 24(4), Borden, M., et al., Structural and human cellular assessment of a novel microsphere-based tissue engineered scaffold for bone repair, p. 597-609, Copyright (2012), with permission from Elsevier) [58]. interconnectivity of the pores can still be a problem [6, 28, 30, 54, 55].

Heat sintering is a technique where the polymer microspheres are heated above glass transition (T_g) of polymer and held for certain period of time, and then cooled down to room

temperature. During the heating process, the sintering occurs due to the intertwining of polymer chains between adjacent microspheres, forming bonds. By controlling the size of the microspheres and heat sintering time, the pore size and porosity can be controlled. Due to the round nature of the microspheres, the pore network is interconnected. Resulting scaffolds (Figure 1.7 C) have porosities in the range 25-40%, with average pore size 50-200 μm , and compressive modulus 140-330 MPa for PLGA [57-59].

Each processing technique has advantages and disadvantages for applications in bone tissue engineering, but all the techniques seek to create scaffolds that mimic trabecular bone alone. Very few techniques and approaches have focused on creating scaffolds that mimic organization and properties of cortical bone tissue. In this project, we will focus on fabricating scaffolds that mimic both structures of the bone, cortical and trabecular. To do this we will utilize the electrospinning technique, which can create nanofiber scaffolds that mimic natural extracellular matrix.

1.4.2.1. *Electrospinning*

Electrospinning is a fabrication technique that can create non-woven meshes with fibers in the nano and micron range from biodegradable polymers. The process relies on the application of an electrostatic force to overcome the surface tension of the polymer solution and drive fiber formation. Typical electrospinning system is composed of a syringe with polymer solution with a needle tip (spinneret), pump that controls the extrusion rate of the polymer solution, high voltage power supply, and collecting plate or mandrel that is grounded or negatively charged (Figure 1.8) [37, 61-63].

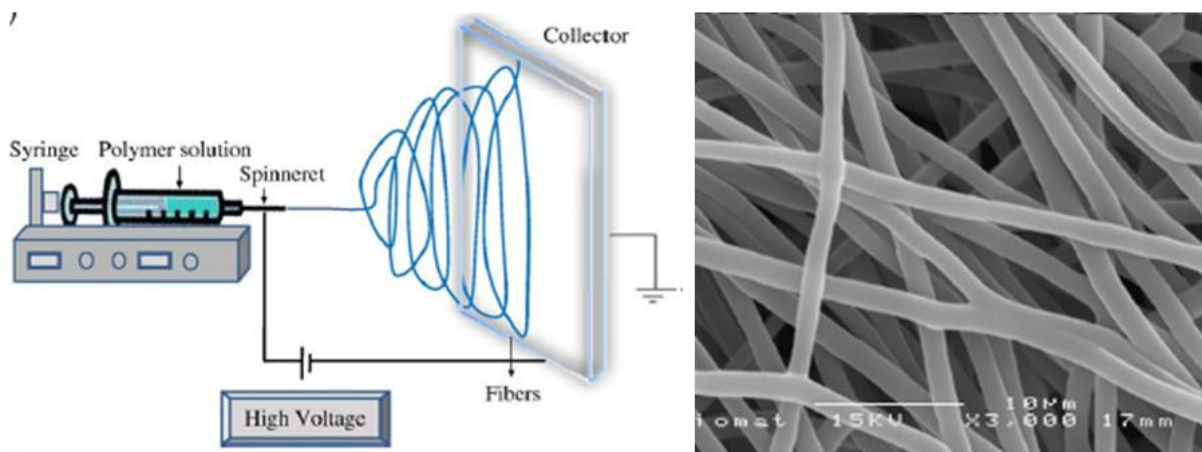


Figure 1.8. Schematic diagram of set up for electrospinning(Reprinted from *Biotechnol Adv.*, 28(3), Bhardwaj, N. and S.C. Kundu , *Electrospinning: a fascinating fiber fabrication technique*, p. 325-47, Copyright (2012), with permission from Elsevier) [37] and SEM of electrospun fibers (Reprinted from *Biomaterials*, 25(11), Chen, V.J. and P.X. Ma, *Nano-fibrous poly(L-lactic acid) scaffolds with interconnected spherical macropores*, p. 2065-73, Copyright (2012), with permission from Elsevier) [54].

In the electrospinning process an electric charge is applied to the polymer solution being extruded from the tip of the syringe needle and is held by surface tension. When the electric charge reaches a critical value and overcomes the surface tension, an electronically charged jet of polymer solution erupts. The jet is unstable and a rapid whipping motion of the jet occurs as it travels toward the collecting plate. During this process the solvent evaporates and the jet is solidified into fibers that are collected/deposited onto a collecting plate or mandrel [37, 64]. Resulting scaffolds are characterized by high surface area, high porosities, and interconnected pore networks. These electrospun scaffolds are desirable for tissue engineering applications because the nano- and microfiber surface morphologies mimic the native extracellular matrix [65, 66].

1.4.2.2. *Electrospinning for Bone Tissue Engineering*

Electrospun scaffolds are desirable candidates for tissue engineering applications as the nano- and microfiber surface morphologies mimic the native extracellular matrix [65, 66]. Various natural and synthetic materials have been successfully electrospun into scaffolds for bone tissue engineering including, poly(ϵ -caprolactone) (PCL) [67, 68], poly(L-lactide) (PLLA)

[69, 70], poly(D,L-lactide) (PDLA) [71], poly(lactide-co-glycolide) (PLGA) [66, 72, 73], collagen type I [66], gelatin [38-40, 42, 43]. Various mixtures of synthetic polymers with either natural polymer like gelatin or collagen [39, 69, 74, 75] or inorganic hydroxyapatite (HA) [39, 70, 73, 75], or both have been investigated to increase cellular attachment, proliferation and differentiation of cells.

While electrospinning has many advantages, it is not without drawbacks, namely the lack of cellular infiltration due to small pore size and lack of three dimensional structures. Electrospun scaffolds are characterized by very high porosities (up to 75% [76]) and pore interconnectivity, but pore size is limited (8-10 μm) by the small fiber diameters [70, 76]. Two techniques have been investigated as means to increase pore size and porosities: addition of salt particles as porogen during electrospinning [77] and dual electrospinning with sacrificial fibers that can be dissolved out [78, 79]. By increasing porosities and pore size these approaches result in better cellular infiltration in the scaffold [77-79].

Up until recently electrospun structures were limited to two dimensional structures and as a result very little to no characterization has been performed to determine the compressive mechanical properties of these scaffolds. Wright *et al.* from our group has developed and characterized two different sintering techniques used to fabricate three dimensional (3D) electrospun scaffolds from electrospun sheets [80]. Briefly, electrospun PDLA layer was electrospun on top of electrospun PLLA mats to serve as bonding layer at higher temperatures and bind multiple layers together into 3D scaffolds. This technique provides the missing step in the investigation of electrospun scaffolds for bone tissue engineering applications, as we now can investigate compressive mechanical properties of these scaffolds. This technique will be utilized in this project to fabricate 3D electrospun scaffolds and create structures that mimic both cortical and trabecular organization of the bone.

1.4.3. Mineralization of Scaffolds

As discussed previously in Section 1.4.1.4, polymers and mineral composites combine the benefits of each material while reducing the drawbacks of each. Various techniques have been investigated for mineralization of electrospun scaffolds: incorporation of mineral particles into polymer solution [39, 70, 74, 75, 81, 82], precipitation of mineral onto nanofiber surface

[68, 76, 79, 83-85], or combination of both [66, 71, 73] . Electrospun PLLA or PCL composites with nano-hydroxyapatite particles incorporated were found to support cellular attachment and proliferation and promote differentiation of the cells. However, the effect of HA on mechanical properties is unclear, as both increases [70, 81] and decreases [39, 75] have been reported.

Incubation of scaffolds in simulated body fluid (SBF), an aqueous solution that has ions concentration similar to human plasma, is considered a biomimetic approach to mineralization as it mimics the way mineral is precipitated *in vivo* [11]. Mineralization in SBF can take up 4 weeks, and mineral precipitated was identified as carbonated hydroxyapatite [83]. Recently, the use of more concentrated SBF solution, like 5X and 10X , is being investigated as mineral precipitation can be achieved faster, on the order of hours [11]. Tas and Bhaduri, reported a method that utilizes ten times concentrated simulated body fluid (10X SBF) achieving mineral deposition within hours of incubation [86]. The same process was utilized for mineralization of electrospun polymer scaffolds [68, 76, 79, 84]. Mineral precipitated was found to be mixtures of dicalcium phosphate dehydrate (DCPC), an amorphous calcium phosphate, and hydroxyapatite [68, 76]. Due the hydrophobic natures of the synthetic polymers, techniques for enhancing mineral deposition by introducing charge sites into the matrix are being investigated and include soaking in NaOH [83], plasma coating [76], and incorporation of gelatin [68]. Another approach is to incorporate nano-hydroxyapatite particles into polymer solutions to serve as nucleation sites for mineralization by incubation in simulated body fluid [72, 73].

1.5. PROJECT DESCRIPTION

The objective of this project is to utilize electrospinning and heat sintering techniques to create a biodegradable full thickness three dimensional biomimetic polymeric scaffolds with macro and nano architecture similar to natural bone for successful bone regeneration. The proposed scaffolds would mimic the structural organization of both trabecular and cortical bone, creating scaffolds that better mimic the natural organization of the bone tissue. To achieve this, the project is divided into 4 steps:

- 1) Evaluation and characterization of the mineralization technique for electrospun scaffolds.** Characterize the mineralization technique for the electrospun scaffolds

with respect to mechanical properties, mineral deposition and distribution, and cytotoxicity.

- 2) **Design, fabrication, and characterization of three dimensional electrospun scaffolds that mimic structural organization of trabecular bone.** Fabricate three dimensional scaffolds and characterize mineralization and fiber alignment effects on compressive mechanical properties of electrospun scaffolds.
- 3) **Design, fabrication, and characterization of three dimensional electrospun scaffolds that mimic structural organization of cortical bone.** Design and fabricate the electrospun scaffolds that mimic the organization of a single osteon. Then, utilize the heat sintering technique to create cortical-like scaffolds by combining multiple osteon-like scaffolds.
- 4) **Design, fabrication, and characterization of full thickness three dimensional electrospun scaffolds.** Combine the cortical and trabecular segments into one three dimensional scaffold, and characterize mechanical properties, mineral deposition and distribution, and cytotoxicity.

1.6. REFERENCES

1. Cowin, S.C. and S.B. Doty, *Tissue mechanics*. 2007, New York, NY: Springer. xvi, 682 p.
2. Hing, K.A., *Bone repair in the twenty-first century: biology, chemistry or engineering?* Philos Transact A Math Phys Eng Sci, 2004. **362**(1825): p. 2821-50.
3. Wheeler, D.L. and W.F. Enneking, *Allograft bone decreases in strength in vivo over time*. Clin Orthop Relat Res, 2005(435): p. 36-42.
4. Rho, J.Y., L. Kuhn-Spearing, and P. Zioupos, *Mechanical properties and the hierarchical structure of bone*. Med Eng Phys, 1998. **20**(2): p. 92-102.
5. Wang, X. and S. Puram, *The toughness of cortical bone and its relationship with age*. Ann Biomed Eng, 2004. **32**(1): p. 123-35.
6. An, Y.H. and R.A. Draughn, *Mechanical testing of bone and the bone-implant interface*. 2000, Boca Raton, Fla.: CRC Press. 624 p.
7. *Bone Structure Figure*. <http://en.wikipedia.org/wiki/Bone>
8. Wagoner Johnson, A.J. and B.A. Herschler, *A review of the mechanical behavior of CaP and CaP/polymer composites for applications in bone replacement and repair*. Acta Biomater. **7**(1): p. 16-30.
9. Beniash, E., *Biominerals--hierarchical nanocomposites: the example of bone*. Wiley Interdiscip Rev Nanomed Nanobiotechnol, 2010. **3**(1): p. 47-69.
10. Frohlich, M., et al., *Tissue engineered bone grafts: biological requirements, tissue culture and clinical relevance*. Curr Stem Cell Res Ther, 2008. **3**(4): p. 254-64.
11. Kretlow, J.D. and A.G. Mikos, *Review: mineralization of synthetic polymer scaffolds for bone tissue engineering*. Tissue Eng, 2007. **13**(5): p. 927-38.
12. Laurencin, C.T. and L.S. Nair, *Biodegradable polymers as biomaterials*. Progress in Polymer Science, 2007. **32**(8-9): p. 762-798.
13. Khan, Y., et al., *Tissue engineering of bone: material and matrix considerations*. J Bone Joint Surg Am, 2008. **90 Suppl 1**: p. 36-42.
14. Agarwal, R., et al., *Osteoinductive bone graft substitutes for lumbar fusion: a systematic review*. J Neurosurg Spine, 2009. **11**(6): p. 729-40.
15. Ambrose, C.G. and T.O. Clanton, *Bioabsorbable implants: review of clinical experience in orthopedic surgery*. Ann Biomed Eng, 2004. **32**(1): p. 171-7.
16. Cornell, C.N., *Osteobiologics*. Bull Hosp Jt Dis, 2004. **62**(1-2): p. 13-7.
17. Giannoudis, P.V., H. Dinopoulos, and E. Tsiridis, *Bone substitutes: an update*. Injury, 2005. **36 Suppl 3**: p. S20-7.
18. Hak, D.J., *The use of osteoconductive bone graft substitutes in orthopaedic trauma*. J Am Acad Orthop Surg, 2007. **15**(9): p. 525-36.
19. Gazdag, A.R., et al., *Alternatives to Autogenous Bone Graft: Efficacy and Indications*. J Am Acad Orthop Surg, 1995. **3**(1): p. 1-8.
20. Laurencin, C., Y. Khan, and S.F. El-Amin, *Bone graft substitutes*. Expert Rev Med Devices, 2006. **3**(1): p. 49-57.
21. Bessa, P.C., M. Casal, and R.L. Reis, *Bone morphogenetic proteins in tissue engineering: the road from laboratory to clinic, part II (BMP delivery)*. J Tissue Eng Regen Med, 2008. **2**(2-3): p. 81-96.
22. Bessa, P.C., M. Casal, and R.L. Reis, *Bone morphogenetic proteins in tissue engineering: the road from the laboratory to the clinic, part I (basic concepts)*. J Tissue Eng Regen Med, 2008. **2**(1): p. 1-13.

23. Seeherman, H. and J.M. Wozney, *Delivery of bone morphogenetic proteins for orthopedic tissue regeneration*. Cytokine Growth Factor Rev, 2005. **16**(3): p. 329-45.
24. White, A.P., et al., *Clinical applications of BMP-7/OP-1 in fractures, nonunions and spinal fusion*. Int Orthop, 2007. **31**(6): p. 735-41.
25. Issa, J.P.M., et al., *Sustained release carriers used to delivery bone morphogenetic proteins in the bone healing process*. Anatomia Histologia Embryologia, 2008. **37**(3): p. 181-187.
26. Ruhe, P.Q., et al., *rhBMP-2 release from injectable poly(DL-lactic-co-glycolic acid)/calcium-phosphate cement composites*. J Bone Joint Surg Am, 2003. **85-A Suppl 3**: p. 75-81.
27. Langer, R. and J.P. Vacanti, *Tissue engineering*. Science, 1993. **260**(5110): p. 920-6.
28. Rezwani, K., et al., *Biodegradable and bioactive porous polymer/inorganic composite scaffolds for bone tissue engineering*. Biomaterials, 2006. **27**(18): p. 3413-3431.
29. An, Y.H., S.K. Wolf, and R.J. Friedman, *Pre-clinical in vivo evaluation of orthopaedic bioabsorbable devices*. Biomaterials, 2000. **21**(24): p. 2635-2652.
30. Liu, X. and P.X. Ma, *Polymeric scaffolds for bone tissue engineering*. Ann Biomed Eng, 2004. **32**(3): p. 477-86.
31. Middleton, J.C. and A.J. Tipton, *Synthetic biodegradable polymers as orthopedic devices*. Biomaterials, 2000. **21**(23): p. 2335-46.
32. Stevens, B., et al., *A review of materials, fabrication methods, and strategies used to enhance bone regeneration in engineered bone tissues*. J Biomed Mater Res B Appl Biomater, 2008. **85**(2): p. 573-82.
33. Ashammakhi, N. and P. Rokkanen, *Absorbable polyglycolide devices in trauma and bone surgery*. Biomaterials, 1997. **18**(1): p. 3-9.
34. Balasundaram, G. and T.J. Webster, *An overview of nano-polymers for orthopedic applications*. Macromol Biosci, 2007. **7**(5): p. 635-42.
35. Tsuji, H., *Poly(lactide) stereocomplexes: formation, structure, properties, degradation, and applications*. Macromol Biosci, 2005. **5**(7): p. 569-97.
36. Tsuji, H., *Poly(lactide) stereocomplexes: Formation, structure, properties, degradation, and applications (vol 5, 569, 2005)*. Macromolecular Bioscience, 2007. **7**(12): p. 1299-1299.
37. Bhardwaj, N. and S.C. Kundu, *Electrospinning: a fascinating fiber fabrication technique*. Biotechnol Adv. **28**(3): p. 325-47.
38. Gu, S.Y., et al., *Electrospinning of gelatin and gelatin/poly(L-lactide) blend and its characteristics for wound dressing*. Materials Science & Engineering C-Materials for Biological Applications, 2009. **29**(6): p. 1822-1828.
39. Gupta, D., et al., *Nanostructured biocomposite substrates by electrospinning and electrospraying for the mineralization of osteoblasts*. Biomaterials, 2009. **30**(11): p. 2085-94.
40. Heydarkhan-Hagvall, S., et al., *Three-dimensional electrospun ECM-based hybrid scaffolds for cardiovascular tissue engineering*. Biomaterials, 2008. **29**(19): p. 2907-14.
41. Sell, S.A., et al., *Electrospinning of collagen/biopolymers for regenerative medicine and cardiovascular tissue engineering*. Adv Drug Deliv Rev, 2009. **61**(12): p. 1007-19.
42. Sisson, K., et al., *Fiber diameters control osteoblastic cell migration and differentiation in electrospun gelatin*. J Biomed Mater Res A. **94**(4): p. 1312-20.

43. Sisson, K., et al., *Evaluation of cross-linking methods for electrospun gelatin on cell growth and viability*. *Biomacromolecules*, 2009. **10**(7): p. 1675-80.
44. Zhang, Y., et al., *Electrospinning of gelatin fibers and gelatin/PCL composite fibrous scaffolds*. *J Biomed Mater Res B Appl Biomater*, 2005. **72**(1): p. 156-65.
45. Nandi, S.K., et al., *Orthopaedic applications of bone graft & graft substitutes: a review*. *Indian J Med Res*. **132**: p. 15-30.
46. Chen, B.Q., et al., *Fabrication and mechanical properties of beta-TCP pieces by gel-casting method*. *Materials Science & Engineering C-Biomimetic and Supramolecular Systems*, 2008. **28**(7): p. 1052-1056.
47. Yang, S., et al., *The design of scaffolds for use in tissue engineering. Part I. Traditional factors*. *Tissue Eng*, 2001. **7**(6): p. 679-89.
48. Yu, N.Y., et al., *Biodegradable poly(alpha-hydroxy acid) polymer scaffolds for bone tissue engineering*. *J Biomed Mater Res B Appl Biomater*. **93**(1): p. 285-95.
49. Hutmacher, D.W., et al., *State of the art and future directions of scaffold-based bone engineering from a biomaterials perspective*. *J Tissue Eng Regen Med*, 2007. **1**(4): p. 245-60.
50. Karageorgiou, V. and D. Kaplan, *Porosity of 3D biomaterial scaffolds and osteogenesis*. *Biomaterials*, 2005. **26**(27): p. 5474-91.
51. Stylios, G., T. Wan, and P. Giannoudis, *Present status and future potential of enhancing bone healing using nanotechnology*. *Injury*, 2007. **38 Suppl 1**: p. S63-74.
52. Ma, P.X. and R. Zhang, *Microtubular architecture of biodegradable polymer scaffolds*. *J Biomed Mater Res*, 2001. **56**(4): p. 469-77.
53. Maquet, V., et al., *Porous poly(alpha-hydroxyacid)/Bioglass composite scaffolds for bone tissue engineering. I: Preparation and in vitro characterisation*. *Biomaterials*, 2004. **25**(18): p. 4185-94.
54. Chen, V.J. and P.X. Ma, *Nano-fibrous poly(L-lactic acid) scaffolds with interconnected spherical macropores*. *Biomaterials*, 2004. **25**(11): p. 2065-73.
55. Liao, C.J., et al., *Fabrication of porous biodegradable polymer scaffolds using a solvent merging/particulate leaching method*. *J Biomed Mater Res*, 2002. **59**(4): p. 676-81.
56. Lu, L., et al., *In vitro and in vivo degradation of porous poly(DL-lactic-co-glycolic acid) foams*. *Biomaterials*, 2000. **21**(18): p. 1837-45.
57. Borden, M., et al., *Tissue engineered microsphere-based matrices for bone repair: design and evaluation*. *Biomaterials*, 2002. **23**(2): p. 551-9.
58. Borden, M., et al., *Structural and human cellular assessment of a novel microsphere-based tissue engineered scaffold for bone repair*. *Biomaterials*, 2003. **24**(4): p. 597-609.
59. Lv, Q., L. Nair, and C.T. Laurencin, *Fabrication, characterization, and in vitro evaluation of poly(lactic acid glycolic acid)/nano-hydroxyapatite composite microsphere-based scaffolds for bone tissue engineering in rotating bioreactors*. *J Biomed Mater Res A*, 2009. **91**(3): p. 679-91.
60. Wei, G. and P.X. Ma, *Structure and properties of nano-hydroxyapatite/polymer composite scaffolds for bone tissue engineering*. *Biomaterials*, 2004. **25**(19): p. 4749-57.
61. Deitzel, J.M., et al., *The effect of processing variables on the morphology of electrospun nanofibers and textiles*. *Polymer*, 2001. **42**(1): p. 261-272.
62. Di Martino, A., et al., *Electrospun scaffolds for bone tissue engineering*. *Musculoskelet Surg*.

63. Li, D. and Y.N. Xia, *Electrospinning of nanofibers: Reinventing the wheel?* Advanced Materials, 2004. **16**(14): p. 1151-1170.
64. Lannutti, J., et al., *Electrospinning for tissue engineering scaffolds*. Materials Science & Engineering C-Biomimetic and Supramolecular Systems, 2007. **27**(3): p. 504-509.
65. Jang, J.H., O. Castano, and H.W. Kim, *Electrospun materials as potential platforms for bone tissue engineering*. Adv Drug Deliv Rev, 2009. **61**(12): p. 1065-83.
66. Liao, S., et al., *Processing nanoengineered scaffolds through electrospinning and mineralization suitable for biomimetic bone tissue engineering*. J Mech Behav Biomed Mater, 2008. **1**(3): p. 252-60.
67. Yoshimoto, H., et al., *A biodegradable nanofiber scaffold by electrospinning and its potential for bone tissue engineering*. Biomaterials, 2003. **24**(12): p. 2077-82.
68. Li, X., et al., *Coating electrospun poly(epsilon-caprolactone) fibers with gelatin and calcium phosphate and their use as biomimetic scaffolds for bone tissue engineering*. Langmuir, 2008. **24**(24): p. 14145-50.
69. Kim, H.W., H.S. Yu, and H.H. Lee, *Nanofibrous matrices of poly(lactic acid) and gelatin polymeric blends for the improvement of cellular responses*. J Biomed Mater Res A, 2008. **87**(1): p. 25-32.
70. Sui, G., et al., *Poly-L-lactic acid/hydroxyapatite hybrid membrane for bone tissue regeneration*. J Biomed Mater Res A, 2007. **82**(2): p. 445-54.
71. Cui, W.U., et al., *In situ growth of hydroxyapatite within electrospun poly(DL-lactide) fibers*. Journal of Biomedical Materials Research Part A, 2007. **82A**(4): p. 831-841.
72. Hild, N., et al., *Two-layer membranes of calcium phosphate/collagen/PLGA nanofibres: in vitro biomineralisation and osteogenic differentiation of human mesenchymal stem cells*. Nanoscale. **3**(2): p. 401-9.
73. Madurantakam, P.A., et al., *Multiple factor interactions in biomimetic mineralization of electrospun scaffolds*. Biomaterials, 2009. **30**(29): p. 5456-5464.
74. Jegal, S.H., et al., *Functional composite nanofibers of poly(lactide-co-caprolactone) containing gelatin-apatite bone mimetic precipitate for bone regeneration*. Acta Biomater. **7**(4): p. 1609-17.
75. Prabhakaran, M.P., J. Venugopal, and S. Ramakrishna, *Electrospun nanostructured scaffolds for bone tissue engineering*. Acta Biomater, 2009.
76. Yang, F., J.G.C. Wolke, and J.A. Jansen, *Biomimetic calcium phosphate coating on electrospun poly (epsilon-caprolactone) scaffolds for bone tissue engineering*. Chemical Engineering Journal, 2008. **137**(1): p. 154-161.
77. Wright, L.D., T. Andric, and J.W. Freeman, *Utilizing NaCl to increase the porosity of electrospun materials*. Materials Science & Engineering C-Materials for Biological Applications, 2011. **31**(1): p. 30-36.
78. Baker, B.M., et al., *The potential to improve cell infiltration in composite fiber-aligned electrospun scaffolds by the selective removal of sacrificial fibers*. Biomaterials, 2008. **29**(15): p. 2348-2358.
79. Whited, B.M., et al., *Pre-osteoblast infiltration and differentiation in highly porous apatite-coated PLLA electrospun scaffolds*. Biomaterials, 2011. **32**(9): p. 2294-2304.
80. Wright, L.D., et al., *Fabrication and mechanical characterization of 3D electrospun scaffolds for tissue engineering*. Biomed Mater, 2010. **5**(5): p. 055006.

81. Peng, F., X. Yu, and M. Wei, *In vitro cell performance on hydroxyapatite particles/poly(l-lactic acid) nanofibrous scaffolds with an excellent particle along nanofiber orientation*. Acta Biomater.
82. Yang, F., et al., *Development of an electrospun nano-apatite/PCL composite membrane for GTR/GBR application*. Acta Biomater, 2009. **5**(9): p. 3295-304.
83. Chen, J., B. Chu, and B.S. Hsiao, *Mineralization of hydroxyapatite in electrospun nanofibrous poly(L-lactic acid) scaffolds*. J Biomed Mater Res A, 2006. **79**(2): p. 307-17.
84. Mavis, B., et al., *Synthesis, characterization and osteoblastic activity of polycaprolactone nanofibers coated with biomimetic calcium phosphate*. Acta Biomaterialia, 2009. **5**(8): p. 3098-3111.
85. Yang, L., et al., *Biomimetic calcium phosphate coatings on recombinant spider silk fibres*. Biomed Mater. **5**(4): p. 045002.
86. Tas, A.C. and S.B. Bhaduri, *Rapid coating of Ti6Al4V at room temperature with a calcium phosphate solution similar to 10x simulated body fluid*. Journal of Materials Research, 2004. **19**(9): p. 2742-2749.

Chapter 2

2.1. Rapid Mineralization of Electrospun Scaffolds for Bone Tissue Engineering

Tea Andric, Lee D. Wright, Joseph W. Freeman

Journal of Biomaterials Science, Polymer Edition 22 (2011) 1535-1550. Used with permission of Taylor and Francis, 2012

2.1.1. ABSTRACT

We investigated different techniques to enhance calcium phosphate mineral precipitation onto electrospun PLLA scaffolds when incubated in concentrated simulated body fluid (SBF)10XSBF. The techniques included the use of vacuum, pretreatment with 0.1M NaOH , and electrospinning gelatin/PLLA blends as means to increase overall mineral precipitation and distribution throughout the scaffolds. Mineral precipitation was evaluated using environmental scanning electron microscopy (SEM), Energy Dispersive Spectroscopy (EDS) mapping, and the determination the mineral weight percents. In addition we evaluated the effect of the techniques on mechanical properties, cellular attachment and cellular proliferation on scaffolds. Two treatments, pretreatment with NaOH and incorporation of 10% gelatin into PLLA solution, both in combination with vacuum, resulted in significantly higher degrees of mineralization (16.79% and 14.9%, respectively) and better mineral distribution on surfaces and through the cross-sections after 2 hours of exposure to SBF. While both scaffolds groups supported cell attachment and proliferation, 10%gelatin/PLLA scaffolds had significantly higher yield stress (1.73 MPa vs. 0.56MPa) and elastic modulus (107MPa vs. 44MPa) than NaOH pretreated scaffolds.

2.1.2. INTRODUCTION

Skeletal loss and bone deficiencies are a major problem with over 600,000 bone grafting procedures performed in the US annually. The market is currently estimated at 2.5 billion dollars annually; however, this number is only expected to increase due to an aging population and increased life expectancy [1]. As current treatment have drawbacks, such as donor site morbidity for autografts and high failure rates for allografts [2], there is a need for alternative bone graft substitutes. Bone tissue engineering has emerged as a promising new approach to design and produce bone graft substitutes [3].

Tissue engineering combines scaffolds, cells, and/or growth factors to regenerate or repair lost or damaged tissues [3-5]. Electrospinning as a scaffold fabrication technique has recently gained interest in applications for bone tissue engineering [4, 6-10]. Electrospun scaffolds are characterized by high surface area, high porosities, and interconnected pore networks. This makes electrospun scaffolds desirable for tissue engineering applications as the nano- and microfiber surface morphologies mimic the native extracellular matrix [4, 6]. Various natural and synthetic materials have been successfully electrospun into scaffolds including, poly(ϵ -caprolactone) (PCL) [7, 8], poly(L-lactide) (PLLA) [9, 10], poly(D,L-lactide) (PDLA) [11], poly(lactide-co-glycolide) (PLGA) [12], collagen type I [6], and gelatin type B [13]. Synthetic polymers are common choices for bone tissue engineering applications because they are biocompatible and easily processed to create the desired porous three-dimensional structures. Among the most frequently used polymers are polyesters such as poly(glycolic) acid (PGA), poly(lactic) acid (PLA), and their copolymer PLGA, which have been approved for medical use by the US Food and Drug Administration. They are also characterized with low glass transition temperatures allowing easy processing, variable degradation rates varying from 6 months (PGA) up to 2 years (PLLA) [14-17].

Composite scaffolds, scaffolds composed of biodegradable polymers and inorganic calcium phosphates, have emerged as great options for bone grafts since their mechanical properties can be altered by varying the two phases. They also mimic natural bone tissue as they can contain both an organic bone phase (protein) with polymer and inorganic bone phase (calcium phosphate). The presence of calcium phosphate has been shown to enhance alkaline

phosphatase (ALP) activity, a marker of osteoblast activity, and improve the mechanical strength of the scaffolds [18, 19].

Different techniques have been investigated for creating polymer and calcium phosphate composite electrospun scaffolds. Hydroxyapatite nanoparticles can be dispersed in the polymer solution and electrospun as a composite [10, 20]. Incorporation of hydroxyapatite in electrospinning polymer solution resulted in increased mechanical properties [10, 20], increased proliferation and ALP activity of human fetal osteoblasts [20]. However uniform dispersion of hydrophilic hydroxyapatite nanoparticles in organic solvents can be difficult to maintain during the electrospinning process [8]. Another approach is the biomimetic mineralization of scaffolds by incubation in simulated body fluid (SBF) which leads to precipitation of the mineral calcium phosphate [21]. An advantage of this approach is that it somewhat mimics biological mineral growth; however, it can take up to 28 days to achieve an apatite layer [21]. An additional challenge is the hydrophobic nature of the synthetic polymers, which can result in reduced mineral precipitation [8, 21]. To enhance calcium phosphate precipitation various surface modification techniques have been investigated to expose or add charged functionalized groups, including argon plasma treatment [22], NaOH hydrolysis [21], and coating with gelatin [8]. Tas and Badhuri developed an accelerated mineral precipitation method that uses 10XSBF to achieve precipitation in a matter of hours [23].

In this study, we investigated different techniques to enhance calcium phosphate mineral precipitation onto electrospun PLLA scaffolds incubated in 10XSBF. These include the use of vacuum pressure, pretreatment with 0.1M NaOH, and electrospinning gelatin/PLLA blends to increase overall mineral precipitation and distribution throughout the scaffolds. Mineral precipitation was evaluated using SEM, EDS mapping, XRD and total mineral weight percents. We also compared mechanical properties and evaluated cellular attachment and proliferation on all the scaffolds.

2.1.3. MATERIALS AND METHODS

2.1.3.1. *Fabrication of Scaffolds by Electrospinning*

PLLA (inherent viscosity =2.0 dl/g, Mw = 152,000) was purchased from Sigma Aldrich (St. Louis, MO, USA). Dichloromethane (DCM) and dimethylformaldehyde (DMF) were

purchased from Fisher Scientific (Pittsburgh, PA, USA). Gelatin, type A, from porcine skin was purchased from Sigma Aldrich (St. Louis, MO, USA). NaCl, KCl, CaCl₂ 2H₂O, MgCl₂ 6H₂O, NaHCO₃, and NaH₂PO₄ were purchased from Fisher Scientific (Pittsburgh, PA, USA).

The electrospinning solution was prepared by dissolving PLLA to 7 % w/v in 75% DCM and 25% DMF. The solution was loaded into a 5 ml plastic syringe with an 18-gauge needle, and extruded at a rate of 5 mL/h. The PLLA was electrospun onto a rotating (~ 1100 RPM) mandrel with a 5 cm diameter and a working distance of 5 cm. The voltage applied was +13kV and -7kV. Negative voltage is utilized in the electrospinning process to help drive the jet toward the target or collecting mandrel.

The gelatin/PLLA mixture was made by dissolving gelatin in 1ml deionized (dI) water and adding it to the 7% PLLA solution. Polymer solutions are made in 16 ml batches, and in order to make overall volume of gelatin/PLLA and PLLA solutions equal, 1ml of DCM was replaced with 1ml of gelatin solution. The amount of gelatin in solution was equal to 10 or 5 %, w/w of the amount of PLLA in the solution, and will be referred to as 5% gel/PLLA and 10% gel/PLLA. As two solutions are not miscible, they were vortexed for 1 hr to mix. This results in a gelatin/PLLA solution mixture that was electrospun. The electrospinning parameters were identical to the parameters used for the PLLA solution alone, except the voltage applied was +18kV and -7kV.

2.1.3.2. Mineralization of Scaffolds

We have adopted a method previously developed and reported by Tas and Bhaduri [23] to prepare 10XSFBF. A stock solution was made using NaCl, KCl, CaCl₂ 2H₂O, MgCl₂ 6H₂O, and NaH₂PO₄, and stored at room temperature. Prior to the mineralization process, NaHCO₃ was added while stirring vigorously, resulting in the following ion concentrations: Ca²⁺ 25 mM, HPO₄²⁻ 10 mM, Na⁺ 1.03 M, K⁺ 5 mM, Mg²⁺ 5mM, Cl⁻ 1.065M, and HCO₃⁻ 10mM . The electrospun mats were incubated in 400 ml of 10XSFBF for two hours at room temperature. One group of PLLA scaffolds was incubated at room temperature, without vacuum, and will be referred to as PLLA_MIN. All other scaffolds were incubated in 10X SBF in vacuum at room temperature, which is denoted with letter V in the group name (Table 2.1.1). After being

removed from 10X SBF , all the samples were rinsed in dI water to remove mineral not attached to scaffolds, and vacuum dried overnight.

The NaOH pretreatment scaffolds were soaked in 0.1 M NaOH solution for 5 min in vacuum and then rinsed in dI water. The samples were then placed in the 10XSBF in vacuum for two hours, rinsed in dI water, and vacuum dried overnight.

Names and the descriptions of all the groups that were analyzed are listed in the Table 2.1.1.

Table 2.1.1. List of group names and descriptions

Group Name	Description
PLLA	PLLA, not mineralized
PLLA_MIN	PLLA, no vacuum, mineralized
PLLA_V_MIN	PLLA, vacuum, mineralized
PLLA_NaOH_V_MIN	PLLA, vacuum, NaOH treatment, mineralized
5%gel/PLLA	PLLA, 5% gelatin, not mineralized
5%gel/PLLA_V_MIN	PLLA, 5% gelatin, vacuum, mineralized
10%gel/PLLA	PLLA, 10% gelatin, not mineralized
10%gel/PLLA_V_MIN	PLLA, 10% gelatin, vacuum, mineralized

2.1.3.3. Mineral Ash Weight

Samples were subjected to high temperatures to burn off the polymer and determine the mineral ash weight percent. Scaffolds tested included PLLA_MIN, PLLA_V_MIN, PLLA_NaOH_V_MIN, 5%gel/PLLA_V_MIN, and 10%gel/PLLA_V_MIN. After the initial weight of the samples was recorded, the samples were placed in ceramic crucibles, and then placed into a high temperature furnace (Model No. FD1535M, Fisher Scientific, Pittsburgh, PA, USA) at 700°C for 24 hours. After cooling down, the mineral ash weight was recorded and the average mineral percent deposition calculated as ratio of mineral ash weight to samples original weight. Each sample was placed in separate crucible, and three samples per group were tested (n=3).

2.1.3.4. Characterization of Scaffolds

Fiber morphology, fiber diameters, mineral deposition and distribution on the scaffolds were imaged by scanning electron microscopy (SEM). Five fiber diameter measurements were taken in four different fields of vision, and the values were averaged to determine average fiber diameters. The scaffolds were soaked in liquid nitrogen and freeze-fractured to view the cross sections. Cross sections were imaged to map out mineral distribution throughout the scaffolds. All the samples were sputter coated with gold and palladium and imaged using an ESEM (Environmental Scanning Electron Microscope) (FEI Quanta 600 FEG). Energy Dispersive Spectroscopy (EDS) analysis was performed using the Bruker EDX Silicon Drifter Detector on the ESEM to map presence of calcium and phosphate across the cross sections. EDS was also utilized to quantify presence of Ca and P ions on surface and determine Ca:P ratio, and quantify presence of gelatin prior and after mineralization by quantifying presence of nitrogen. Spectra of three fields of view for each group were quantified, and data reported as atomic percentages.

X-ray diffraction (XRD) was used to determine the crystallographic structure of the calcium phosphate mineral. Samples were tested using X-ray Diffraction System (Philips Xpert Pro) with 45kV, 40mA, step size of 0.03° and scanning range from 10° to 60°. Two groups of samples were analyzed, 10%gel/PLLA_V_MIN and PLLA_NaOH_V_MIN, as they had highest mineral content.

2.1.3.5. Mechanical Testing

The scaffolds were mechanically tested in tension using an Instron 5869 with Bioplus Bath (Norwood, MA, USA). Scaffolds tested included electrospun PLLA (n=7), PLLA_MIN (n=6), PLLA_V_MIN (n=7), PLLA_NaOH_V_MIN (n=7), 5% gel/PLLA (n=5), 5% gel/PLLA_V_MIN (n=5), 10% gel/PLLA (n=5), and 10% gel/PLLA_V_MIN (n=5). The tests were performed in phosphate buffered saline (PBS) (pH= 7.4) at 37°C. The samples were cut in into 1 x 5 cm strips, the gauge length was set to 2 cm, and the strain rate was 2 mm/min (10% stain/min). The samples were tested until failure. The data was analyzed to determine yield stress and elastic modulus.

2.1.3.6. Cell Culture

Mouse pre-osteoblastic cells (MC3T3-E1, ATCC) were cultured in Dubelcco's Modified Eagle Medium (DMEM, Cellgro, Mediatech, Manassas, VA, USA) supplemented with 10% fetal bovine serum (FBS, Cellgro, Mediatech, Manassas, VA, USA) and 1% streptomycin/ penicillin (Cellgro, Mediatech, Manassas, VA, USA). The scaffolds were cut into 15mm discs with 0.2 mm thickness and secured into 24-well tissue culture treated polystyrene (TCPS) plates using Silastic Medical Adhesive (Dow Corning, Midland, MI, USA). The samples were sterilized in 70% ethanol for 30 minutes followed by exposure to UV light for 30 minutes on each side. The scaffolds were then washed with PBS and soaked in cell culture medium overnight. Approximately 50,000 cells were seeded onto each scaffolds and control (TCPS alone). The cells were allowed to attach for one hour before adding culture medium to a final volume of 1 ml. The medium was changed every other day, and the cultures were incubated at 37°C in a humidified atmosphere and 5% CO₂. Cells were cultured for period of 28 days, and data was collected on days 7, 14, 21, and 28.

Cell viability was measured using a Cell Titer 96TM Aqueous Solution Cell Proliferation Assay (MTS Assay) (Promega, Madison, WI, USA) on following scaffolds PLLA (n=3), PLLA_V_MIN (n=3), PLLA_NaOH_V_MIN(n=3), 10%gel/PLLA (n=3), and 10%gel/PLLA_V_MIN (n=3). At each time point (7, 14, 21, and 28 days) the media was removed, then 400 µl of fresh media and 80 µl of the MTS solution were added to each well and incubated at 37°C and 5 % CO₂ for three hours. After incubation, 300 µl of the mixture was transferred to a 48-well plate and diluted with 300µl of dI water. The plate was read at 490 nm using a SpectroMax M2 spectrophotometer (Sunnyvale, CA, USA).

Cell attachment was visualized qualitatively using ESEM at the same time points for the same groups. Cells on the scaffolds were rinsed three times with PBS and fixed at 4°C in 1% and 3% gluteraldehyde for one hour and 20 hours, respectively. The scaffolds were then dehydrated using a series of methanol dilutions from 10% to 100% for 15 minutes each. The scaffolds were dried and sputter coated using gold and palladium and viewed using ESEM.

2.1.3.7. Statistical Analysis

Statistical analysis was performed using JMP 7 software. All the data was analyzed using one way analysis of variance (ANOVA) with Tukey's test to determine statistically significant differences between groups. Statistical significance was tested at $p < 0.05$.

2.1.4. RESULTS

PLLA and PLLA/gelatin blends (5 % and 10%) were electrospun onto a rotating mandrel to create a non-woven nanofibrous scaffolds. Surface morphologies of electrospun PLLA and 10% gel/PLLA can be seen in Figure 2.1.1. Scaffolds electrospun with 10% gelatin/PLLA had significantly larger average fiber diameters of $1.184 \pm 0.384 \mu\text{m}$ than PLLA scaffolds, $0.670 \pm 0.170 \mu\text{m}$. PLLA scaffolds were then incubated in 10XSBF, with and without vacuum, to achieve calcium phosphate precipitation. Treatment with 0.1M NaOH and incorporation of gelatin into PLLA solution were investigated as ways to enhance mineral precipitation.

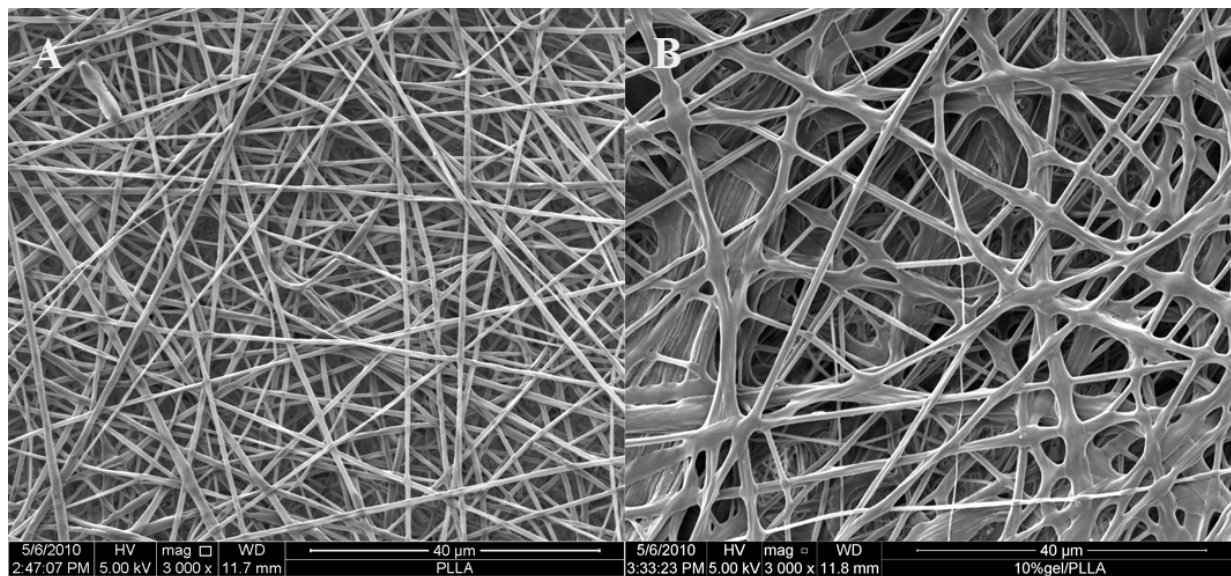


Figure 2.1.1. SEM images of electrospun PLLA (A) and 10%Gel/PLLA (B). 10%Gel/PLLA scaffolds were found to have significantly larger fiber diameters.

2.1.4.1. Mineral Ash Weight

The amount of calcium phosphate coating was quantified as average ash weight percent after burning off the PLLA and measuring the resulting mineral ash weight. The ash weights are reported as average weight percent (Table 2.1.2). Scaffolds that were pretreated with NaOH (PLLA_NaOH_V_MIN) and 10% gel/PLLA_V_MIN scaffolds had significantly higher mineral weight percents than scaffolds that were mineralized without any pretreatments and no vacuum (PLLA_MIN) (Table 2.1.2).

Table 2.1.2. Average mineral ash weight percent. (*) denotes significant difference from PLLA_MIN group (p<0.05)

Group	Average mineral ash weight
PLLA_MIN	4.59% ± 2.95%
PLLA_V_MIN	11.04% ± 1.22%
PLLA_NaOH_V_MIN	16.55% ± 0.83%*
5%gel/PLLA_V_MIN	10.12% ± 2.42%
10%gel/PLLA_V_MIN	15.14% ± 2.04%*

2.1.4.2. Mineralization of the Scaffolds

Calcium phosphate deposition was qualitatively observed using SEM and EDS. SEM was used to observe the way mineral precipitated on the fibers and scaffolds. In groups mineralized without vacuum (PLLA_MIN), mineral was deposited sparsely in the form of large and small crystals on fibers on the surface (Figure 2.1.2 A). In the group that was mineralized without any pretreatment in vacuum (PLLA_V_MIN), mineral was also deposited in the form of large and small crystals on the surface (Figure 2.1.2 B). The mineral was deposited more uniformly and in larger quantities in the form of small crystal grains on polymer fibers (Figure 2.1.2 C) for the scaffolds pretreated with 0.1 M NaOH (PLLA_NaOH_V_MIN). Similarly, smaller grain crystals were also observed covering the surface of the scaffolds with 10% gelatin (Figure 2.1.2 D).

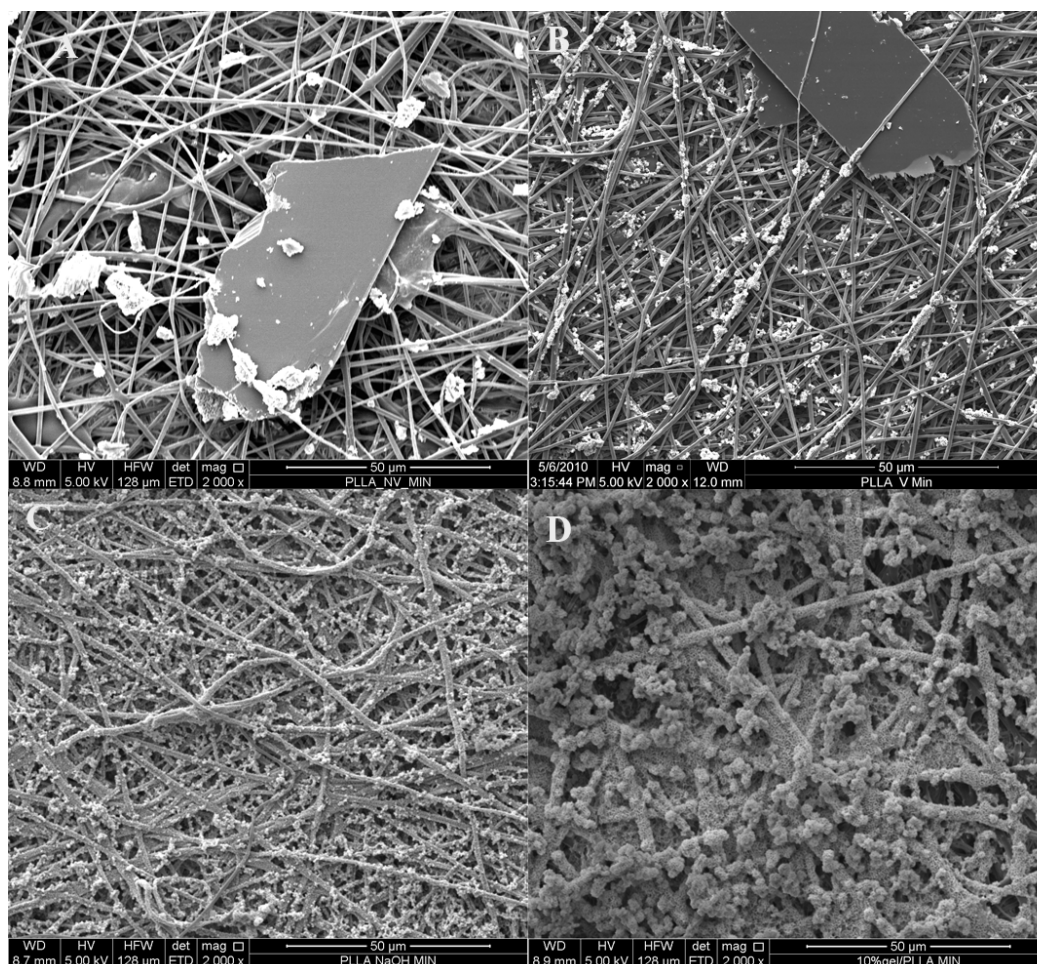


Figure 2.1.2. SEM images of mineralized scaffolds: **A)** PLLA_MIN - Mineralized PLLA no vacuum, larger crystals can be seen of surface, **B)** PLLA_V_MIN - mineralized PLLA in vacuum, combination of large crystals with smaller crystals grain can be seen, **C)** PLLA_NaOH_V_MIN – mineralized PLLA in vacuum, pretreated with NaOH, small mineral crystals cover surface, but fiber morphology is preserved, **D)** 10%gel/PLLA_V_MIN – 10% gelatin/PLLA mineralized, surface is covered with small grain mineral crystals and fiber morphology is still visible

EDS mapping was used to confirm presence of calcium and phosphorus in the cross-sections of the scaffolds to qualitatively assess how well the mineral had deposited across the thickness of the scaffolds, see Figure 2.1.3. The presence of Ca and P was detected on the surfaces of the cross sections, but very little was detected in the middle of the cross-sections that were incubated without vacuum (Figure 2.1.3 A) and without any pretreatment (Figure 2.1.3 B). However, Ca and P were present across the cross-section for scaffolds pretreated with 0.1M NaOH (Figure 2.1.3 D). A similar trend was observed in the scaffolds that were electrospun with

10% gelatin (Figure 2.1.3 C). The combination of vacuum and pretreatment or incorporation of gelatin resulted in increased mineral deposition throughout the thickness of the scaffolds.

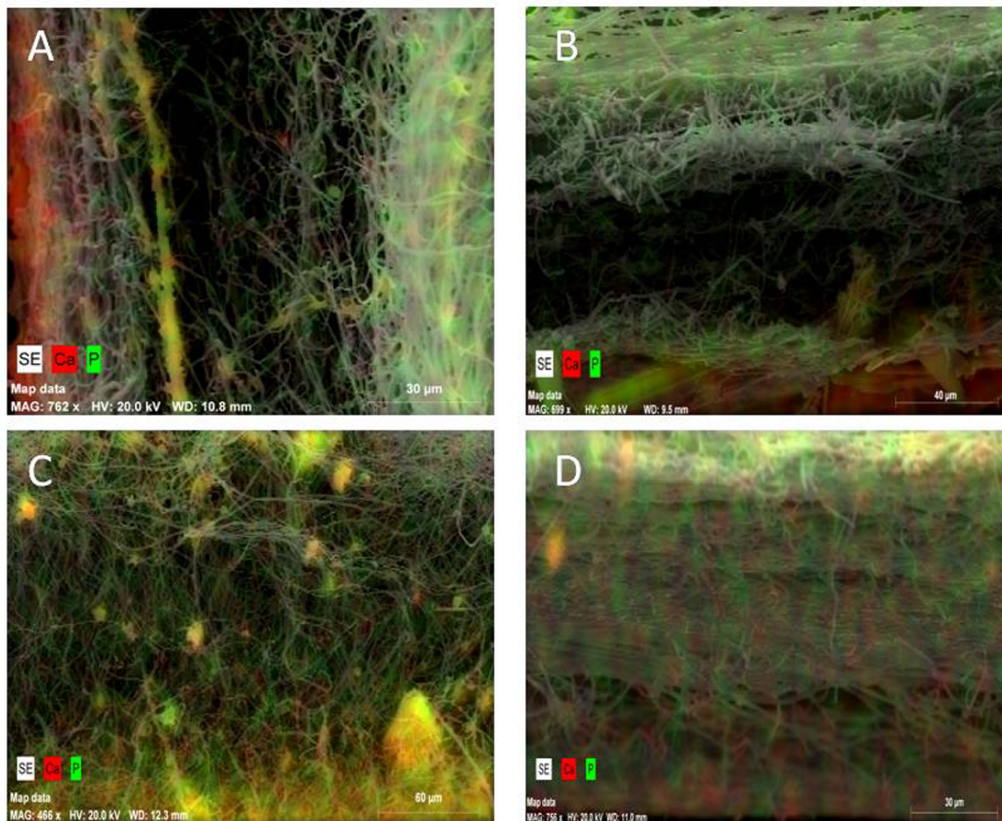


Figure 2.1.3. EDS map of mineralized scaffolds cross-sections where calcium is tagged with red, and phosphorus is tagged with green: **A)** PLLA no vacuum, presence of Ca and P on surfaces, scale bar shown **30 μ m**, **B)** PLLA vacuum, no pretreatment (PLLA_MIN), presence of Ca and P on the surfaces with very little present in the center, scale bar shown **40 μ m**, **C)** PLLA pretreated with 0.1M NaOH (PLLA_T_MIN), presence of Ca and P can be seen across the cross-section, scale bar shown **60 μ m**, **D)** 10% gelatin/PLLA mineralized, presence of Ca and P can be seen across the cross-section, scale bar shown **30 μ m**.

EDS mapping and XRD were utilized to identify the type of mineral that was formed on the surface of the scaffolds. EDS spectra showed presence of calcium, phosphorus and oxygen. The amount of each element was quantified to determine Ca:P ratio for each group of samples. All the values were very close to 1, which corresponds to several calcium phosphates: dicalcium phosphate dehydrate (DCPD), also known as brushite, dicalcium phosphate (DCP), and calcium phosphate (CPP) [24]. X-ray diffraction patterns show presence of two types of minerals on the surfaces, brushite and hydroxyapatite, with peaks clearly labeled in Figure 2.1.4.

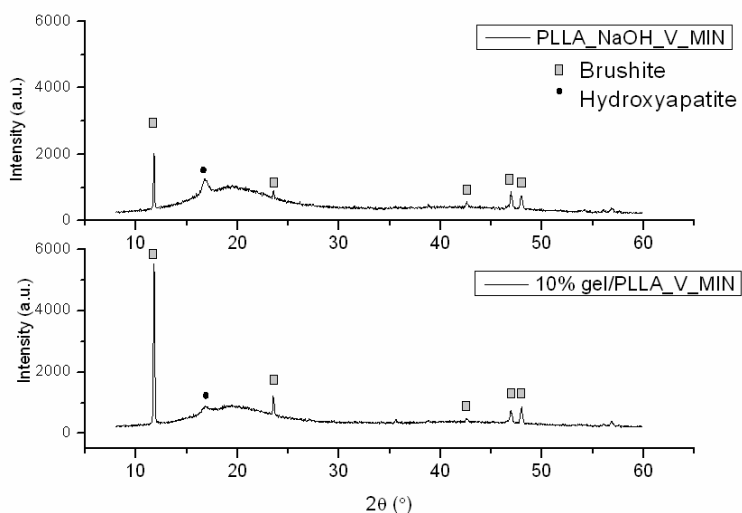


Figure 2.1.4. X-ray diffraction pattern of PLLA_NaOH_V_MIN (top) and 10% gel/PLLA_V_MIN (bottom) scaffolds mineralized by incubation in 10X SBF for 2 h in vacuum.

To determine presence of gelatin in scaffolds prior and after the mineralization, EDS spectra of the scaffolds were plotted and quantified. Average atomic percentages of nitrogen on the surfaces are $7.91 \pm 1.56\%$ prior to mineralization and $0.43 \pm 0.26\%$ after mineralization. Majority of the gelatin was lost during the mineralization process, as expected, since it was not cross-linked. However, it did not significantly affect mineralization process.

2.1.4.3. Mechanical Properties

Mechanical tests were performed to determine the effect of the 10XSBF, treatment with 0.1 M NaOH, and incorporation of 5% and 10% gelatin on PLLA electrospun scaffolds. All the values are graphed as averages with standard deviations in Figure 2.1.5. Electrospun PLLA scaffolds, PLLA scaffolds mineralized with no vacuum, and mineralized NaOH pretreated PLLA scaffolds were found to have a significantly lower yield stress than the other groups. The addition of vacuum during mineralization process resulted in significant increase in mechanical properties of PLLA scaffolds. There were not any significant differences between 5% and 10% gelatin, mineralized or not mineralized. PLLA scaffolds, mineralized without vacuum PLLA scaffolds, and mineralized NaOH treated PLLA scaffolds were found to have statistically lower elastic modulus than all other groups. Mineralizing electrospun PLLA scaffolds and/or

incorporation of 5% or 10% gelatin resulted in scaffolds with significantly higher yield stresses and elastic moduli than electrospun PLLA alone. However treatment with 0.1 M NaOH and mineralization did not result in any changes in yield stress and elastic modulus when compared to PLLA alone.

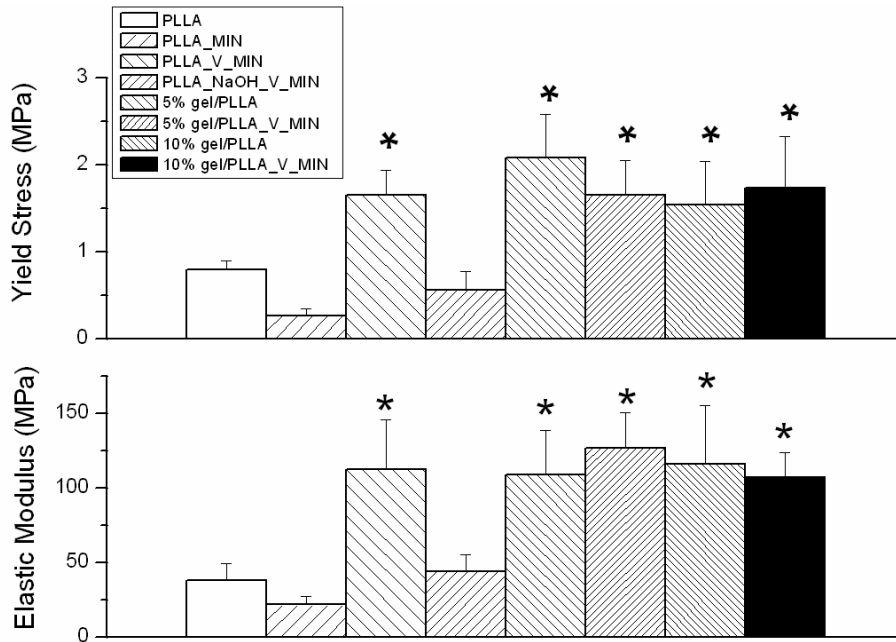


Figure 2.1.5. Mechanical testing data graphs include yield stress (top) and elastic moduli (bottom) averages as bars, and standard deviations as error bars. (*) denotes statistically significant difference from PLLA, PLLA_MIN and PLLA_NaOH_V_MIN groups ($p < 0.05$)

2.1.4.4. Cell Culture

Attachment and proliferation of MC3T3 cells were evaluated qualitatively using SEM and quantitatively using an MTS assay on the following scaffolds: electrospun PLLA alone, PLLA mineralized in vacuum, PLLA mineralized pretreated with 0.1 M NaOH, 10% gel/PLLA, 10% gel/PLLA mineralized, and TCPS as a control. Cell attachment and deposition of ECM on the scaffolds can be seen after 21 days in culture on electrospun PLLA alone and PLLA mineralized in vacuum (Figure 2.1.6 A and B). This also visible after 21 days on 10%gel/PLLA scaffolds and 10%gel/PLLA_MIN scaffolds (Figure 2.1.6 C and D).

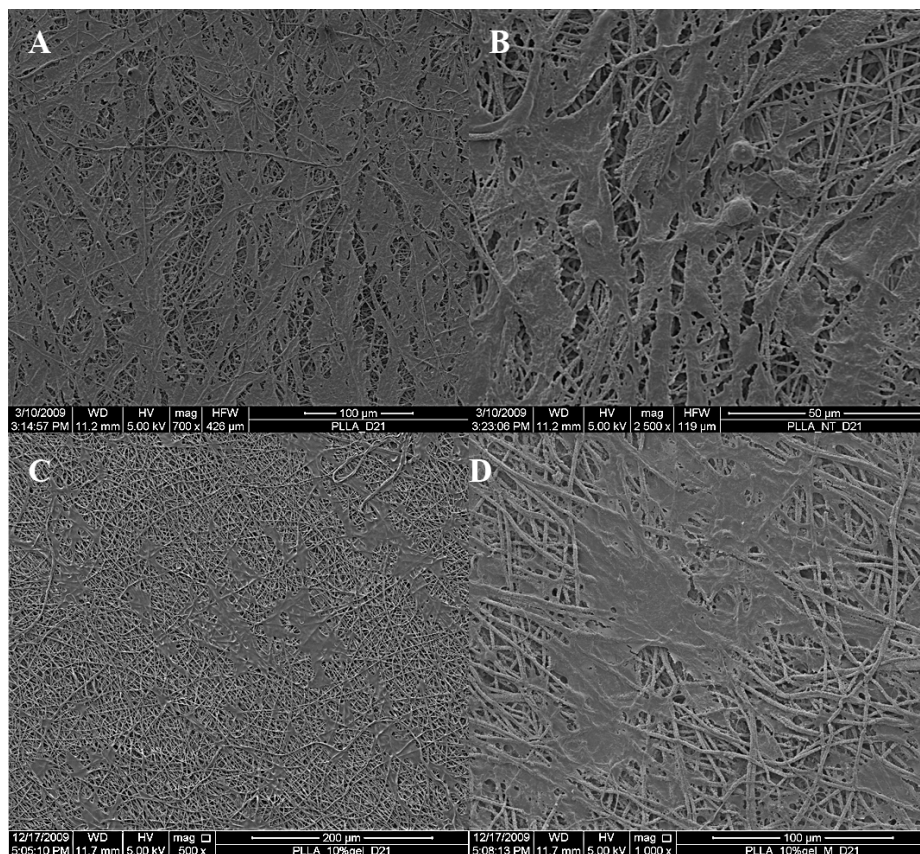


Figure 2.1.6. Cellular attachment and ECM after 21 days of MC3T3 cells culture on following electrospun scaffolds (note the scale bars as the pictures are at different magnifications): **A)** PLLA, scale bar shown 100 μ m, **B)** PLLA_V_MIN, scale bar shown 50 μ m, **C)** 10% gel/PLLA, scale bar shown 200 μ m, and **D)** 10% gel/PLLA_V_MIN, scale bar shown 100 μ m.

Cellular proliferation on the scaffolds was quantified using MTS assay on days 7, 14, 21, and 28 and the absorbances at 490 nm are shown in Figure 2.1.7. On day 7, absorbance on PLLA_NaOH_MIN was significantly lower than on PLLA, 10% gel/PLLA, and 10% gel/PLLA_V_MIN. On day 14 absorbance on 10% gel/PLLA_V_MIN was significantly lower than absorbances on control, PLLA, PLLA_V_MIN, and PLLA_NaOH_V_MIN. On day 21 absorbance for 10% gel/PLLA_V_MIN was significantly lower than PLLA and control. On day 28, the absorbance for PLLA had an outlying low value which affected the overall average, resulting in significantly lower absorbance than for PLLA_V_MIN and PLLA_NaOH_V_MIN. On day 14 absorbances were significantly increased over those on day 7 for the following groups: 10% gel/PLLA, PLLA_V_MIN, PLLA_NaOH_V_MIN, and control. On day 21 absorbances significantly increased for all scaffolds except PLLA when compared to that of day

14. An outlying low value on day 28 on PLLA scaffolds affected the statistical analysis of MTS data for PLLA group, resulting in no significance between time points. When statistical analysis was performed without data for day 28, significant increase in absorbances from day 7 to day 14 to day 21 was found. Cells proliferation started to plateau by day 28; there were no significant increases in absorbances on day 28 when compared to day 21.

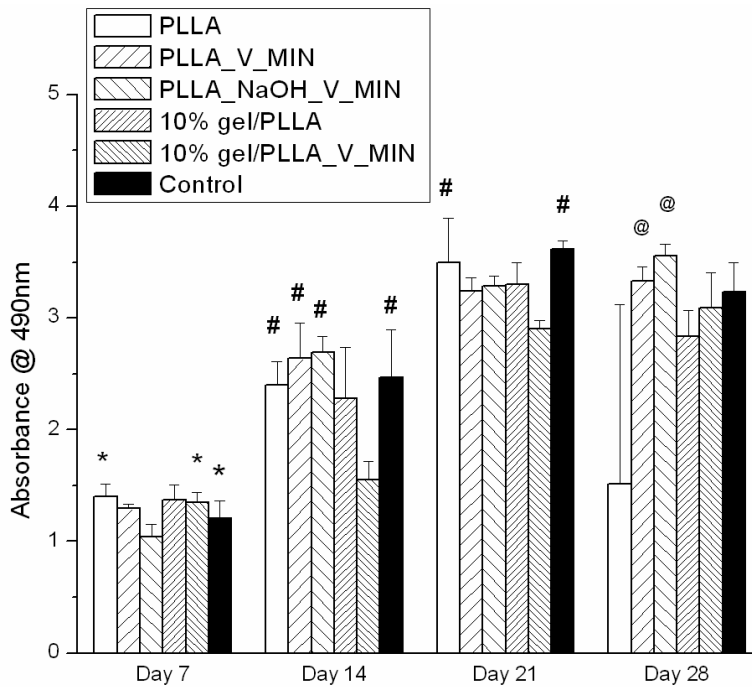


Figure 2.1.7. Average absorbances of MTS assay with standard deviations as error bars of MCT3T3-E1 cells. (*) denotes significant difference from PLLA_NaOH_V_MIN, (#) denotes significant difference from 10% gel/PLLA_V_MIN, (@) denotes significant difference from PLLA, $p < 0.05$

2.1.5. DISCUSSION

In this study electrospun PLLA scaffolds were rapidly mineralized by incubation with 10X SBF, which significantly reduces incubation time from the order of week to hours. To further improve this process we investigated the use of vacuum during the mineralization process, treatment with NaOH and incorporation of various amounts of gelatin into PLLA solutions prior to electrospinning as ways to increase mineral deposition throughout the thickness of the scaffold, improve mechanical properties, and improve cellular adhesion and proliferation. The addition of gelatin resulted in increased fiber diameters, when compared to electrospun

PLLA. Mineral precipitated on the scaffolds was identified using EDS and X-ray diffraction as brushite and hydroxyapatite. Similar results were also reported previously with mineralization by incubation in 10X SBF [8, 12, 22]. Also, it has been reported that brushite can be potential starting material for bone substitutes, and can be converted to hydroxyapatite [22, 25].

Scaffolds pretreated with 0.1M NaOH (PLLA_NaOH_V_MIN) and scaffolds electrospun from 10% gel/PLLA mixture (10% gel/PLLA_V_MIN) had significantly higher mineral weight percents, 16.55% and 15.14% respectively, than scaffolds mineralized without vacuum, 4.59% (PLLA_MIN) (Table 2). Exposure of scaffolds to NaOH resulted in degradation and exposure of carboxyl groups, which then resulted in an increased number of mineral nucleation sites. The addition of gelatin to the electrospinning PLLA solution had a similar effect. Gelatin, a denatured collagen, provided exposed carboxyl groups which increased mineral percent deposition with increased gelatin concentration. Treatment with NaOH and the addition of gelatin affected the way mineral was deposited in addition to overall mineral deposition. Mineral on the scaffolds without NaOH treatment and without gelatin, (PLLA_MIN, PLLA_V_MIN) was deposited in the form of large crystals which can block scaffolds pores (Figure 2.1.2). Mineral on the scaffolds treated with NaOH and scaffolds electrospun with gelatin/PLLA mixture formed small granules directly on the fibers (Figure 2.1.2). This can be more beneficial for applications in tissue engineering as the mineral is deposited in such way that electrospun fiber morphology is preserved and it does not block pores. Treatment with NaOH and addition of 10% gelatin resulted in scaffolds with more uniform distribution of mineral throughout the scaffolds compared to scaffolds mineralized without any treatment, as seen in EDS cross-section maps of Ca and P in Figure 2.1.3. More uniform mineral distribution throughout the scaffolds can be beneficial for uniform mechanical properties and also provide uniform environment for cellular infiltration.

The effect of the vacuum, NaOH treatment and addition of gelatin to PLLA solutions on mechanical properties was also evaluated. Addition of vacuum during mineralization process resulted in significant increase in mechanical properties of PLLA scaffolds. Although pretreatment with NaOH resulted in increased mineral deposition, mechanical properties were no different from PLLA alone and were significantly lower than all other mineralized groups. This decrease in mechanical properties compared to other mineralized groups was due to the

hydrolytic effects of the NaOH on the scaffolds. Chen *et al.* reported visible fiber degradation of electrospun PLLA scaffolds after 10 min exposure to 0.5 M NaOH [21]. Although the concentration and exposure time used was lower (0.1 M), this could still cause degradation and weakening of the fibers, resulting in decreased mechanical properties. Any possible increase in strength from mineralization was negated by scaffold degradation. Therefore this process is not effective for the replacement of load bearing bone.

Incorporation of gelatin resulted in significantly higher mechanical properties than PLLA alone. However there were no significant differences in mechanical properties between the mineralized and unmineralized gelatin scaffolds. An increase in mechanical properties with the incorporation of gelatin into polymer solution was also observed by Gupta *et al.*, mechanical properties of electrospun poly (L-lactic acid)-co-poly (ϵ -caprolactone) (PLACL) increased with the addition of 10% gelatin [26]. This is thought to be due to the higher mechanical properties of the electrospun gelatin scaffolds which is reported to have a tensile strength of 5.77 MPa and an elastic modulus of 499 MPa [27]. These data indicate that the incorporation of gelatin into the scaffold is better for the production of load bearing bone scaffolds than the use of NaOH. Incorporation of gelatin yields increased mineral deposition and sponsored cell growth, while also increasing mechanical properties whereas NaOH treatment did not increase the mechanical properties with mineralization.

Cellular attachment and proliferation was evaluated over the period of 4 weeks in culture. All the scaffolds supported cell attachment and proliferation over the period of 28 days. Cell attachment and deposition of ECM on the scaffolds can be seen after 21 days in culture on electrospun PLLA alone and PLLA mineralized (Figure 2.1.7A and B). This was also visible after 21 days on 10%gel/PLLA scaffolds, and 10%gel/PLLA_MIN scaffolds (Figure 2.1.7 C and D). The decrease in cell numbers from day 21 to day 28 on PLLA scaffolds was observed due to a low outlier value on one of the scaffolds. This affected the statistical analysis of MTS data for PLLA group, resulting in no significance between time points. We suspect that the low outlier value could be to the cells decreasing their activity or possibly dying due to over population. When statistical analysis was performed without data for day 28, significant increase in absorbances from day7 to day14 to day 21 was found. MTS absorbances for every group have

significantly increased by day 21 in culture, indicating that the scaffolds had no cytotoxic effect on the cells.

We observed no difference in proliferation between scaffolds with and without gelatin. Gelatin has been reported to increase cell proliferation, but mostly in the cross-linked state [8]. We believe that such effect was not observed in our system due to dissolution of gelatin in the media and mineralization solution, as the gelatin was not cross-linked and is soluble in water. EDS surface analysis revealed that most of the gelatin was dissolved during 2h mineralization process, thus no effect of increased proliferation due to gelatin was observed. We also did not observe any increased proliferation of cells on mineralized scaffolds compared to non-mineralized scaffolds. This could possibly be due to dissolution of mineral and gelatin on the scaffolds. The mineral present on the scaffolds was identified as brushite, which is a soluble calcium phosphate, and over time some of the mineral could be lost [24]. This dissolution of mineral can result in loss of cells that were bound to mineral on the surface. While no significant effect in cell proliferation was observed on the modified scaffolds over PLLA alone scaffolds, they all supported cellular attachment and proliferation and no cytotoxic effects.

2.1.6. CONCLUSION

In this study we investigated different treatment techniques for increasing mineral precipitation on electrospun PLLA scaffolds. Two treatments, pretreatment with NaOH and incorporation of 10% gelatin into PLLA solution, in combination with vacuum resulted in significantly higher degrees of mineralization as evidenced by the ash weight percent. They also had better mineral distribution on scaffold surfaces and through the cross-sections. While both scaffold groups supported cell attachment and proliferation, 10% gelatin/PLLA scaffolds had significantly higher mechanical properties than NaOH treated scaffolds and PLLA alone. Pretreatment of PLLA scaffolds with NaOH resulted in scaffold degradation and decreased mechanical properties. Addition of 10% gelatin to PLLA solution resulted in the higher fiber diameters, significantly higher degree of mineralization, increased mechanical properties, and scaffolds that supported cellular adhesion and proliferation. Based on these findings, electrospun blends of 10% gelatin and PLLA that are mineralized in 10X SBF under vacuum may be a better method for enhancing mineral precipitation for bone tissue engineering.

2.1.7. REFERENCES

1. Hing, K.A., *Bone repair in the twenty-first century: biology, chemistry or engineering?* Philos Transact A Math Phys Eng Sci, 2004. **362**(1825): p. 2821-50.
2. Wheeler, D.L. and W.F. Enneking, *Allograft bone decreases in strength in vivo over time.* Clin Orthop Relat Res, 2005(435): p. 36-42.
3. Laurencin, C.T., et al., *Tissue engineering: orthopedic applications.* Annu Rev Biomed Eng, 1999. **1**: p. 19-46.
4. Jang, J.H., O. Castano, and H.W. Kim, *Electrospun materials as potential platforms for bone tissue engineering.* Adv Drug Deliv Rev, 2009. **61**(12): p. 1065-83.
5. Lv, Q., L. Nair, and C.T. Laurencin, *Fabrication, characterization, and in vitro evaluation of poly(lactic acid glycolic acid)/nano-hydroxyapatite composite microsphere-based scaffolds for bone tissue engineering in rotating bioreactors.* J Biomed Mater Res A, 2009. **91**(3): p. 679-91.
6. Liao, S., et al., *Processing nanoengineered scaffolds through electrospinning and mineralization suitable for biomimetic bone tissue engineering.* J Mech Behav Biomed Mater, 2008. **1**(3): p. 252-60.
7. Yoshimoto, H., et al., *A biodegradable nanofiber scaffold by electrospinning and its potential for bone tissue engineering.* Biomaterials, 2003. **24**(12): p. 2077-82.
8. Li, X., et al., *Coating electrospun poly(epsilon-caprolactone) fibers with gelatin and calcium phosphate and their use as biomimetic scaffolds for bone tissue engineering.* Langmuir, 2008. **24**(24): p. 14145-50.
9. Kim, H.W., H.S. Yu, and H.H. Lee, *Nanofibrous matrices of poly(lactic acid) and gelatin polymeric blends for the improvement of cellular responses.* J Biomed Mater Res A, 2008. **87**(1): p. 25-32.
10. Sui, G., et al., *Poly-L-lactic acid/hydroxyapatite hybrid membrane for bone tissue regeneration.* J Biomed Mater Res A, 2007. **82**(2): p. 445-54.
11. Cui, W., et al., *In situ growth of hydroxyapatite within electrospun poly(DL-lactide) fibers.* J Biomed Mater Res A, 2007. **82**(4): p. 831-41.
12. Zhao, J., et al., *Preparation and mineralization of PLGA/Gt electrospun fiber mats.* Chinese Science Bulletin, 2009. **54**(8): p. 1328-1333.
13. Heydarkhan-Hagvall, S., et al., *Three-dimensional electrospun ECM-based hybrid scaffolds for cardiovascular tissue engineering.* Biomaterials, 2008. **29**(19): p. 2907-14.
14. Agrawal, C.M. and R.B. Ray, *Biodegradable polymeric scaffolds for musculoskeletal tissue engineering.* J Biomed Mater Res, 2001. **55**(2): p. 141-50.
15. Khan, Y., et al., *Tissue engineering of bone: material and matrix considerations.* J Bone Joint Surg Am, 2008. **90 Suppl 1**: p. 36-42.
16. Middleton, J.C. and A.J. Tipton, *Synthetic biodegradable polymers as orthopedic devices.* Biomaterials, 2000. **21**(23): p. 2335-46.
17. Rezwani, K., et al., *Biodegradable and bioactive porous polymer/inorganic composite scaffolds for bone tissue engineering.* Biomaterials, 2006. **27**(18): p. 3413-31.
18. Kretlow, J.D. and A.G. Mikos, *Review: mineralization of synthetic polymer scaffolds for bone tissue engineering.* Tissue Eng, 2007. **13**(5): p. 927-38.
19. Lv, Q., L. Nair, and C.T. Laurencin, *Fabrication, characterization, and in vitro evaluation of poly(lactic acid glycolic acid)/nano-hydroxyapatite composite microsphere-*

- based scaffolds for bone tissue engineering in rotating bioreactors.* J Biomed Mater Res A, 2008.
20. Prabhakaran, M.P., J. Venugopal, and S. Ramakrishna, *Electrospun nanostructured scaffolds for bone tissue engineering.* Acta Biomater, 2009. **5**(8): p. 2884-93.
 21. Chen, J., B. Chu, and B.S. Hsiao, *Mineralization of hydroxyapatite in electrospun nanofibrous poly(L-lactic acid) scaffolds.* J Biomed Mater Res A, 2006. **79**(2): p. 307-17.
 22. Yang, F., J.G.C. Wolke, and J.A. Jansen, *Biomimetic calcium phosphate coating on electrospun poly (epsilon-caprolactone) scaffolds for bone tissue engineering.* Chemical Engineering Journal, 2008. **137**(1): p. 154-161.
 23. Tas, A.C. and S.B. Bhaduri, *Rapid coating of Ti6Al4V at room temperature with a calcium phosphate solution similar to 10x simulated body fluid.* Journal of Materials Research, 2004. **19**(9): p. 2742-2749.
 24. Vallet-Regi, M., *Revisiting ceramics for medical applications.* Dalton Trans, 2006(44): p. 5211-20.
 25. Tas, A.C. and S.B. Bhaduri, *Chemical processing of CaHPO(4).(.)2H(2)O: Its conversion to hydroxyapatite.* Journal of the American Ceramic Society, 2004. **87**(12): p. 2195-2200.
 26. Gupta, D., et al., *Nanostructured biocomposite substrates by electrospinning and electrospraying for the mineralization of osteoblasts.* Biomaterials, 2009. **30**(11): p. 2085-94.
 27. Li, M., et al., *Electrospinning polyaniline-contained gelatin nanofibers for tissue engineering applications.* Biomaterials, 2006. **27**(13): p. 2705-15.

2.2. Biological Evaluation of Electrospun Cross-linked PLLA/gelatin Scaffolds

2.2.1 INTRODUCTION

In our previous work we investigated addition of gelatin to electrospinning PLLA solution as means to increase mineral deposition and distribution throughout the scaffolds, section 1 of this chapter [1]. The addition of the gelatin resulted in increases in mineral deposition, mineral distribution, and mechanical properties, but there was no difference in cellular proliferation compared to electrospun PLLA scaffolds alone.

Gelatin is natural molecule derived from denaturing collagen triple helical structure. As it is derived from collagen, it resembles collagen, but it eliminates high cost associated with use of collagen. It is very abundant and used in many industries, including food, pharmacy and cosmetics, making it biocompatible and commercially available at low cost [2-7]. All of these characteristic make it an attractive candidate for tissue engineering applications. However gelatin is water soluble and cannot retain 3D structures in aqueous environments, and as a result it is either cross-liked [4, 6, 7] or mixed with polymers to stabilize it for longer periods of time [4, 8]. Electrospun gelatin is commonly cross-linked in glutaraldehyde vapor, which is also a cross-linking method for electrospun collagen. The cross-linking by glutaraldehyde occurs between the carboxyl groups on the glutaraldehyde and the amine groups of the gelatin [7]. Gelatin has been successfully electrospun alone [2, 4, 6, 7] and in combination with natural proteins [4] and synthetic polymers [2, 3]. Li et al. have coated electrospun PCL with gelatin and mineralized it for 2 hours in 10x SBF and saw increased cellular proliferation over PCL scaffolds alone with MC3T3-E1 cells after 7 days in culture [9]. Gupta et al. reported increase in proliferation on poly (L-lactic acid)-co-poly (ϵ -caprolactone) (PLACL)/gelatin blend sprayed with hydroxyapatite over PLACL and PLACL/gel and TCP with human fetal osteoblasts after 15 days in culture [3]. Gu et al. reported increase in proliferation of WI-38 human embryonic fibroblast, lung derived, cultured on PLLA/gelatin electrospun scaffolds over PLLA scaffolds alone over period of 4 days [2].

In this study, we further investigated the effects of addition of gelatin to electrospun PLLA scaffolds on the proliferation, differentiation and mineral deposition of MC3T3-E1 cells. Electrospun PLLA/gelatin scaffolds were cross-linked in glutaraldehyde vapor for 2 hours, and

also mineralized by incubation in 10x SBF. We evaluated cellular proliferation, attachment, ALP production, and mineral production over the period of 4 weeks.

2.2.2. MATERIALS AND METHODS

2.2.2.1. Scaffold Fabrication by Electrospinning

PLLA (inherent viscosity =2.0 dl/g, Mw = 152,000) was purchased from Sigma Aldrich (St. Louis, MO, USA). PGA fibers were purchased from Concordia Medical (Warwick, RI, 02886). Dichloromethane (DCM) and dimethylformaldehyde (DMF) were purchased from Fisher Scientific (Pittsburgh, PA, USA). Gelatin, type A, from porcine skin was purchased from Sigma Aldrich (St. Louis, MO, USA). NaCl, KCl, CaCl₂·2H₂O, MgCl₂·6H₂O, NaHCO₃, and NaH₂PO₄ were purchased from Fisher Scientific (Pittsburgh, PA, USA).

The electrospinning solutions were prepared by dissolving PLLA to 7 % w/v in 75% DCM and 25% DMF. The gelatin/PLLA mixture was made by dissolving gelatin in 1ml deionized (DI) water and adding it to the 7% PLLA solution. Polymer solutions are made in 16 ml batches, and in order to make overall volume of gelatin/PLLA and PLLA solutions equal, 1ml of DCM was replaced with 1ml of gelatin solution. The amount of gelatin in solution was equal to 10 %, w/w of the amount of PLLA in the solution. As two solutions are not miscible, they were vortexed for 1 hr to mix before electrospinning.

The gel/PLLA was electrospun a rotating (~ 1100 RPM) 5 cm diameter mandrel for a total volume of 5ml with a working distance of 5 cm. The voltage applied was +18kV and -7kV. Negative voltage is utilized in the electrospinning process to help drive the jet toward the target or collecting mandrel. Gelatin in the scaffolds was cross-linked in the vapor of 2.5% glutaraldehyde for 2 hours.

2.2.2.2. Mineralization of Scaffolds

We have adopted a method previously developed and reported by Tas and Bhaduri [10] to prepare 10XSBF. A stock solution was made using NaCl, KCl, CaCl₂·2H₂O, MgCl₂·6H₂O, and NaH₂PO₄, and stored at room temperature. Prior to the mineralization process, NaHCO₃ was added while stirring vigorously, resulting in the following ion concentrations: Ca²⁺ 25 mM, HPO₄²⁻ 10 mM, Na⁺ 1.03 M, K⁺ 5 mM, Mg²⁺ 5mM, Cl⁻ 1.065M, and HCO₃⁻ 10mM . The

electrospun mats were incubated in 400 ml of 10XSBF in vacuum for two hours at room temperature. After being removed from 10X SBF, all the samples were rinsed in dI water to remove mineral not attached to scaffolds, and vacuum dried overnight.

2.2.2.3. Scaffold Characterization

Scaffold morphology, the presence of gelatin with or without cross-linking, mineral deposition and distribution on the scaffolds were imaged by scanning electron microscopy (SEM). All the samples were sputter coated with gold and palladium and imaged using an ESEM (Environmental Scanning Electron Microscope) (FEI Quanta 600 FEG) in high vacuum mode. Energy Dispersive Spectroscopy (EDS) analysis was performed using the Bruker EDX Silicon Drifter Detector on the ESEM to map presence of gelatin on the scaffolds.

2.2.2.4. Cell Study

2.2.2.4.1. Cellular Proliferation

Mouse pre-osteoblastic cells (MC3T3-E1, ATCC) were cultured in Alpha Minimum Essential Medium (α -MEM, Cellgro, Mediatech, Manassas, VA, USA) supplemented with 10% fetal bovine serum (FBS, Cellgro, Mediatech, Manassas, VA, USA) and 1% streptomycin/penicillin (Cellgro, Mediatech, Manassas, VA, USA). Scaffolds were cut into 15mm disks and secured into 24-well tissue culture polystyrene (TCP) plates using Silastic Medical Adhesive (Dow Corning, Midland, MI, USA). The samples were then sterilized in 70% ethanol for 30 minutes followed by exposure to UV light for 30 minutes. The scaffolds were then washed with PBS and soaked in cell culture medium overnight. Approximately 30,000 cells were seeded onto each scaffold and control (well plate without scaffold). The cells were allowed to attach for one hour before adding culture medium to a final volume of 1 ml. After the cells were seeded the media was supplemented with 3mM β -glycerophosphate and 10 μ g/ml of L-ascorbic acid. The media was changed every other day and the cultures were incubated at 37°C in a humidified atmosphere and 5% CO₂. Cells were cultured for a period of 28 days and data was collected on days 7, 14, 21, and 28.

Cell viability was measured using a Cell Titer 96TM Aqueous Solution Cell Proliferation Assay (MTS Assay) (Promega, Madison, WI, USA) on the following scaffolds PLLAgel (n=4),

PLLAGelCL (n=4), PLLAgelCL_MIN (n=4), and a control(TCP) (n=4). At each time point (7, 14, 21, and 28 days) the media was removed, then 300 µl of fresh media and 60 µl of the MTS solution were added to each well and incubated at 37°C with 5 % CO₂ for three hours. After incubation, 300 µl of the mixture was transferred to a 48-well plate and diluted 1:1 with 300µl of dI water. The plate was read at 490 nm using a SpectroMax M2 spectrophotometer (Sunnyvale, CA, USA).

2.2.2.4.2. Alkaline Phosphatase Activity

Alkaline phosphatase (ALP) activity was measured as an early marker of osteoblastic phenotype using an ALP substrate kit (Bio-Rad, Hercules, CA) on the following scaffolds PLLAgel (n=4), PLLAgelCL (n=4), PLLAgelCL_MIN (n=4), and a control (TCP) (n=4). At each time point, scaffolds were washed twice with sterile PBS and transferred to a new well. Cells were lysed with 1ml of 1% Triton X-100 solutions and then subjected to three freeze-thawing cycles at -80°C. All the cells lysates were stored at -80°C until the end of the study, when all the samples were thawed and assayed together. A 100µL of the sample was mixed with 400µL of substrate solution (mixture of p-nitrophenylphosphate, diethanolamine buffer, and dI water) and incubated at 37°C for 30 minutes. The reaction was stopped with 500µL of 0.4N NaOH, and the resulting solution was read at 405nm using a SpectroMax M2 spectrophotometer (Sunnyvale, CA, USA). The amount of ALP was normalized to total protein content from the same cell lysates, which was determined using BCA protein assay (Thermo Scientific, Rockford, IL).

2.2.2.4.3. Alizarin Red and Fluorescence Stain

Mineral deposition and distribution was characterized by Alizarin red staining. At each time point, the scaffolds were washed with PBS and transferred into new well plates. The scaffolds were then fixed in 70% ethanol for 1hr at 4°C, and stained with 40 mM Alizarin red solution for 10 min. The scaffolds were then washed with dI water five times and air dried. The sections of the scaffolds were imaged using a stereoscope. After the images were taken, the scaffolds were placed in 1ml of 10% w/v of cetylpyridinium chloride (CPC) in 10 mM Na₂HPO₄ and incubated for 15 mins for the stain to dissolve. The absorbances were read at 562 nm on SpectroMax M2 spectrophotometer (Sunnyvale, CA, USA).

Cellular attachment on the scaffolds was qualitatively observed by fluorescence staining. Scaffolds were fixed in 3.7% paraformaldehyde and 0.5% Triton X-100 at room temperatures and stained with phalloidin and DAPI. The scaffolds were imaged using a fluorescence microscope (Leica Microsystems, Bannockburn, IL, USA).

2.2.2.5. Statistical Analysis

Statistical analysis was performed using JMP 9 software. All the data was analyzed using one way analysis of variance (ANOVA) with Tukey's test to determine statistically significant differences between groups. Statistical significance was tested at $p < 0.05$.

2.2.3. RESULTS

2.3.1. Scaffold Characterization

Scaffold fiber morphology before and after cross-linking were imaged using ESEM. Images revealed that the fibers morphology and porosity of the scaffolds was not affected by the cross-linking process. Some webbing was still present, but the fibers round morphology was not affected (Figure 2.2.1).

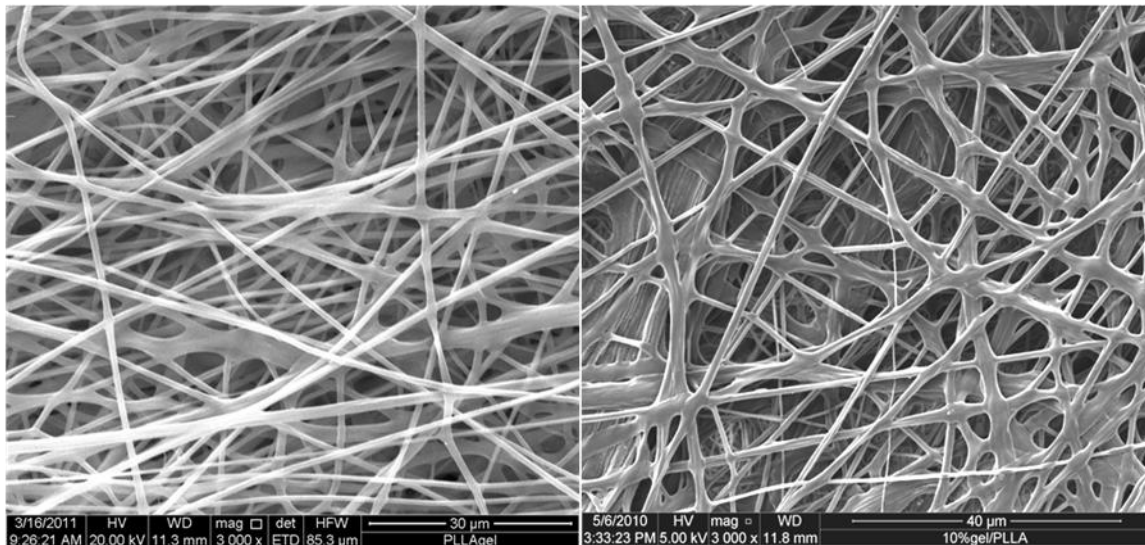


Figure 2.2.1. SEM images of electrospun PLLA gelatin mixtures, not cross-linked (left) and cross-linked (right)

2.2.3.2. Cellular Proliferation

Proliferation of the M3T3-E1 cells on the scaffolds was quantified using MTS assay on days 7, 14, 21, and 28 with absorbances at 490 nm are shown in Figure 2.2.2. Absorbances for all the scaffolds were significantly lower than controls for every time point. On day 7 and day 21 PLLAgel and PLLAgelCL scaffolds had significantly higher absorbances than PLLAgelCL_MIN scaffolds. On day 14, PLLAgel scaffolds and on day 28, PLLAgelCL scaffolds had significantly higher absorbances than PLLAgelCL_MIN scaffolds. Every group of scaffolds had experienced significant increase in absorbances over the 28 day period: PLLAgel from day 7 to day 14, PLLAgelCL from day 7 to day 14 to day 21, PLLAgelCL_MIN from day 7 to day 14, and Control from day 7 to day 14. Surface fluorescence images of scaffolds (Figure 2.2.3), stained for actin (green) and nuclei (blue), show cellular attachment and dispersion of the cells on the surfaces of all three groups of scaffolds on day 28 of cell study.

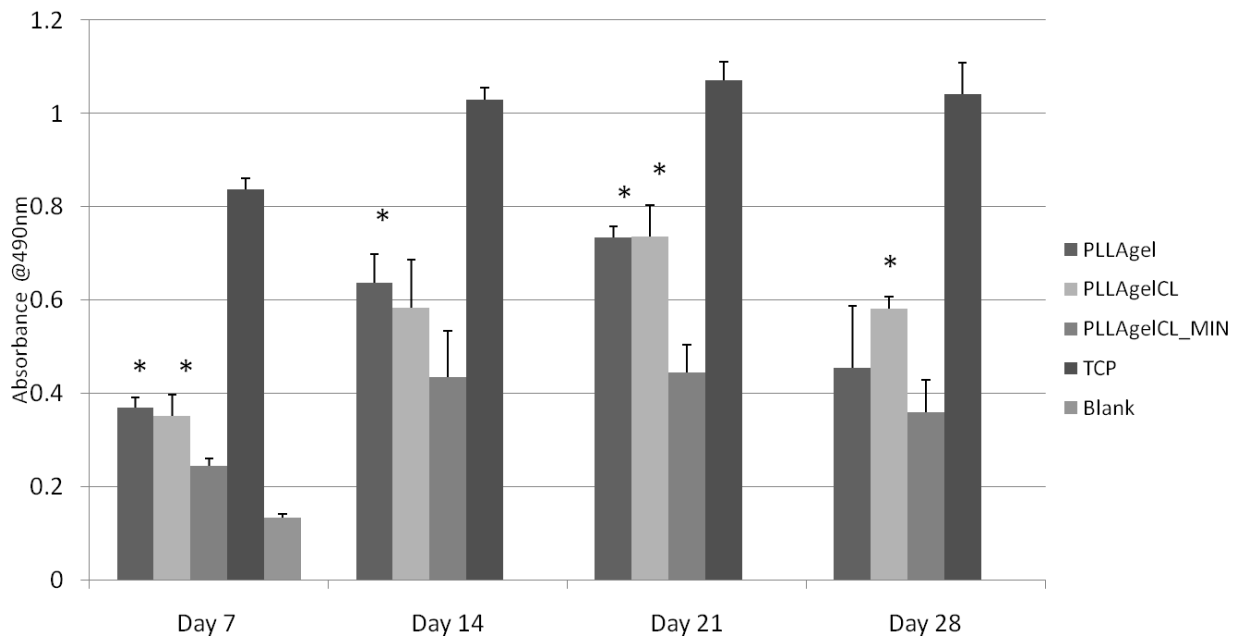


Figure 2.2.2. MTS assay absorbances of cell viability. (*) – Significantly different from PLLAgelCL_MIN ($p < 0.05$)

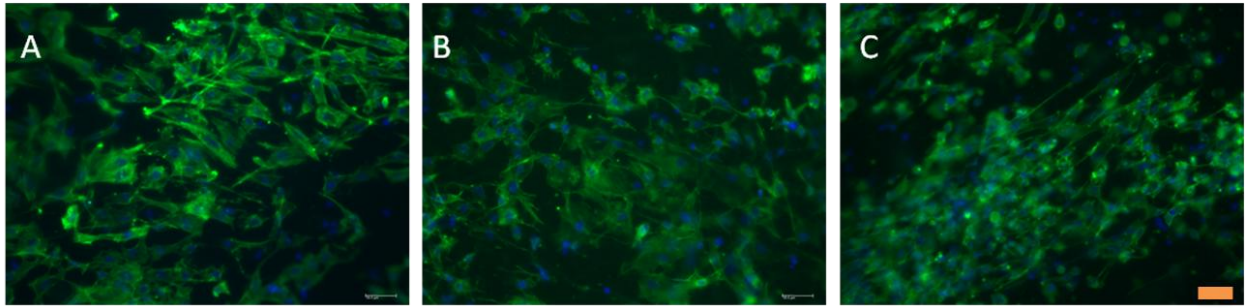


Figure 2.2.3. Fluorescent stains of actin (green) and nuclei (blue) on scaffolds after 28 days in culture. **A)** PLLAgel, **B)** PLLAgelCL and **C)** PLLAgelCL_MIN. Scale bar **50 μ m**.

2.2.3.3. Alkaline Phosphatase Activity

Alkaline phosphatase activity was measured using an ALP substrate kit and all the values are expressed as fractions of total cell protein in Figure 2.2.4. On day 21, PLLAgel and PLLAgelCL scaffolds have significantly higher fraction of ALP expression than PLLAgelCL_MIN scaffolds. On day 28, PLLAgelCL_MIN have significantly lower expression of ALP than remaining three groups. For PLLAgelCL and PLLAgelCL_MIN scaffolds there was no significant change in fraction of ALP expressed over the period of 4 weeks. Scaffolds PLLAgel showed a significant change in ALP expression for every time point, from day 7 to day 14 to day 21 to day 28. Significant change in ALP expression over 4 weeks was also seen in Control group, from day 7 to day 14 to day 21.

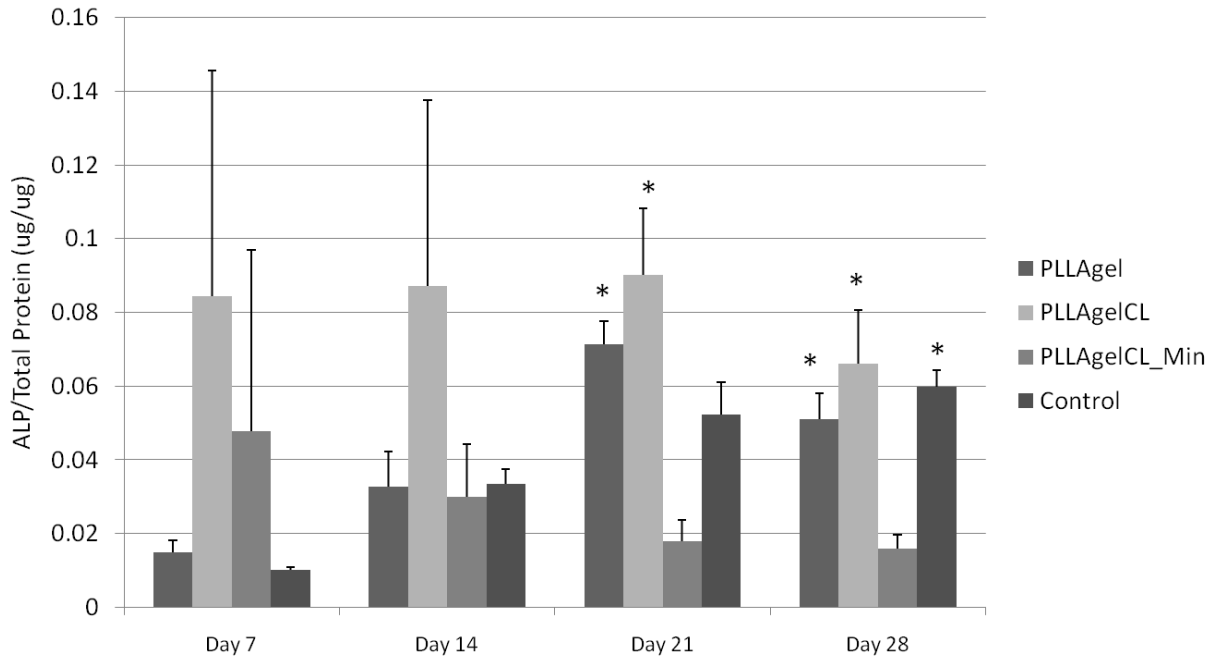


Figure 2.2.4. ALP expression as a function of total protein. (*) –Significantly different from PLLAgelCL_MIN (p<0.05)

To normalize the ALP expression, total protein was also measured and is shown in Figure 2.2.5. At every time point, Control groups have a significantly higher protein concentration than the scaffolds. On day 7, PLLAgel scaffolds have significantly higher protein concentration than PLLAgelCL_MIN scaffolds. Significantly higher protein concentration was found on PLLAgelCL scaffolds than on PLLAgelCL_MIN scaffolds on day 28. All groups of scaffolds exhibited significant increase in the total protein over the 4 week period: scaffolds PLLAgel, PLLAgelCL, and PLLAgelCL_MIN from day 21 to day 28, while control group exhibited significant increase at every time point.

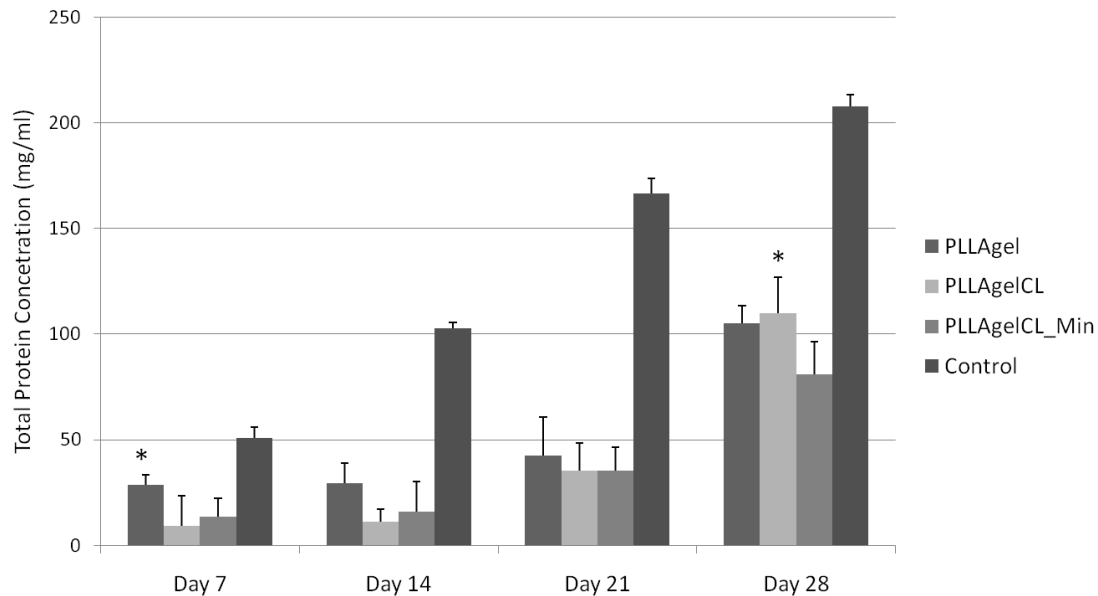


Figure 2.2.5. Average total protein concentration on the scaffolds over the 4 week period. (*)Significantly different from PLLAgelCL_MIN ($p < 0.05$)

2.2.3.4. Alizarin Red and Fluorescence Stain

Mineral deposition and distribution was observed by Alizarin red staining at each time point (Figure 2.2.6). On day 7, little to no mineral can be seen on scaffolds that are not cross-linked; slightly more can be seen on the cross-linked scaffolds, while premineralized scaffolds have the most mineral. By day 28, mineral staining can be seen on every scaffold, but premineralized scaffolds have the most mineral present on the surface, indicated by deep dark red stains.

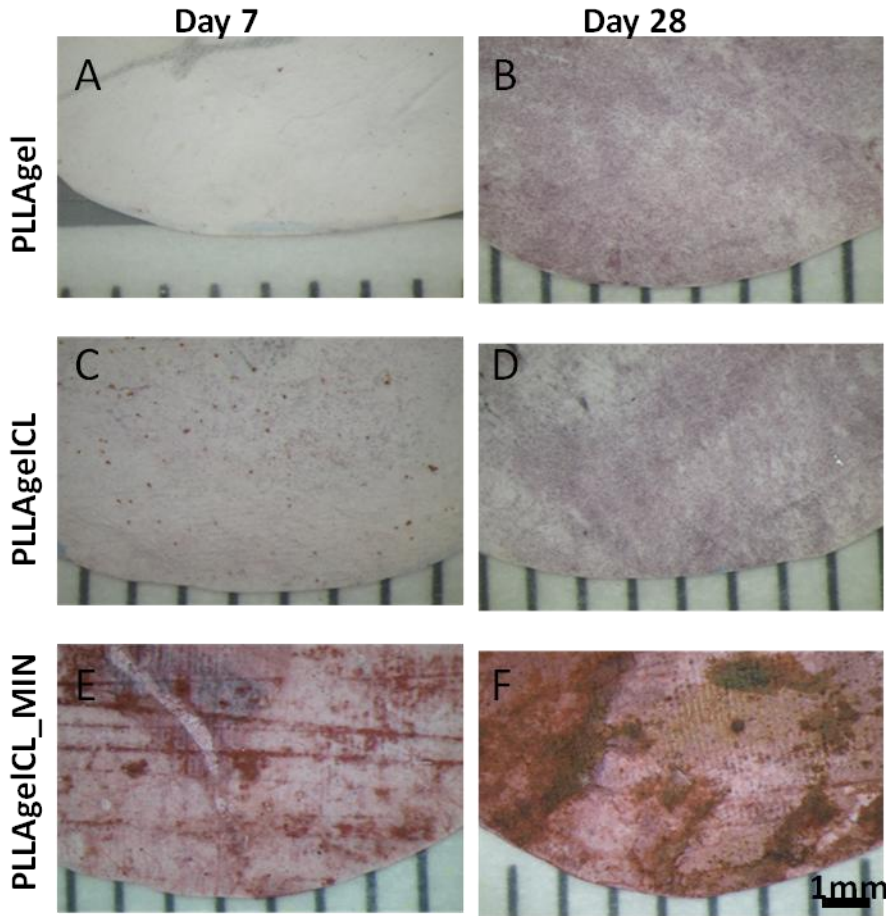


Figure 2.2.6. Alizarin red stains of the following scaffolds PLLAgel (**A, B**), PLLAgelCL(**C, D**) and PLLAgelCL_MIN(**E, F**). Images were taken on day 7 (**A, C, E**) and day 28 (**B, D, F**).

Mineral stains were quantified by dissolving in 10% CPC and reading absorbances at 562nm, averages can be seen in Figure 2.2.7. At every time point, PLLAgelCL_MIN scaffolds are significantly higher than for any other scaffold group. There were no significant differences between other the two groups. Scaffolds that were not cross-lined exhibited significant increase in stain absorbance from day 7 to day 14. Scaffolds that were cross-linked exhibited increase in stain absorbance from day 7 to day 21. Mineralized scaffolds showed no significant change in stain absorbances over the period of 4 weeks.

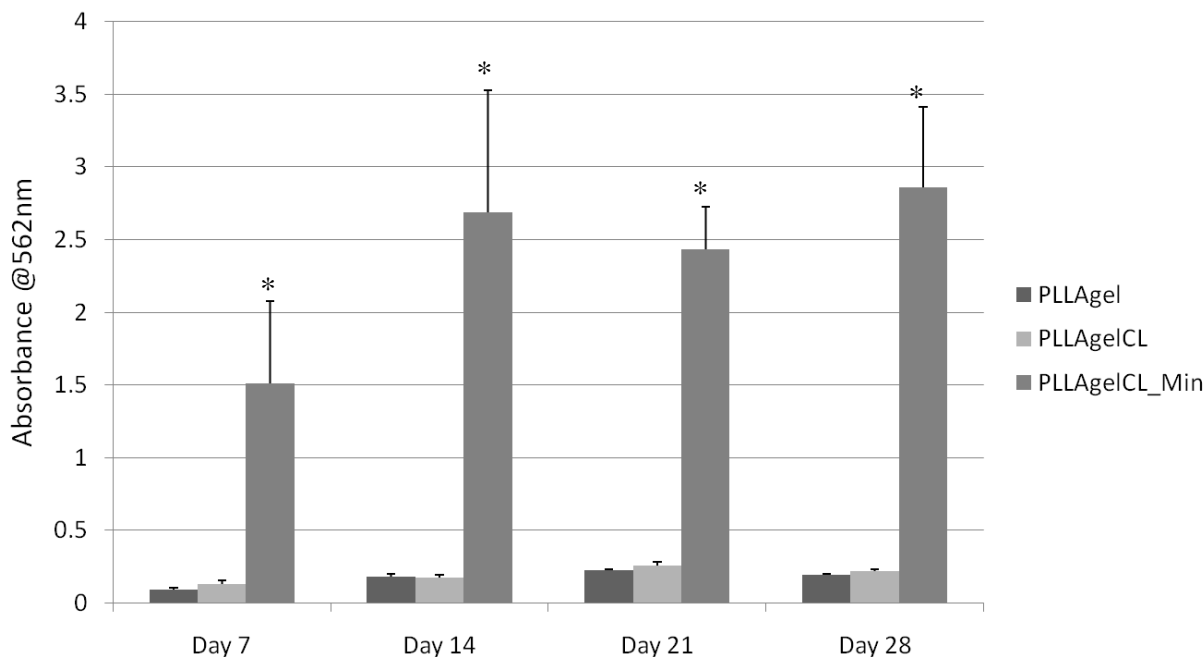


Figure 2.2.7. Alizarin red stain absorbances over the period of 4 weeks. (*) –Significantly different from PLLAgel and PLLAgelCL($p < 0.05$)

2.2.4. DISCUSSION

In this study, we were able to successfully electrospin PLLA /gelatin mixture solutions, and cross-link them using incubation in 2.5% glutaraldehyde vapor. SEM images revealed that the fiber morphology was not affected by the cross-linking process as can be seen in Figure 2.2.1. Glutaraldehyde is commonly used cross-linking agent for electrospun collagen and gelatin structures [3, 4, 6, 7]. Some webbing of the fibers can be observed due to the water in the cross-linking solution, but the fiber morphology is still preserved.

Proliferation of the MC3T3-E1 cells was also evaluated on following electrospun scaffolds: PLLAgel not cross-linked, PLLAgel cross-linked, PLLAgel cross-linked and mineralized, and control (TCP). There were no significant differences between uncross-linked and cross-linked PLLAgel scaffolds, indicating that the cross-linking process did not make scaffolds more cytotoxic (which was also observed in similar studies where glutaraldehyde was also used as cross-linking agent for gelatin [6, 7]). However, non mineralized scaffolds had significantly higher absorbances than mineralized scaffolds at every time point, both types on days 7 and 21, and not cross-linked on day 24 and cross-linked on day 28. A similar trend was

also observed in previous study [1], and is thought to be due to dissolution of mineral on the scaffolds. The mineral present on the scaffolds was identified as brushite, which is a soluble calcium phosphate, and over time some of the mineral could be lost [11]. This dissolution of mineral can result in loss of cells that were bound to mineral on the surface. While there were some differences between scaffolds, all the scaffolds supported cellular attachment and proliferation, as every group of scaffolds had significant increase in absorbance over the period of 4 weeks. Surface fluorescence images of scaffolds, stained for actin (green) and nuclei (blue), show cellular attachment and dispersion of the cells on the surfaces of all three groups of scaffolds on day 28 of cell study. Total protein concentrations in Figure 2.2.5 showed different trends than MTS assay, which measures cellular activity. MTS graphs (Figure 2.2.2) show plateau by 21 and start decreasing by day 28, while total protein graph shows continuous increase of protein concentration up to day 28. The difference seen between MTS and BCA protein assay are most likely due to differences in what they measure. MTS measures cellular metabolic activity, which can change over the course of the study. Total amount of protein can change as cells keep dividing or their activity changes.

Alkaline phosphatase activity was measured and expressed as the fraction of total protein for the corresponding scaffolds group. Only significant differences were observed compared to PLLAgelCL_MIN scaffolds, on day 21 PLLAgel and PLLAgelCL and on day 28 all three groups of scaffolds were significantly higher than PLLAgelCL_MIN. No significant changes in ALP expressions were observed in cross-linked and cross-linked mineralized scaffolds over the period of 28 days. This could be due to the fact that the subclone of the MC3T3-E1 cells that was used, subclone 4, did not test positive for ALP expression [12]. The subclone 4 cells, used in our study, did express collagen I, osteocalcin, bone sialoprotein, and successfully produced mineral, but were negative for ALP gene expression [12]. In the future, more extensive testing should be utilized to confirm cellular differentiation, for an example looking at osteocalcin or osteopontin expression.

Alizarin red staining was also utilized to assess mineral distribution and deposition over the course of the 4 week study. At the beginning very little to none staining can be seen on the non mineralized scaffolds, while mineralized scaffolds show light red stain. At the end of the study, red stains can be seen on every scaffolds group, indicating that the cells produced mineral.

This was also found in the absorbances of the dissolved alizarin red stains, where absorbances for non-mineralized scaffolds increased significantly over the period of the study. No significant changes were found in absorbances of the mineralized scaffolds, although an increasing trend can be seen. This may be due to a high outlier value on day 14. However, significant changes in the intensity of the stain color can be seen from day 7 to day 28, indicating more mineral was produced by the cells.

2.2.5. CONCLUSION

In this study, we were able to successfully electrospin PLLA /gelatin mixture solutions, and cross-link them using incubation in 2.5% glutaraldehyde vapor for 2 hours. SEM images revealed that the fiber morphology was not affected by the cross-linking process. Cellular attachment, proliferation, and mineral deposition were evaluated on following electrospun scaffolds: PLLAgel not cross-linked, PLLAgel cross-linked, PLLAgel cross-linked and mineralized, and TCP control. Cross-linking process did not have cytotoxic effects on the cellular proliferation. After 28 days in cell culture, significant increase in presence of the mineral is seen of the surface of the scaffolds, as stained by alizarin red stain, indicating that the cells produced the mineral deposited. All the scaffolds supported cellular attachment and proliferation, as every group of scaffolds had significant increase in absorbance over the period of 4 weeks. Surface fluorescence images of scaffolds show cellular attachment and dispersion of the cells on the surfaces of all three groups of scaffolds on day 28 of cell study.

2.2.6. REFERENCES

1. Andric, T., L.D. Wright, and J.W. Freeman, *Rapid Mineralization of Electrospun Scaffolds for Bone Tissue Engineering*. J Biomater Sci Polym Ed.
2. Gu, S.Y., et al., *Electrospinning of gelatin and gelatin/poly(L-lactide) blend and its characteristics for wound dressing*. Materials Science & Engineering C-Materials for Biological Applications, 2009. **29**(6): p. 1822-1828.
3. Gupta, D., et al., *Nanostructured biocomposite substrates by electrospinning and electrospraying for the mineralization of osteoblasts*. Biomaterials, 2009. **30**(11): p. 2085-94.
4. Heydarkhan-Hagvall, S., et al., *Three-dimensional electrospun ECM-based hybrid scaffolds for cardiovascular tissue engineering*. Biomaterials, 2008. **29**(19): p. 2907-14.
5. Sell, S.A., et al., *Electrospinning of collagen/biopolymers for regenerative medicine and cardiovascular tissue engineering*. Adv Drug Deliv Rev, 2009. **61**(12): p. 1007-19.
6. Sisson, K., et al., *Fiber diameters control osteoblastic cell migration and differentiation in electrospun gelatin*. J Biomed Mater Res A. **94**(4): p. 1312-20.
7. Sisson, K., et al., *Evaluation of cross-linking methods for electrospun gelatin on cell growth and viability*. Biomacromolecules, 2009. **10**(7): p. 1675-80.
8. Zhang, Y., et al., *Electrospinning of gelatin fibers and gelatin/PCL composite fibrous scaffolds*. J Biomed Mater Res B Appl Biomater, 2005. **72**(1): p. 156-65.
9. Li, X., et al., *Coating electrospun poly(epsilon-caprolactone) fibers with gelatin and calcium phosphate and their use as biomimetic scaffolds for bone tissue engineering*. Langmuir, 2008. **24**(24): p. 14145-50.
10. Tas, A.C. and S.B. Bhaduri, *Rapid coating of Ti6Al4V at room temperature with a calcium phosphate solution similar to 10x simulated body fluid*. Journal of Materials Research, 2004. **19**(9): p. 2742-2749.
11. Vallet-Regi, M., *Revisiting ceramics for medical applications*. Dalton Trans, 2006(44): p. 5211-20.
12. Wang, D., et al., *Isolation and characterization of MC3T3-E1 preosteoblast subclones with distinct in vitro and in vivo differentiation/mineralization potential*. J Bone Miner Res, 1999. **14**(6): p. 893-903.

Chapter 3

Fabrication and Characterization of Three Dimensional Electrospun Scaffolds for Bone Tissue Engineering

Tea Andric, Lee D. Wright, Joseph W. Freeman
Journal of Biomedical Materials: A (accepted)

3.1. ABSTRACT

When traumatic injury, tumor removal, or disease results in significant bone loss, reconstructive surgery is required. Bone grafts are used in orthopaedic reconstructive procedures to provide mechanical support and promote bone regeneration. In this study, we applied a heat sintering technique to fabricate 3D electrospun scaffolds that were used to evaluate effects of mineralization and fiber orientation on scaffold strength. We electrospun PLLA/gelatin scaffolds with a layer of PDLA and heat sintered them into three dimensional cylindrical scaffolds. Scaffolds were mineralized by incubation in 10X simulated body fluid for 6h, 24h, and 48 h to evaluate the effect of mineralization on scaffolds compressive mechanical properties. The effects of heat sintering hydroxyapatite (HA) microparticles directly to the scaffolds on mineral deposition, distribution and mechanical properties of the scaffolds were also evaluated. We found that orientation of the fibers had little effect on the compressive mechanical properties of the scaffolds. However, increasing the mineralization times resulted in an increase in compressive mechanical properties. Also, the direct addition of HA microparticles had no effect on the scaffold mechanical properties, but had a significant effect on the mineral deposition on PLLA/gelatin scaffolds.

3.2. INTRODUCTION

When traumatic injury, tumor removal, or disease, results in significant bone loss, reconstructive surgery is required. Bone grafts are used in these orthopaedic reconstructive procedures to provide mechanical support and promote bone regeneration. It is estimated that 600,000 of bone grafting procedures are performed annually, making bone one of the most transplanted tissues, second only to blood [1]. The current treatment or “gold standard” for bone grafting procedures is an autograft, autologous bone tissue harvested from the patient. Although

autografts have very high success rates, they do have drawbacks, namely donor site morbidity and limited supply. Incidence of donor site morbidity has been reported to be as high as 44% [2]. In cases of bone disease, the amount of tissue that can be harvested can be very limited or even nonexistent. The current alternatives to autografts are allografts. Although the use of allografts eliminates the potential drawbacks of the autografts, they do have limitations of their own. Whenever donor tissue is transplanted, there is a chance of disease transmission. In addition, the harsh sterilization techniques also denature the bone matrix and deteriorate its mechanical properties. Recent reports on long term use of allografts *in vivo* report that they exhibit a decrease in mechanical strength and have failure rates of 30-60 % over a period of ten years [3].

The field of tissue engineering has emerged with a goal to bridge this gap between the need and lack of ideal bone graft. Some of the necessary properties that should be considered in scaffold design are porosity, degradation rate, and mechanical properties. Porosity and pore interconnectivity of the scaffolds is essential to allow infiltration of the cells and new tissue growth. The degradation rate of the scaffolds should be comparable to the tissue growth rate, as the implant needs to maintain mechanical properties initially to bear loads, but over time the load bearing should transfer onto the newly forming tissue. The mechanical properties of the scaffold should match the properties of the surrounding tissue. Additional attributes that should be considered when discussing bone grafts are: *biocompatibility* – performing with an appropriate host response [4]; *osteoconductivity* - allowing and promoting cell attachment, proliferation, and migration throughout the scaffold; *osteoinductivity* – possessing necessary bioactive molecules that can induce differentiation of progenitor cells toward osteoblastic lineage; *osteoogenicity* – allowing osteobalsts that are on site to produce minerals and calcify the surrounding matrix [1, 5].

Various scaffold fabrication techniques have been investigated for creating three dimensional (3D) porous composite polymeric scaffolds for bone tissue engineering [5-7]. Thermally induced phase separation is used to create foam scaffolds by freezing polymer solution into molds, and sublimating solvent out at low temperatures leaving an interconnected porous network behind [6, 8-10]. Solvent casting with particulate leaching involves the use of porogens (salt sugar or paraffin particles) that are incorporated into the polymer solution and then poured into 3D mold. Once the polymer has set, the solvent evaporates and the porogen is

leached out, leaving a porous network behind. While the pore size can be controlled by controlling the size of the porogen particles, porogen entrapped and closed off pores can be problematic [6, 7].

Sintered microsphere scaffolds are produced by packing polymeric microspheres into 3D molds, and heat sintered above glass transition temperature. Due to the shape of the microspheres, the interconnected pore network is created in-between the microspheres, and pore size can be controlled by controlling the microsphere size. These scaffolds have been reported to have mechanical properties in the range of trabecular bone, with incorporation of either amorphous calcium phosphates or hydroxyapatite (HA) nanoparticles [6, 7, 11-13].

Electrospinning is a scaffold fabrication technique that has recently gained interest in applications for bone tissue engineering [4, 6-10]. Electrospun scaffolds are characterized by high surface area, high porosities, and interconnected pore networks. This makes electrospun scaffolds desirable for tissue engineering applications as the nano- and microfiber surface morphologies mimic the native extracellular matrix [14, 15]. Various techniques have been investigated to create fiber alignment in electrospun mats to improve mechanical properties and better mimic native tissue, and they include electrospinning onto rotating mandrel and parallel plate deposition. While use of the rotating mandrel allows creation of thicker larger electrospun mats, the degree of fiber alignment is far from perfect. In parallel plate set up, fibers are collected on two conductive electrode strips separated by a gap. Almost perfect alignment of fibers collected between two electrodes can be achieved, but the mats are very small (due to small gap region) and thin [16].

Various natural and synthetic materials have been successfully electrospun into scaffolds including, poly(ϵ -caprolactone) (PCL) [17, 18], poly(L-lactide) (PLLA) [19, 20], poly(D,L-lactide) (PDLLA) [21], poly(lactide-co-glycolide) (PLGA) [22], collagen type I [15], gelatin type B [23-27]. Various mixtures of synthetic polymers with either natural polymer like gelatin or collagen [19, 24, 28, 29] or inorganic hydroxyapatite (HA) [20, 24, 29, 30], or both have been investigated to increase cellular attachment, proliferation and differentiation of cells.

Scaffolds produced by electrospinning technique are two dimensional meshes with thickness up to a couple hundred microns. As a result, very little to no characterization has been done to determine the compressive mechanical properties of these scaffolds. Our group has

developed and characterized a sintering technique to fabricate 3D electrospun scaffolds from electrospun sheets[31]. Briefly, a layer of PDLA was electrospun onto an electrospun PLLA mat to serve as a bonding layer at higher temperatures to bind multiple layers together into 3D scaffolds. This technique has been utilized in this study to fabricate 3D PLLA/gelatin with PDLA layer electrospun scaffolds and the effects of mineralization and fiber orientation on compressive mechanical properties were evaluated.

3.3. MATERIALS AND METHODS

3.3.1. *Fabrication of Scaffolds by Electrospinning*

PLLA (inherent viscosity =2.0 dl/g, Mw = 152,000) was purchased from Sigma Aldrich (St. Louis, MO, USA). PDLA (inherent viscosity 0.6-0.8 dL/g) was purchased from SurModics Pharmaceuticals (Birmingham, AL, USA). Dichloromethane (DCM), tetrahydrofuran (THF), and dimethylformaldehyde (DMF) were purchased from Fisher Scientific (Pittsburgh, PA, USA). Gelatin, type A, from porcine skin was purchased from Sigma Aldrich (St. Louis, MO, USA). NaCl, KCl, CaCl 2H₂O, MgCl₂ 6H₂O, NaHCO₃, and NaH₂PO₄ were purchased from Fisher Scientific (Pittsburgh, PA, USA).

The electrospinning solutions were prepared by dissolving PLLA to 7 % w/v in 75% DCM and 25% DMF, and dissolving PDLA to 22 % w/v in 75% THF and 25%DMF. The PLLA/gelatin mixture was made by dissolving gelatin in 1ml deionized (dI) water and adding it to the 7% PLLA solution. The amount of gelatin in solution is equal to 10 %, w/w of the amount of PLLA in the solution. As two solutions are not miscible, they were vortexed for 1 hr to mix before electrospinning. Polymer solutions were made in 16 ml batches and to make overall volume of gelatin/PLLA and PLLA solutions equal, 1ml of DCM is replaced with 1ml of gelatin.

First, the PDLA solution was loaded into a 5 ml plastic syringe with an 18-gauge needle, and extruded at a rate of 5 mL/h. PDLA was electrospun on a rotating (~ 2000 RPM) 5 cm diameter mandrel for a total volume of 1ml, at a distance of 15cm with voltages of +12kV and -5kV applied. The gelatin/PLLA was then electrospun directly onto the PDLA layer with a working distance of 5 cm. The voltages applied were +18kV and -7kV. The negative voltage is utilized in the electrospinning process to help drive the jet toward the collecting mandrel. For scaffolds that were used for heat sintering HA, an additional layer of 1ml PDLA was electrospun

on top of gelatin/PLLA layer, with idea that one layer or PDLA is used for heat sintering HA and the other for sintering into 3D scaffolds. Gelatin in all the scaffolds was cross-linked in vapor of 2.5% glutaraldehyde for 2 hours.

3.3.2. Heat Sintering

To fabricate three dimensional electrospun scaffolds, we will be utilizing heat sintering method previously reported by our group [31]. For heat sintering process, the electrospun mats were cut into 1cm wide strips, and rolled around 24-guge blunt needle into cylinders with 5 mm diameter. The cylinders were sintered in the oven at 54°C for 45 min.

3.3.3. Variation of the Angles

The effect of fiber alignment and orientation on mechanical properties of electrospun scaffolds in compression was investigated. Electrospun scaffolds were cut into 1cm wide strips at various angles (0°, 15°, 30°, 45°, and 90°), with 0° being vertical orientation of the fibers and 90° being horizontal orientation of the fibers (Figure 3.1). The strips were then rolled and sintered into 10mm by 5mm cylinders as described above, and tested in compression under physiological conditions (PBS pH7.4 at 37°C) until failure (n=6).

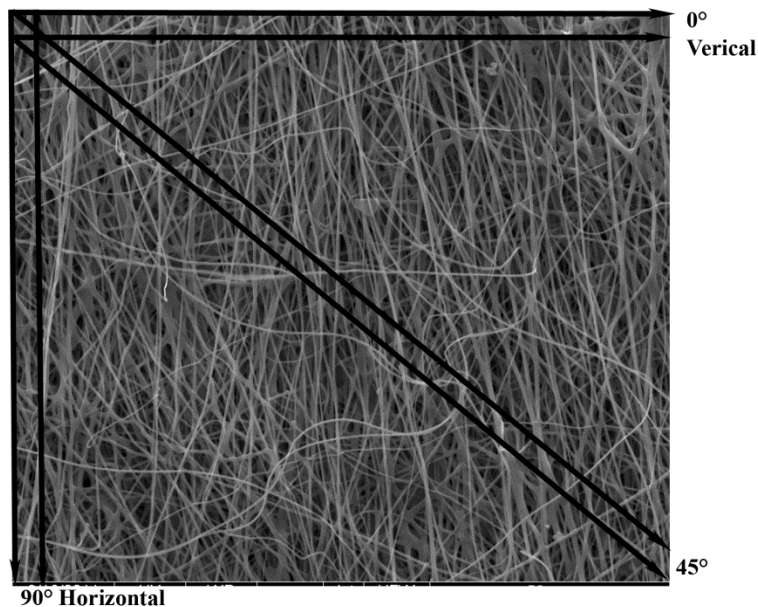


Figure 3.1. Schematic representation of cutting 1 cm strips at angles: 0°, 45°, and 90 °

3.3.4. Addition of Hydroxyapatite

Hydroxyapatite (HA) microparticles (10-20 μ m) were added by heat sintering to electrospun scaffolds to investigate potential effects on overall increase in mineralization and increase in mechanical properties. Amount of HA was determined as weight percentage of the weight of the entire electrospun mat. Two different amounts of HA microparticles were investigated, 50% or 100% w/w of the entire electrospun mat. Scaffolds that were used for HA sintering had 2 layers of PDLA, 1ml of PDLA on the bottom and 1ml of PDLA on the top of the PLLA/gelatin layer. HA was spread on one side of the mat and heat sintered for 45 min at 54°C. Afterwards, the mats were cut into 1cm strips as described above and heat sintered into cylinders for further mineralization and testing.

3.3.5. *Mineralization of the Scaffolds*

All the scaffolds were mineralized using a previously reported method by incubation in 10X SBF [32]. Briefly, a stock solution was made using NaCl, KCl, CaCl 2H₂O, MgCl₂ 6H₂O, and NaH₂PO₄, and stored at room temperature. Prior to the mineralization process, NaHCO₃ was added while stirring vigorously, resulting in the following ion concentrations: Ca²⁺ 25 mM, HPO₄²⁻ 10 mM, Na⁺ 1.03 M, K⁺ 5 mM, Mg²⁺ 5mM, Cl⁻ 1.065M, and HCO₃⁻ 10mM . The electrospun scaffolds were incubated in 300 ml of 10XSBF for various times at room temperature, with mineralizing solution replaced every 2 hours. After being removed from 10X SBF , all the samples were rinsed in dI water to remove mineral not attached to scaffolds, and vacuum dried overnight.

3.3.6. *Scaffold Characterization*

Scaffold morphology, HA microparticles, and mineral deposition and distribution on the scaffolds were imaged by scanning electron microscopy (SEM). All the samples were sputter coated with gold and palladium and imaged using an ESEM (Environmental Scanning Electron Microscope) (FEI Quanta 600 FEG) in high vacuum mode.

3.3.7. *Mechanical Properties*

The scaffolds were mechanically tested in compression using an Instron 5869 with Bioplus Bath (Norwood, MA, USA). The tests were performed in phosphate buffered saline (PBS) (pH= 7.4) at 37°C. The scaffolds were fabricated into 10mm high cylinders with 5mm

diameter (2:1 height to diameter ratio) and tested in compression (n=6) until failure with uniform strain rate of 1mm/min (10% stain/min). The data was analyzed to determine yield stress and elastic modulus.

3.3.8. *Mineral Ash Weights*

Samples were subjected to high temperatures to burn off the polymer and determine the mineral ash weight percent. After the initial weight of the samples was recorded, the samples were placed in ceramic crucibles, and then placed into a high temperature furnace (Model No. FD1535M, Fisher Scientific, Pittsburgh, PA, USA) at 700°C for 24 hours. After cooling down, the mineral ash weight was recorded and the average mineral percent deposition calculated as ratio of mineral ash weight to samples original weight. Each sample was placed in separate crucible, and three samples per group were tested (n=3).

3.3.9. *Alizarin Red Stains*

Mineral deposition and distribution was characterized by the Alizarin red stain. At each time point, the scaffolds were washed with PBS and transferred into new well plates. The scaffolds were then fixed in 70% ethanol for 1hr at 4°C, and stained with 40 mM Alizarin red solution for 10 min. The scaffolds were then washed with dI water five times, placed into cryomolds, imbedded in OCT imbedding medium, and frozen at -20°C. The scaffolds were cut into 200µm section using a Cryostat HM 550 (Thermo Scientific Microm, Walldorf, Germany), and imaged using stereoscope.

3.3.10. *Statistical Analysis*

Statistical analysis was performed using JMP 9 software. All the data was analyzed using one way analysis of variance (ANOVA) with Tukey's test to determine statistically significant differences between groups. Statistical significance was tested at $p < 0.05$.

3.4. RESULTS

We were able to successfully create three dimensional heat sintered scaffolds from electrospun materials. The resulting scaffolds were in the shape of the cylinders with 2:1 height

to width ratio, with 5mm diameter and 10mm height. The scaffolds were used to investigate the effect of fiber orientation on the mechanical properties in compression.

3.4.1. Variation of the Angles

The effect of fiber alignment and orientation on compressive mechanical properties of scaffolds in compression can be seen in Figure 3.2. The alignment of the fibers that were electrospun can be seen in Figure 2A. No noticeable trends were observed as the angle of the orientation of the fibers was changed. Scaffolds with vertical orientation (0°) of the fibers had significantly higher compressive yield stress than scaffolds with fiber orientation at 45° . The same scaffolds, 45° orientation had significantly lower compressive modulus than scaffolds at 30° fiber orientation. As there were no differences between vertical and 30° orientation scaffolds, vertical orientation was chosen for continuing studies.

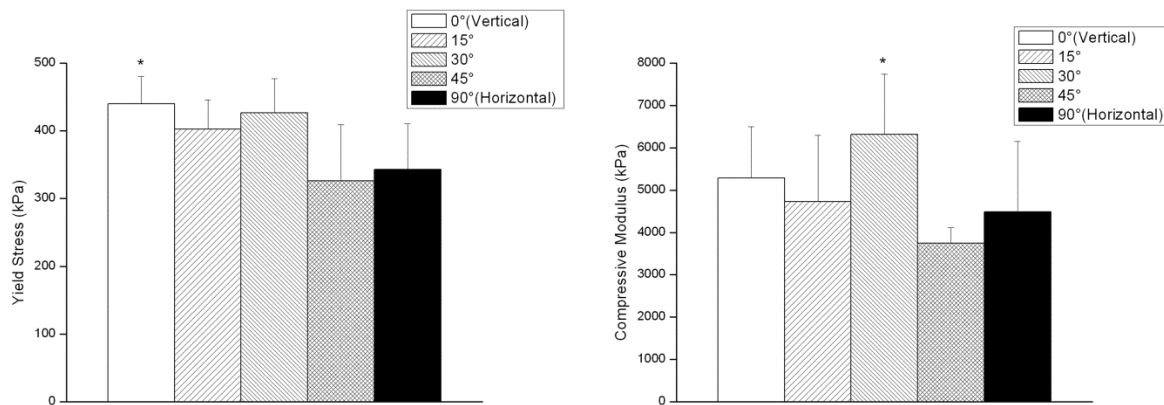


Figure 3.2. Effects of fiber alignment on compressive mechanical properties of the scaffolds. (*) - Statistically different from 45° ($p < 0.05$)

3.4.2. Addition of Hydroxyapatite and Mineralization

The hydroxyapatite microparticles were sintered to the surface of the electrospun scaffolds and can be seen in Figure 3.2. There were no differences in the amount of HA microparticles present between 50wt% and 100wt%, but the particles were distributed evenly on the surfaces.

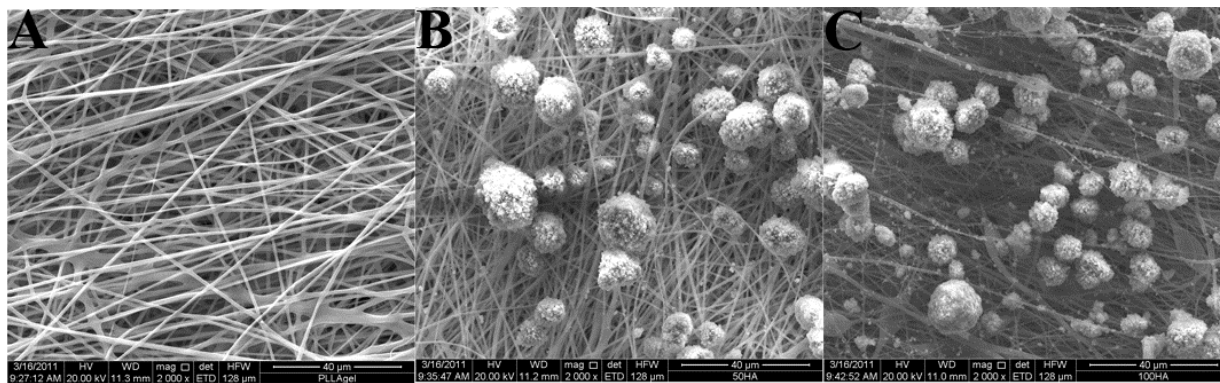


Figure 3.3. SEM images of electrospun PLLAgelatin cross-linked scaffolds (**A**) and scaffolds with hydroxyapatite (HA) microparticles on the surface (**B, C**). No difference is seen between 50wt% HA (**B**) and 100wt% HA (**C**). Scale bar 40 μ m

Mineral formation on the scaffolds was also qualitatively observed using SEM and can be seen in Figure 3.4. After 6 hour of mineralization (A, D, and F), fiber morphology of the electrospun scaffolds is still preserved, but some large crystals can be seen on the surface. However, as the mineralization time is increased to 24 hours (B, E, and G), the surfaces of the scaffolds become completely covered in calcium phosphate crystals. Some fiber morphology can be seen on the 100wt% HA scaffolds (G), but it still dominated by large crystals. After 48 hours of mineralization (C and H), surface of the scaffolds are covered in calcium phosphate crystals, and no fiber morphology is visible, and there are no differences in appearances of the scaffolds.

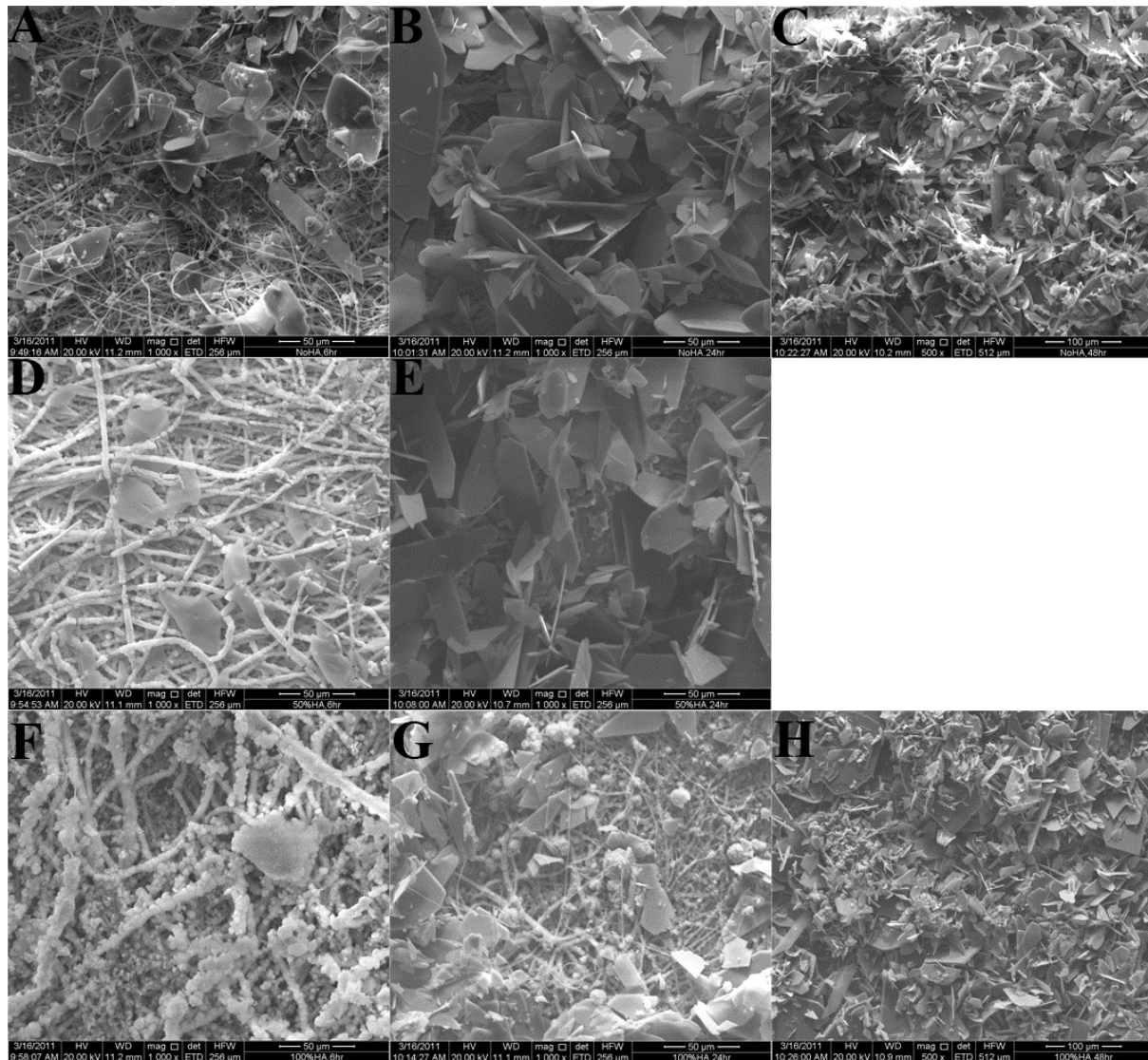


Figure 3.4. SEM images of the following scaffolds: NoHA (A, B, C), 50wt%HA (D, E), and 100wt%HA (F,G, H). Imaging was performed after 6 hour (A, D, F), 24 hr (B, E, G) and 48 hr (C, H) of mineralization

3.4.3. Mechanical Properties

Effects of heat sintering and prolonged mineralization times on compressive mechanical properties were investigated under simulated physiological conditions (Figure 3.5). Scaffolds were tested in pH 7.4 PBS at 37°C at 10% strain rate until failure.

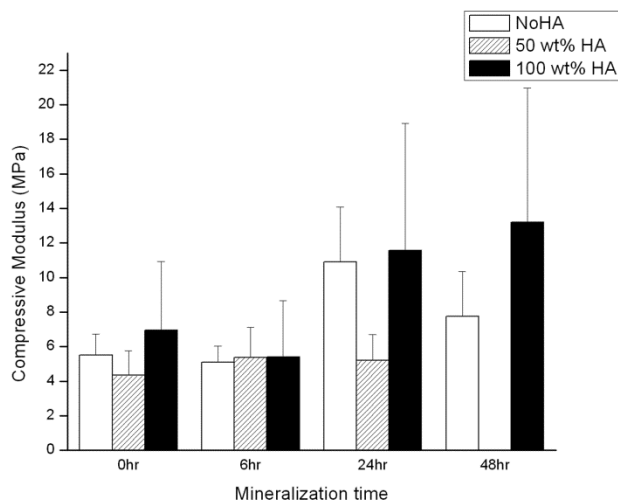
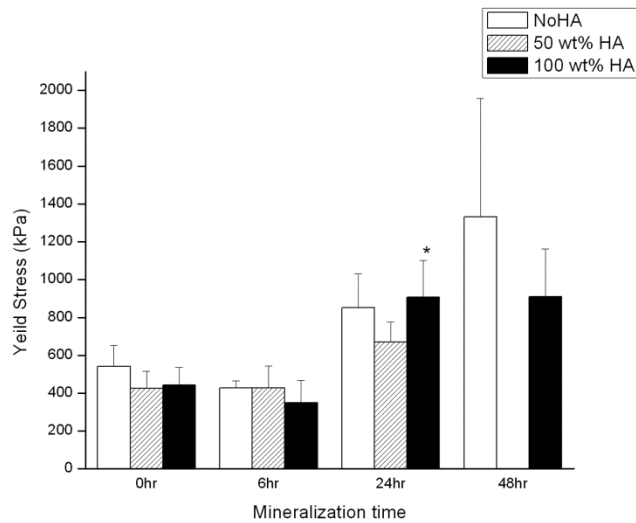


Figure 3.5. Mechanical properties of the scaffolds in compression after mineralization up to 48 hrs. (*) - Statistically different from 50wt%HA, 24hr ($p < 0.05$)

No effect on the yield stress was seen from the addition and heat sintering of HA to the electrospun scaffolds. There were also no significant differences between groups after 6 hours of mineralization. After 24 hours of mineralization, scaffolds that contained 100wt% HA had a significantly higher yield stress than scaffolds with 50% wt HA. However, no differences between scaffolds were found on after 48 hours of mineralization. Mineralization time had an effect on the yield stresses of scaffolds without HA and with 100 wt% HA, but not on scaffolds with 50 wt% HA. Scaffolds with no HA showed significant increase in yield stress from 6 hr to 24 hr to 48hr. With scaffolds with 100 wt% HA, a significant increase in yield stress was

observed from 6hr to 24hr mineralization. Prolonged mineralization times resulted in increase in compressive mechanical properties, however the addition of the HA had no significant effect on the mechanical properties of the scaffolds.

3.4.4. Ash Weights

The amount of mineral deposited onto each scaffolds was determined by determining mineral ash weights. The percentages are reported in Table 1. After heat sintering HA to the mats and then heat sintering mats into 3D scaffolds, reaming HA in the scaffolds only around 10-11 wt%. Increasing the mineralization times resulted in a significant increase in mineral ash for 50% HA and 100%HA, from 6hr to 24hr, and also from 24hr to 48 hr for groups with 0%HA and 100%HA. Addition of HA to the scaffolds resulted in significantly higher amount of mineral present on the scaffolds after 6, 24 and 48 hours of mineralization. No significant differences in amount of mineral present were seen between scaffolds with 50%HA and 100%HA, therefore the ash weight of 48h for 50% HA was not included in Table 3.1.

Table 3.1. Average mineral ash weight percents

	0%HA	50%HA	100%HA
0h		10.07±2.69	11.68±0.49
6h	2.19±1.56	15.79±0.32	15.29±1.10
24h	7.86±2.67	24.33±0.75	26.78±2.93
48h	15.64±3.84		34.50±0.59

3.4.5. Alizarin Red Stains

The mineral presence and distribution were visualized by staining with alizarin red for calcium (Figure 3.6). The presence of calcium is most noticeable on the outer most layers of the scaffolds. Very little to no mineral can be seen on the inside layers of the scaffolds, but the scaffolds with increased mineralization time did show some mineral on the inside layers. The addition of HA to the scaffolds made no noticeable difference.

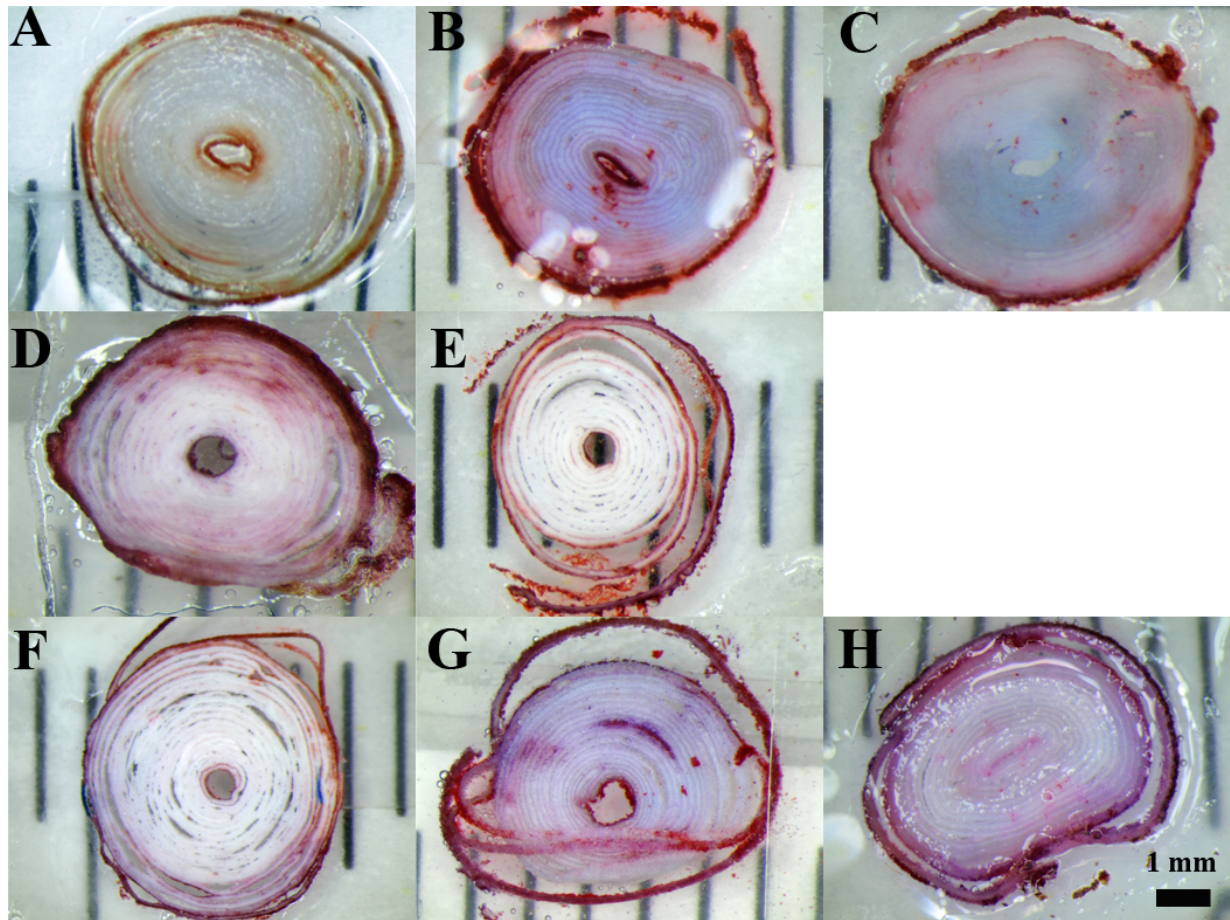


Figure 3.6. Alizarin red cross-sections stains of the following scaffolds: NoHA (A, B, C), 50wt%HA (D, E), and 100wt%HA (F, G, H). Staining was performed after 6 hour (A, D, F), 24 hr (B, E, G) and 48 hr (C, H) of mineralization

3.5.DISCUSSION

In this study we utilized previously reported heat sintering technique for the electrospun scaffolds [31] to investigate the effect of fiber orientation and degree of mineralization on compressive mechanical properties of the electrospun scaffolds. While the effect of fiber alignment on tensile mechanical properties of electrospun scaffolds has been investigated [33], the effect of the alignment on compressive properties is still unknown. Scaffolds with vertical orientation of the fibers had significantly higher yield stress than scaffolds with fiber orientation of 45°. Scaffolds with fiber orientation at 30° had significantly higher compressive modulus than scaffolds with 45° orientation. Overall, no trends were observed as the orientation was varied,

indicating that the alignment may not affect the compressive mechanical properties. This could also be due to the limitation of the speed of the rotating mandrel that was used to collect the nanofibers. In our system, the speed of the mandrel maxes out at 2000 RPM, but higher speeds are possible with other setups. With increasing rotation speed of the collecting mandrel, even better alignment can be obtained and the differences or trends in mechanical properties may become more prominent.

Addition of the HA by heat sintering and prolonged mineralization times were evaluated as means to increase mineral deposition and mechanical properties of the scaffolds. SEM images of the scaffolds before mineralization (Figure 2) and during the various stages of mineralization (Figure 3) are shown. Before mineralization HA can be seen on the surface and there were no differences between two amounts of HA added. Increased mineralization times resulted in increase of the mineral deposited on the scaffolds (Figure 3). After 6 hour of mineralization, mineral deposition can be seen, but the fiber morphology is preserved. Scaffolds with 100% HA seem to have the highest amount of mineral present. As the mineralization times increases scaffolds become completely covered in large mineral crystals, as seen in Figure 3 C and H, and no difference can be seen between the groups of the scaffolds.

Effects of increased mineralization and addition of hydroxyapatite on compressive mechanical properties of the scaffolds were also investigated. There were no differences in compressive mechanical properties between scaffolds with HA and without HA, and any time point of the mineralization. The effects of incorporation of HA into electrospinning polymer solution have only been investigated on tensile mechanical properties, with some conflicting data suggesting increase in yield stresses and elastic modulus for PLLA/HA vs. PLLA [20], but also reports of decrease in tensile mechanical properties [24, 29]. However these are tensile properties and the HA was incorporated directly into polymer solution. Lv et al. also investigated heat sintering nanoHA to PLGA microspheres and heat sintering 3D scaffolds. They found that addition of nanoHA can increase mechanical properties in compression, however if too much HA was added it interfered with heat sintering, resulting in the decrease in mechanical properties [34]. This could also explain the results we are observing with our data, that sintering the HA to the surface of the mats is interfering with the sintering of polymeric layers to one another. Increased mineralization times had positive effect on the mechanical properties of the scaffolds,

with significant increases in mechanical properties for scaffolds without HA and with 100wt%HA.

Mineral ash weight percentages were calculated after the polymer was burned off. After heat sintering HA to the mats and then heat sintering mats into 3D scaffolds, only 10-11 wt% HA remained in the scaffolds. This indicated that most of the HA was lost during the fabrication process probably due to lack sintering to the polymer fibers. Also, there were no differences in the amount of HA sintered in the scaffolds between 50wt%HA and 100wt% HA, indicating that there may be a limit to the amount of HA that can be sintered to the mats. Increasing mineralization times resulted in increased mineral content, as expected. Addition of HA to the scaffolds resulted in significantly higher amount of mineral present on the scaffolds after 6, 24 and 48 hours of mineralization. While the presence of HA increased overall mineral weight percentage, it also provides nucleation sites during the incubation in 10X SBF, resulting in the increased mineral precipitation. Similar reports have also been reported by Dr. Bowlin's group, where incorporation of nanoHA significantly increased mineral precipitation during incubation in SBF [30].

Alizarin red staining of the scaffolds cross-sections was used to observe mineral deposition and distribution in the scaffolds. Some increase in mineral distribution could be seen with increased mineralization, but a majority of the mineral was found on the outer layers of the scaffolds. This is a common drawback of mineralization by incubation in simulated body fluid under static condition. Until now, electrospun scaffolds were 2 dimensional so mineralization at the centers was possible with the use of vacuum [35], but these 3D scaffolds are too big to achieve mineralization throughout the scaffolds using these methods. Recently Teo et al. utilized flow chamber for mineralization of electrospun scaffolds by alternate immersion in CaCl_2 and Na_2HPO_4 . This resulted in more uniform mineral deposition throughout the scaffolds and improved mechanical properties over scaffolds mineralized in static conditions [36].

The porosity of the scaffolds was not investigated in this study, but the mineral presence on the surface could affect the cellular infiltration. Mineral deposited by incubation in 10X SBF was shown to deposit mainly as brushite, which is a reabsorbable and amorphous CaP, and does not

have negative effects on cellular proliferation[35]. Future work will focus on in vitro studies to further investigate these scaffolds.

3.6.CONCLUSION

In this study we utilized a heat sintering technique to create 3D electrospun scaffolds and explored the effect of fiber orientation and degree of mineralization on compressive mechanical properties. Scaffolds with vertical fiber orientation had a significantly higher yield stress compared to those with a 45° nanofiber orientation. Scaffolds with a nanofiber orientation at 30° had a significantly higher compressive modulus than scaffolds with 45° orientation. Longer mineralization times resulted in an increase in compressive mechanical properties. HA incorporation had no effect on the mechanical properties of the scaffolds, but had significant effect on the mineral deposition on PLLA/gelatin scaffolds. SEM images showed significant amounts of mineral deposited on the scaffolds; however, alizarin red cross-sectional stains indicate that the majority of the mineral is located on the outer surfaces of the scaffolds.

Based on this data we can conclude that fiber orientation can make a slight difference in nanofibrous scaffold compression, but this difference is not as profound as the difference seen with increased mineralization. The data also shows that there is a balance when utilizing HA for increased compressive strength. HA deposition through mineralization in an SBF bath increases compressive strength by reinforcing the nanofibrous matrix. On the other hand, the use of HA microparticles can interfere with nanofiber sintering and decrease scaffold strength. In addition, the use of static mineralization techniques limits the depth of mineralization into the scaffold. Future work will focus on the use of flow to improve mineral distribution throughout the scaffolds.

3.7.ACKNOWLEDGEMENTS

The authors would like to thank National Science Foundation (grant no. 0926970) and Institute for Critical Technology and Applied Science for funding this research.

3.8. REFERENCES

1. Hing, K.A., *Bone repair in the twenty-first century: biology, chemistry or engineering?* Philos Transact A Math Phys Eng Sci, 2004. **362**(1825): p. 2821-50.
2. Kretlow, J.D. and A.G. Mikos, *Review: mineralization of synthetic polymer scaffolds for bone tissue engineering.* Tissue Eng, 2007. **13**(5): p. 927-38.
3. Wheeler, D.L. and W.F. Enneking, *Allograft bone decreases in strength in vivo over time.* Clin Orthop Relat Res, 2005(435): p. 36-42.
4. Jabbarzadeh, E., et al., *Human endothelial cell growth and phenotypic expression on three dimensional poly(lactide-co-glycolide) sintered microsphere scaffolds for bone tissue engineering.* Biotechnol Bioeng, 2007. **98**(5): p. 1094-102.
5. Khan, Y., et al., *Tissue engineering of bone: material and matrix considerations.* J Bone Joint Surg Am, 2008. **90 Suppl 1**: p. 36-42.
6. Rezwani, K., et al., *Biodegradable and bioactive porous polymer/inorganic composite scaffolds for bone tissue engineering.* Biomaterials, 2006. **27**(18): p. 3413-31.
7. Stevens, B., et al., *A review of materials, fabrication methods, and strategies used to enhance bone regeneration in engineered bone tissues.* J Biomed Mater Res B Appl Biomater, 2008. **85**(2): p. 573-82.
8. Hsu, Y.Y., et al., *Mechanisms of isoniazid release from poly(D,L-lactide-co-glycolide) matrices prepared by dry-mixing and low density polymeric foam methods.* J Pharm Sci, 1996. **85**(7): p. 706-13.
9. Hsu, Y.Y., et al., *Effect of polymer foam morphology and density on kinetics of in vitro controlled release of isoniazid from compressed foam matrices.* J Biomed Mater Res, 1997. **35**(1): p. 107-16.
10. Wei, G. and P.X. Ma, *Structure and properties of nano-hydroxyapatite/polymer composite scaffolds for bone tissue engineering.* Biomaterials, 2004. **25**(19): p. 4749-57.
11. Borden, M., et al., *Tissue-engineered bone formation in vivo using a novel sintered polymeric microsphere matrix.* J Bone Joint Surg Br, 2004. **86**(8): p. 1200-8.
12. Borden, M., et al., *Tissue engineered microsphere-based matrices for bone repair: design and evaluation.* Biomaterials, 2002. **23**(2): p. 551-9.
13. Lv, Q., L. Nair, and C.T. Laurencin, *Fabrication, characterization, and in vitro evaluation of poly(lactic acid glycolic acid)/nano-hydroxyapatite composite microsphere-based scaffolds for bone tissue engineering in rotating bioreactors.* J Biomed Mater Res A, 2008.
14. Jang, J.H., O. Castano, and H.W. Kim, *Electrospun materials as potential platforms for bone tissue engineering.* Adv Drug Deliv Rev, 2009. **61**(12): p. 1065-83.
15. Liao, S., et al., *Processing nanoengineered scaffolds through electrospinning and mineralization suitable for biomimetic bone tissue engineering.* J Mech Behav Biomed Mater, 2008. **1**(3): p. 252-60.
16. Li, D. and Y.N. Xia, *Electrospinning of nanofibers: Reinventing the wheel?* Advanced Materials, 2004. **16**(14): p. 1151-1170.
17. Yoshimoto, H., et al., *A biodegradable nanofiber scaffold by electrospinning and its potential for bone tissue engineering.* Biomaterials, 2003. **24**(12): p. 2077-82.
18. Li, X., et al., *Coating electrospun poly(epsilon-caprolactone) fibers with gelatin and calcium phosphate and their use as biomimetic scaffolds for bone tissue engineering.* Langmuir, 2008. **24**(24): p. 14145-50.

19. Kim, H.W., H.S. Yu, and H.H. Lee, *Nanofibrous matrices of poly(lactic acid) and gelatin polymeric blends for the improvement of cellular responses*. J Biomed Mater Res A, 2008. **87**(1): p. 25-32.
20. Sui, G., et al., *Poly-L-lactic acid/hydroxyapatite hybrid membrane for bone tissue regeneration*. J Biomed Mater Res A, 2007. **82**(2): p. 445-54.
21. Cui, W.U., et al., *In situ growth of hydroxyapatite within electrospun poly(DL-lactide) fibers*. Journal of Biomedical Materials Research Part A, 2007. **82A**(4): p. 831-841.
22. Zhao, J., et al., *Preparation and mineralization of PLGA/Gt electrospun fiber mats*. Chinese Science Bulletin, 2009. **54**(8): p. 1328-1333.
23. Gu, S.Y., et al., *Electrospinning of gelatin and gelatin/poly(L-lactide) blend and its characteristics for wound dressing*. Materials Science & Engineering C-Materials for Biological Applications, 2009. **29**(6): p. 1822-1828.
24. Gupta, D., et al., *Nanostructured biocomposite substrates by electrospinning and electrospraying for the mineralization of osteoblasts*. Biomaterials, 2009. **30**(11): p. 2085-94.
25. Heydarkhan-Hagvall, S., et al., *Three-dimensional electrospun ECM-based hybrid scaffolds for cardiovascular tissue engineering*. Biomaterials, 2008. **29**(19): p. 2907-14.
26. Sisson, K., et al., *Fiber diameters control osteoblastic cell migration and differentiation in electrospun gelatin*. J Biomed Mater Res A. **94**(4): p. 1312-20.
27. Sisson, K., et al., *Evaluation of cross-linking methods for electrospun gelatin on cell growth and viability*. Biomacromolecules, 2009. **10**(7): p. 1675-80.
28. Jegal, S.H., et al., *Functional composite nanofibers of poly(lactide-co-caprolactone) containing gelatin-apatite bone mimetic precipitate for bone regeneration*. Acta Biomater. **7**(4): p. 1609-17.
29. Prabhakaran, M.P., J. Venugopal, and S. Ramakrishna, *Electrospun nanostructured scaffolds for bone tissue engineering*. Acta Biomater, 2009. **5**(8): p. 2884-93.
30. Madurantakam, P.A., et al., *Multiple factor interactions in biomimetic mineralization of electrospun scaffolds*. Biomaterials, 2009. **30**(29): p. 5456-64.
31. Wright, L.D., et al., *Fabrication and mechanical characterization of 3D electrospun scaffolds for tissue engineering*. Biomed Mater. **5**(5): p. 055006.
32. Tas, A.C. and S.B. Bhaduri, *Rapid coating of Ti6Al4V at room temperature with a calcium phosphate solution similar to 10x simulated body fluid*. Journal of Materials Research, 2004. **19**(9): p. 2742-2749.
33. Li, W.J., et al., *Engineering controllable anisotropy in electrospun biodegradable nanofibrous scaffolds for musculoskeletal tissue engineering*. J Biomech, 2007. **40**(8): p. 1686-93.
34. Lv, Q., L. Nair, and C.T. Laurencin, *Fabrication, characterization, and in vitro evaluation of poly(lactic acid glycolic acid)/nano-hydroxyapatite composite microsphere-based scaffolds for bone tissue engineering in rotating bioreactors*. J Biomed Mater Res A, 2009. **91**(3): p. 679-91.
35. Andric, T., L.D. Wright, and J.W. Freeman, *Rapid Mineralization of Electrospun Scaffolds for Bone Tissue Engineering*. J Biomater Sci Polym Ed.
36. Teo, W.E., et al., *Fabrication and characterization of hierarchically organized nanoparticle-reinforced nanofibrous composite scaffolds*. Acta Biomater. **7**(1): p. 193-202.

Chapter 4

Fabrication and Characterization of Electrospun Osteon Mimicking Scaffolds for Bone Tissue Engineering

Tea Andric, Alana C. Sampson, Joseph W. Freeman

Materials Science and Engineering C 31(2011) 2-8

4.1. ABSTRACT

Skeletal loss and bone deficiencies are a major worldwide problem with over 600,000 procedures performed in the US alone annually, making bone one of the most transplanted tissues, second to blood only. Bone is a composite tissue composed of organic matrix, inorganic bone mineral, and water. Structurally bone is organized into two distinct types: trabecular (or cancellous) and cortical (or compact) bone. Trabecular bone is characterized by an extensive interconnected network of pores. Cortical bone is composed of tightly packed units, called osteons, oriented parallel along to the axis of the bone. While the majority of scaffolds attempt to replicate the structure of the trabecular bone, fewer attempts have been made to create scaffolds to mimic the structure of cortical bone. The aim of this study was to develop a technique to fabricate scaffolds that mimic the organization of an osteon, the structural unit of cortical bone. We built a rotating stage for PGA fibers and utilized it for collecting electrospun nanofibers and creating scaffolds. Resulting scaffolds consisted of concentric layers of electrospun PLLA or gelatin/PLLA nanofibers wrapped around PGA microfiber core with diameters that ranged from 200-600 μm . Scaffolds were mineralized by incubation in 10x simulated body fluid, and scaffolds composed of 10% gelatin/PLLA had significantly higher amounts of calcium phosphate. Electrospun scaffolds also supported cellular attachment and proliferation of MC3T3 cells over the period of 28 days.

4.2. INTRODUCTION

Skeletal loss and bone deficiencies are major worldwide problem with over 600,000 procedures performed in the US alone annually, making bone second most transplanted tissues, second to blood only [1, 2] . This number is only expected to increase due to the aging population and increased life expectancies. The annual market is estimated at 2.5 billion annually. The current standard in orthopedic reconstructive surgeries is the autograft, autologous tissue harvested from the patient. Although autografts have very high success rates, they do have drawbacks, namely donor site morbidity and limited supply. The current alternative to autografts is allografts or tissue from donors. Although the use of allografts eliminates the potential drawbacks of the autografts, they do have the limitations of their own, such as chance of disease transmission and high failure rates. As current standards in treatment are not without drawbacks, there is a need for alternative bone grafts substitutes.

Bone is a composite tissue composed of organic matrix (20-30 wt%), inorganic bone mineral (60-70 wt%), and water (10 wt%) [3]. The majority of the bone's organic matrix, over 90 %, is composed of type I collagen fibrils [1, 4]. The inorganic phase of the bone is composed of hydrated calcium phosphate, known as hydroxyapatite [1, 4]. While the mineral content of the bone contributes to tissue stiffness, collagen matrix contributes to the toughness of the tissue [5].

Structurally, bone is organized into two distinct types: trabecular (or cancellous) and cortical (or compact) bone. The two types of bone are distinguished by their degree of porosity. Cortical bone is highly organized, dense and compact. It has a low porosity that range from 5 to 30% [4] and is usually found on the outside of the bone. Cortical bone is composed of tightly packed units, called osteons, oriented parallel along to the axis of the bone. Osteons are composed of concentric layers of mineralized collagen fibers around central channel, haversian canal, where vasculature and nerves are housed [6-8]. Osteons can range from 100 to 300 μm in diameter [6, 7]. The high organization and compact nature provide excellent micro-crack propagation prevention and high tensile and compressive mechanical properties. Trabecular bone is generally found surrounded by cortical bone. Trabecular bone is often referred to as spongy bone, due to extensive interconnected network of pores, with porosity as high as 90% [4, 7, 9]. The variation in bone structure and composition results in a wide range of mechanical properties. Cortical bone has compressive and tensile strengths in the range of 167-215 MPa and

107-140 MPa respectively, and the Young's modulus is 10-20 GPa [4]. Trabecular bone has compressive strength in the range of 3- 9 MPa, and Young's modulus of 0.01 – 0.9 GPa [4]

Many fabrication and polymer processing techniques have been investigated for possible bone tissue engineering scaffolds, including sintered microspheres [10, 11], thermally induced phase separation [12-14], particulate leaching [15, 16], and 3D printing [17-20]. All of the scaffolds are characterized by high porosities, pore interconnectivity, and architectures that mimic the structure of the trabecular bone. No fabrication technique, to the best of our knowledge, has attempted to create scaffolds that replicate the structural organization of the cortical bone.

Electrospinning as a scaffold fabrication technique has recently gained interest in applications for bone tissue engineering [4, 6-10]. Electrospun scaffolds are characterized by high surface area, high porosities, and interconnected pore networks. This makes electrospun scaffolds desirable for tissue engineering applications as the nano- and microfiber surface morphologies mimic the native extracellular matrix [21, 22]. One limitation on the electrospun scaffolds for bone tissue engineering is that scaffolds are sheets with thicknesses up to 500 μ m [23].

In this study, the aim was to develop a technique to fabricate scaffolds that mimic the structural organization of an osteon, the structural unit of the cortical bone. We successfully built rotating stage for PGA fibers and utilized it for collecting electrospun nanofibers and creating scaffolds. Resulting scaffolds consisted of concentric layers of electrospun PLLA or gelatin/PLLA nanofibers wrapped around PGA microfiber core. Scaffolds were successfully mineralized utilizing incubation in 10X simulated body fluid (SBF) solution and evaluated for cellular attachment and proliferation.

4.3. MATERIALS AND METHODS

4.3.1. Scaffold Fabrication by Electrospinning

PLLA (inherent viscosity =2.0 dl/g, Mw = 152,000) was purchased from Sigma Aldrich (St. Louis, MO, USA). PGA fibers were purchased from Concordia Medical (Warwick, RI, 02886). Dichloromethane (DCM) and dimethylformaldehyde (DMF) were purchased from Fisher Scientific (Pittsburgh, PA, USA). Gelatin, type A, from porcine skin was purchased from

Sigma Aldrich (St. Louis, MO, USA). NaCl, KCl, CaCl₂·2H₂O, MgCl₂·6H₂O, NaHCO₃, and NaH₂PO₄ were purchased from Fisher Scientific (Pittsburgh, PA, USA).

The electrospinning solution was prepared by dissolving PLLA to 7 weight percent (wt %) in 75% DCM and 25% DMF. The solution was loaded into a 5 ml plastic syringe with an 18-gauge needle, and extruded at a rate of 5 ml/hr. The PLLA was electrospun onto a rotating PGA fibers placed in front of negatively charged plate with a 5 cm diameter and a working distance of 5 cm. The voltage applied was +13kV and -7kV. A stage for rotating PGA fibers was custom built and allowed three fibers to be rotated at one time, see Figure 4.1. A total of 1ml of polymer solution was electrospun for every set of scaffolds.

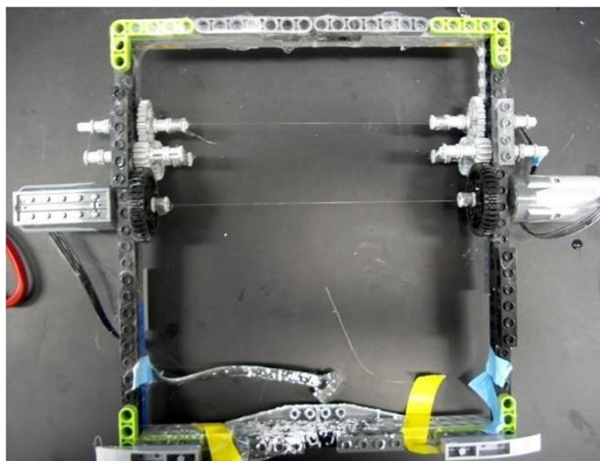


Figure 4.1. Set up that was used for rotation of PGA fibers and scaffolds fabrication

The gelatin/PLLA mixture was made by dissolving gelatin in 1ml deionized (dI) water and adding it to the 7% PLLA solution. The amount of gelatin in solution was equal to 10 or 5 %, w/w of the amount of PLLA in the solution, and will be referred to as 5% gel/PLLA and 10% gel/PLLA. As the two solutions are not miscible, they were vortexed for 1 hr prior to electrospinning. The electrospinning parameters were identical to the parameters used for the PLLA solution alone, except the voltage applied was +18kV and -7kV.

4.3.2. Mineralization of Scaffolds

We have adopted a method previously developed and reported by Tas and Bhaduri [24] to prepare 10XSBF. A stock solution was made using NaCl, KCl, CaCl₂·2H₂O, MgCl₂·6H₂O, and NaH₂PO₄, and stored at room temperature. Prior to the mineralization process, NaHCO₃ was

added while stirring vigorously, resulting in the following ion concentrations: Ca^{2+} 25 mM, HPO_4^{2-} 10 mM, Na^+ 1.03 M, K^+ 5 mM, Mg^{2+} 5mM, Cl^- 1.065M, and HCO_3^- 10mM . The electrospun mats were incubated in 400 ml of 10XSBF in vacuum for two hours at room temperature After being removed from 10X SBF , all the samples were rinsed in dI water to remove mineral not attached to scaffolds, and vacuum dried overnight.

4.3.3. *Mineral Ash Weight*

Samples were subjected to high temperatures to burn off the polymer and determine the mineral ash weight percent. After the initial weight of the samples was recorded, the samples were placed in ceramic crucibles, and then placed into a high temperature furnace (Model No. FD1535M, Fisher Scientific, Pittsburgh, PA, USA) at 700°C for 24 hours. After cooling down, the mineral ash weight was recorded and the average mineral percent deposition calculated as ratio of mineral ash weight to samples original weight. Scaffolds were tested in groups of five fibers (n=3).

4.3.4. *Scaffold Characterization*

Scaffold morphology, size, mineral deposition and distribution on the scaffolds were imaged by scanning electron microscopy (SEM). The scaffolds were soaked in liquid nitrogen and freeze-fractured to view the cross-sections. Cross-sections were imaged to map out mineral distribution throughout the scaffolds. All the samples were sputter coated with gold and palladium and imaged using an ESEM (Environmental Scanning Electron Microscope) (FEI Quanta 600 FEG) in high vacuum mode. Energy Dispersive Spectroscopy (EDS) analysis was performed using the Bruker EDX Silicon Drifter Detector on the ESEM to map presence of calcium and phosphate on the scaffolds.

X-ray diffraction (XRD) was used to determine the crystallographic structure of the calcium phosphate mineral. Samples were tested using X-ray Diffraction System (Philips Xpert Pro) with 45kV, 40mA, step size of 0.03° and scanning range from 10° to 60°.

4.3.5. Degradation Study

Four groups of scaffolds, PLLA (n=5), PLLA_MIN (n=5), 10% gel/PLLA (n=5), and 10% gel/PLLA_MIN (N=5) were subjected to *in vitro* degradation study. The weights of five samples were recorded and the samples were placed in 15ml conical tubes with 10ml of PBS, and placed in an agitated water bath (Stovall Life Science Inc., Greensboro, NC, USA) at 37°C for period of 4 weeks. At the end of every week, samples were removed from the conical tubes, rinsed in dI water, vacuum dried overnight, and weighed. Weight percent change for every group was calculated as change in weight divided by the original weight. To evaluate the presence of PGA fibers in the osteons, the scaffolds were freeze-fractured using liquid nitrogen, and cross-sections were imaged using ESEM.

4.3.6. Cell Study

4.3.6.1. Cellular Proliferation

Mouse pre-osteoblastic cells (MC3T3-E1, ATCC) were cultured in Alpha Minimum Essential Medium (α -MEM, Cellgro, Mediatech, Manassas, VA, USA) supplemented with 10% fetal bovine serum (FBS, Cellgro, Mediatech, Manassas, VA, USA) and 1% streptomycin/penicillin (Cellgro, Mediatech, Manassas, VA, USA). The scaffolds were cut into 15mm fibers and secured into 24-well Ultra-Low Cluster plates (Costar) using Silastic Medical Adhesive (Dow Corning, Midland, MI, USA). The samples were sterilized in 70% ethanol for 30 minutes followed by exposure to UV light for 30 minutes. The scaffolds were then washed with PBS and soaked in cell culture medium overnight. Approximately 20,000 cells were seeded onto each scaffold and control (well plate without scaffold). The cells were allowed to attach for one hour before adding culture medium to a final volume of 1 ml. After the cells were seeded the media was supplemented with 3mM β -glycerophosphate and 10 μ g/ml of L-ascorbic acid. The media was changed every other day and the cultures were incubated at 37°C in a humidified atmosphere and 5% CO₂. Cells were cultured for a period of 28 days and data was collected on days 7, 14, 21, and 28.

Cell viability was measured using a Cell Titer 96TM Aqueous Solution Cell Proliferation Assay (MTS Assay) (Promega, Madison, WI, USA) on the following scaffolds PLLA (n=4), PLLA_MIN (n=4), 10% gel/PLLA (n=4), 10% gel/PLLA_MIN (n=4) and a control (n=4). At

each time point (7, 14, 21, and 28 days) the media was removed, then 300 μ l of fresh media and 60 μ l of the MTS solution were added to each well and incubated at 37°C with 5 % CO₂ for three hours. After incubation, 300 μ l of the mixture was transferred to a 48-well plate. The plate was read at 490 nm using a SpectroMax M2 spectrophotometer (Sunnyvale, CA, USA).

4.3.6.2. Alkaline Phosphatase Activity

Alkaline phosphatase (ALP) activity was measured as an early marker of osteoblastic phenotype using an ALP substrate kit (Bio-Rad, Hercules, CA) on the following scaffolds PLLA (n=4), PLLA_MIN (n=4), 10% gel/PLLA (n=4), and 10% gel/PLLA_MIN (n=4). At each time point, scaffolds were washed twice with sterile PBS. Cells were lysed with 1ml of 1% Triton X-100 solutions and then subjected to three freeze-thawing cycles at -80°C. All the cells lysates were stored at -80°C until the end of the study, when all the samples were thawed and assayed together. A 100 μ L of the sample was mixed with 400 μ L of substrate solution (mixture of p-nitrophenylphosphate, diethanolamine buffer, and dI water) and incubated at 37°C for 30 minutes. The reaction was stopped with 500 μ L of 0.4N NaOH, and the resulting solution was read at 405nm using a SpectroMax M2 spectrophotometer (Sunnyvale, CA, USA). The amount of ALP was normalized to total protein content from the same cell lysates, which was determined using BCA protein assay (Thermo Scientific, Rockford, IL).

4.3.6.3. Alizarin Red and Fluorescence Stain

Mineral deposition and distribution was characterized by the Alizarin red stain. At each time point, the scaffolds were washed with PBS and transferred into new well plates. The scaffolds were then fixed in 70% ethanol for 1hr at 4°C, and stained with 40 mM Alizarin red solution for 10 min. The scaffolds were then washed with dI water five times, placed into cryomolds, imbedded in OCT imbedding medium, and frozen at -20°C. The scaffolds were cut into 50 μ m section using a Cryostat HM 550 (Thermo Scientific Microm, Walldorf, Germany), and imaged using light microscope (Leica Microsystems LAS AF 6000, Bannockburn, IL, USA).

Cellular attachment on the scaffolds was qualitatively observed by fluorescence staining. Scaffolds were fixed in 3.7% paraformaldehyde and 0.5% Triton X-100 at room temperatures and stained with phalloidin and DAPI. The scaffolds were imaged using a fluorescence microscope (Leica Microsystems, Bannockburn, IL, USA).

3.3.7. Statistical Analysis

Statistical analysis was performed using JMP 7 software. All the data was analyzed using one way analysis of variance (ANOVA) with Tukey's test to determine statistically significant differences between groups. Statistical significance was tested at $p < 0.05$.

4.4. RESULTS

Scaffolds were fabricated by electrospinning polymer solutions onto rotating PGA fibers. ESEM images of the scaffolds showed that they consisted of concentric layers of polymer nanofibers with PGA fibers as the cores. ESEM picture shows a cross-section of a single scaffold (Figure 4.2). Scaffolds were found to have average diameters that ranged from 200-600 μm . In our previous work, we have showed that scaffolds electrospun with PLLA/gelatin mixture were found to have higher fiber diameters [25]. Osteon-like scaffolds electrospun with 10%gel/PLLA were found to have significantly higher average diameter (704 $\mu\text{m} \pm 172 \mu\text{m}$) than PLLA scaffolds (481 $\mu\text{m} \pm 260\mu\text{m}$).

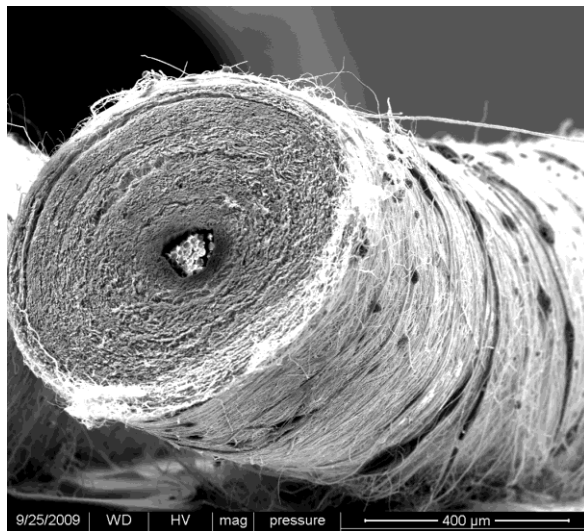


Figure 4.2. ESEM of scaffold cross-section, where PGA fibers are visible in the core surrounded by concentric layers of PLLA fibers

4.4.1 Mineralization of Scaffolds

Mineral content of the scaffolds was quantitatively evaluated by determining mineral ash weights. All ash weights are listed in the Table 4.1. Scaffolds with 10% gelatin were found to have significantly higher mineral ash weight percentages than PLLA and 5% gel/PLLA scaffolds.

Table 4.1. Average mineral ash weight percentages. * than PLLA (p<0.05)

Group Name	Avg. Mineral Ash Weight %
PLLA	2.65 ±2.02
5%gel/PLLA	6.08±2.23
10% gel/PLLA	13.50±1.85*

The amount and distribution of mineral on the scaffolds was qualitatively assessed using ESEM and EDS mapping. EDS maps of scaffolds revealed presence of calcium and phosphorus ions on the surfaces of all osteons (Figure 4.3), but the highest amounts of mineral can be seen on 10% gel/PLLA scaffolds in Figure 4.3 C and F. In the pictures, calcium is tagged with red and phosphorus with green, and in places where the two overlap the color becomes yellow.

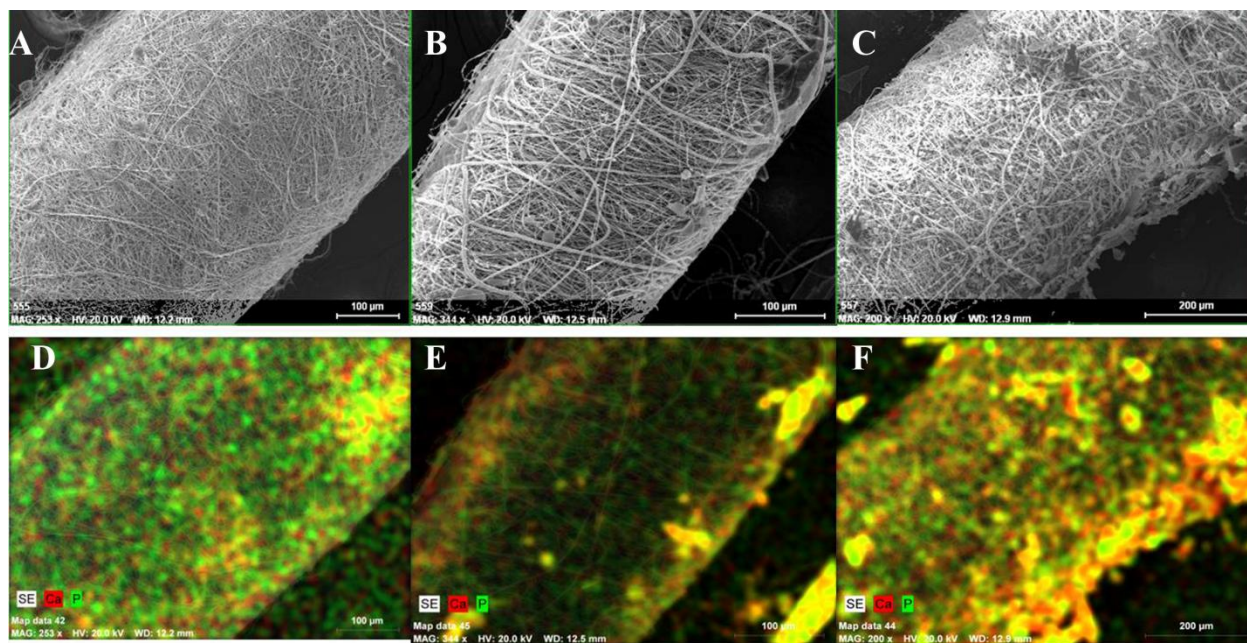


Figure 4.3. ESEM pictures of PLLA_MIN (A), 5% gel/PLLA_MIN (B), and 10% gel/PLLA_MIN (C) scaffolds and corresponding EDS maps (D,E,F). The highest amount calcium phosphate can be seen on the 10% gel/PLLA scaffolds (F)

Crystallographic structure of the calcium phosphate mineral on the surface on the scaffolds was investigated using a X-ray diffraction (XRD). Diffraction pattern can be seen in Figure 4.4, where the peaks identified as the combination of hydroxyapatite and brushite.

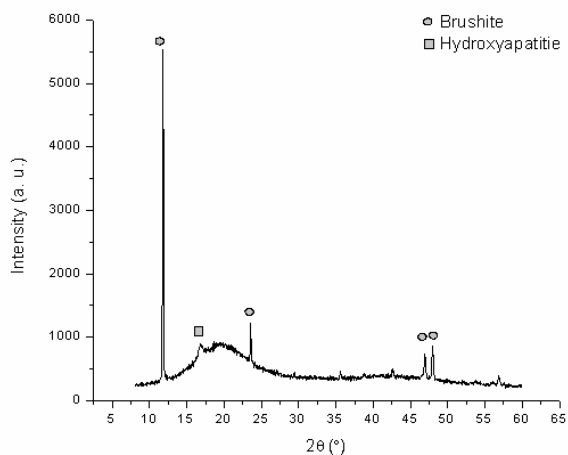


Figure 4.4. Diffraction pattern of the 10% gel/PLLA_MIN scaffolds with brushite and hydroxyapatite peaks labeled

4.4.2 Degradation Study

Osteons found in cortical bone are characterized by concentric layers of mineralized collagen fibers around the haversian canal. We performed 4 week degradation study to degrade PGA fibers found in the core of the scaffolds, to create channels that would mimic haversian canals. After 4 weeks, there was no significant weight loss due to degradation between groups, but significant weight loss was observed for PLLA scaffolds from day 21 to day 28 point and for PLLA_MIN scaffolds from day14 to day 28. Overall, average percent weight loss was between 14-21 weight percents (Figure 4.5).

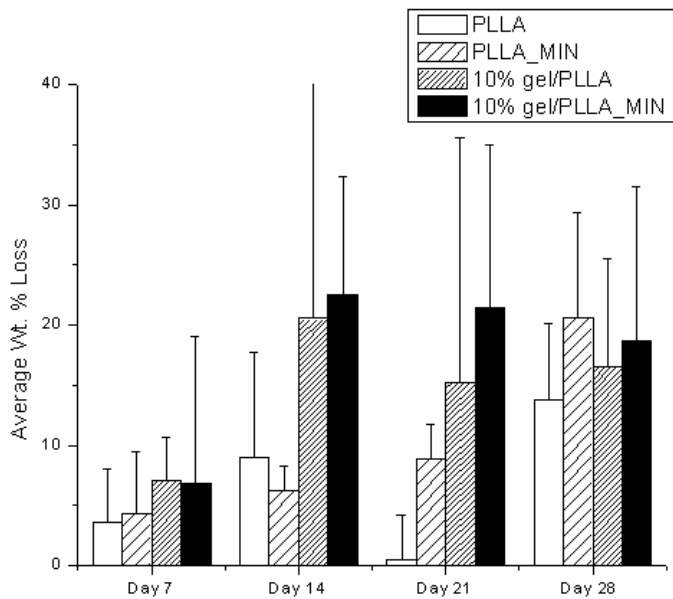


Figure 4.5. Average weight percent loss over the 4 week degradation study

ESEM pictures of these scaffolds were taken after 4 weeks to assess the degradation of PGA fibers in the cores of the scaffolds. Pictures shown in Figure 4.6 reveal the presence of PGA fibers in the cores of the scaffolds. PGA fibers did not degrade completely during the 4 week study.

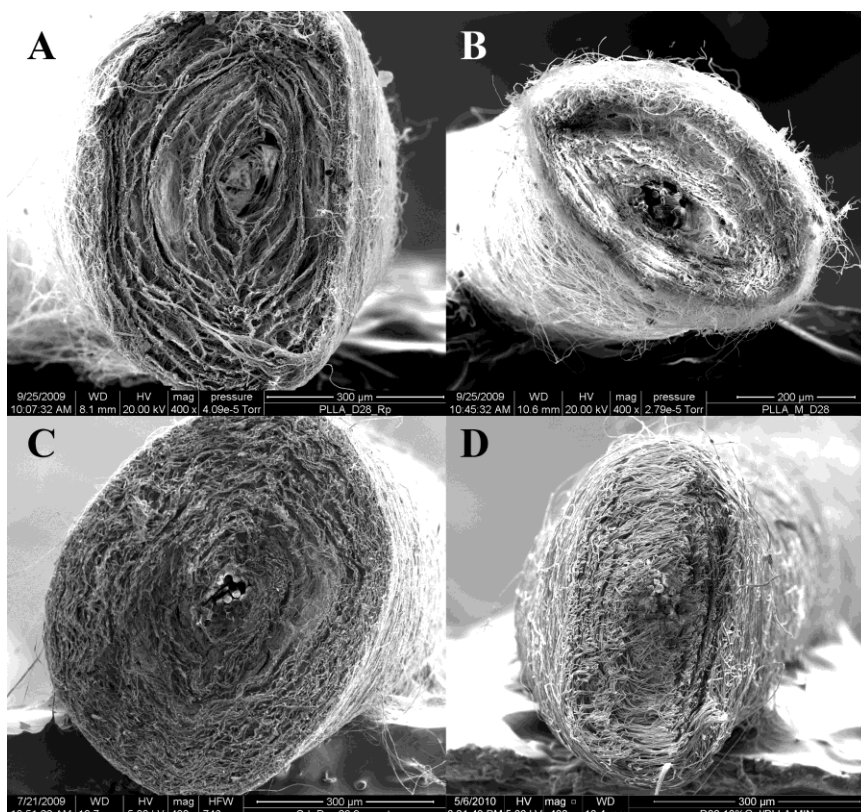


Figure 4.6. ESEM of scaffold cross-section on day 28 of degradation study. PGA fibers can be seen in the cores of the scaffolds: **A)** PLLA, **B)** PLLA_MIN, **C)** 10% gel/PLLA, and **D)** 10% gel/PLLA_MIN

4.4.3. Cell Study

4.4.3.1. Cellular Proliferation

Proliferation of the M3T3-E1 cells on the scaffolds was quantified using MTS assay on days 7, 14, 21, and 28 and the absorbances at 490 nm are shown in Figure 4.7. All absorbances were significantly higher than negative controls for every time point. On day 7, absorbance for PLLA was significantly higher than for all the other groups. Absorbance for PLLA scaffolds was significantly higher than absorbances for PLLA_MIN and 10%gel/PLLA_MIN group on day 14. On day 21, PLLA and 10%gel/PLLA scaffolds showed significantly higher absorbances than PLLA_MIN and 10%gel/PLLA_MIN scaffolds. On day 28, PLLA scaffolds had significantly higher absorbances than PLLA_MIN scaffolds.

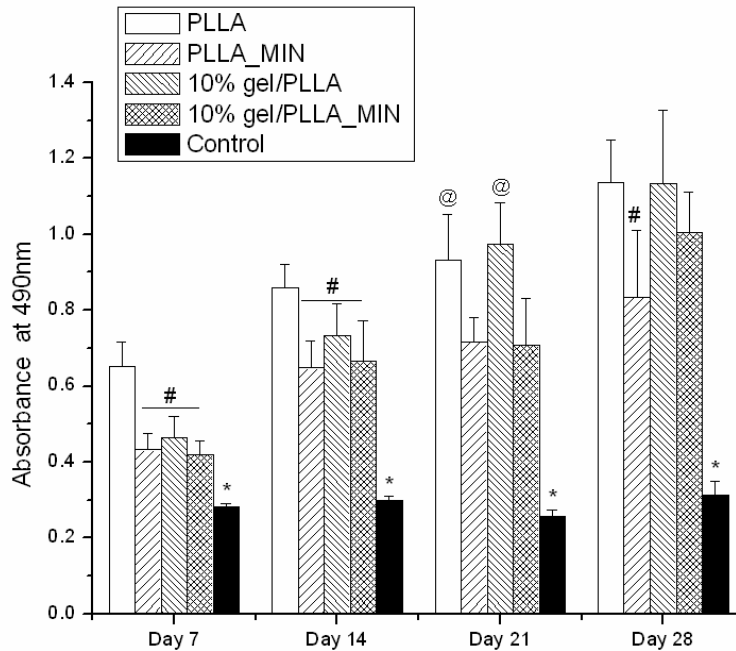


Figure 4.7. MTS assay absorbances over the period of 4 week cell study. * - significantly different from all groups ($p < 0.05$); # - significantly different from PLLA ($p < 0.05$), @ - significantly different from PLLA_MIN and 10% gel/PLLA_MIN ($p < 0.05$)

Over the period of 28 days, all groups exhibited significant increase in absorbance. Significant increase in absorbances was observed from day 7 to day 14 for groups PLLA_MIN, 10% gel/PLLA, 10% gel/PLLA_MIN, from day 7 to day 21 for PLLA, from day 14 to day 21 for 10% gel/PLLA, and from day 21 to day 28 for 10% gel/PLLA_MIN. Cells can also be seen on the surfaces of the scaffolds where actin filaments are stained green and nuclei stained blue (Figure 4.8).

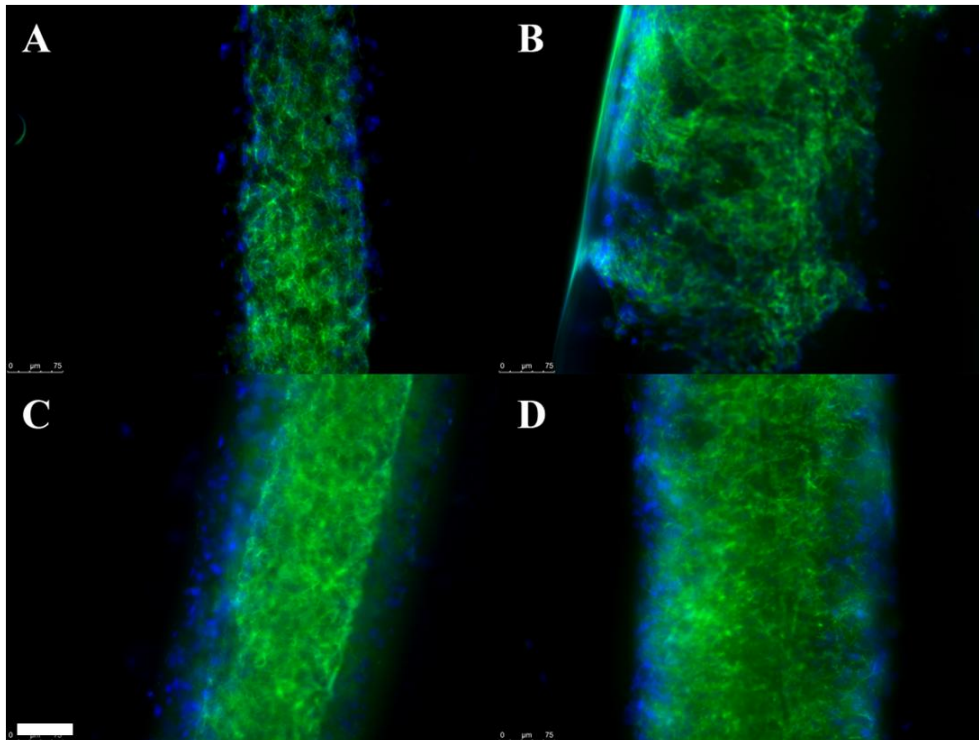


Figure 4.8. Fluorescently labeled scaffolds after 28 days of cell culture, actin filaments are stained green and the cell's nuclei stained blue for the following scaffolds: **A)** PLLA , **B)** PLLA_MIN, **C)** 10% gel/PLLA, and **D)** 10% gel/PLLA_MIN (scale bar 75 μ m)

4.4.3.2. Alkaline Phosphatase Activity

Alkaline phosphatase activity was measured using an ALP substrate kit, all of the values are expressed as fractions of total cell protein in Figure 4.9. On day 14 scaffolds for 10% gel/PLLA_MIN had higher levels of ALP than PLLA scaffolds. On day 21 and 28 there were no significant differences between scaffolds.

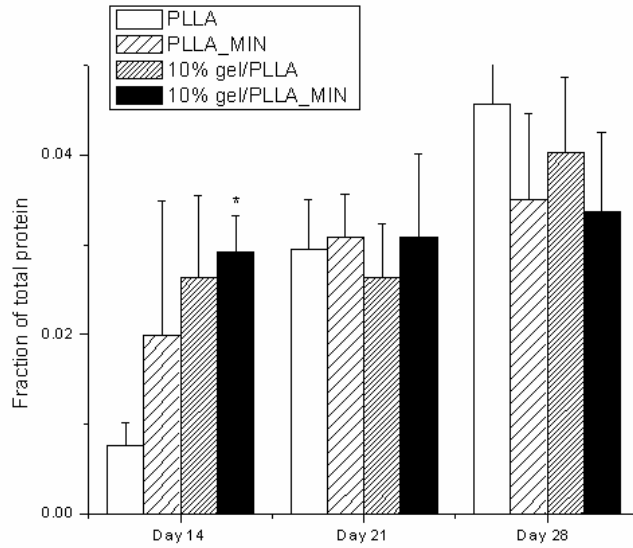


Figure 4.9. ALP expression as the fraction of the total cell protein. * - significantly different from PLLA ($p < 0.05$)

4.4.3.3. Alizarin Red Stain

Mineral deposition and distribution was observed by Alizarin red staining at the end of each time point in the cell study (Figure 4.10). On day 7, very little of the alizarin red stain can be seen in the cross-sections, especially on the nonmineralized scaffolds. By day 28, mineral stains can be seen on all scaffolds. Scaffolds that were originally nonmineralized have a thin surface layer of mineral. Presence of mineral across the entire cross-section after 28 days of cell culture can be seen on the mineralized scaffolds, PLLA and gel/PLLA.

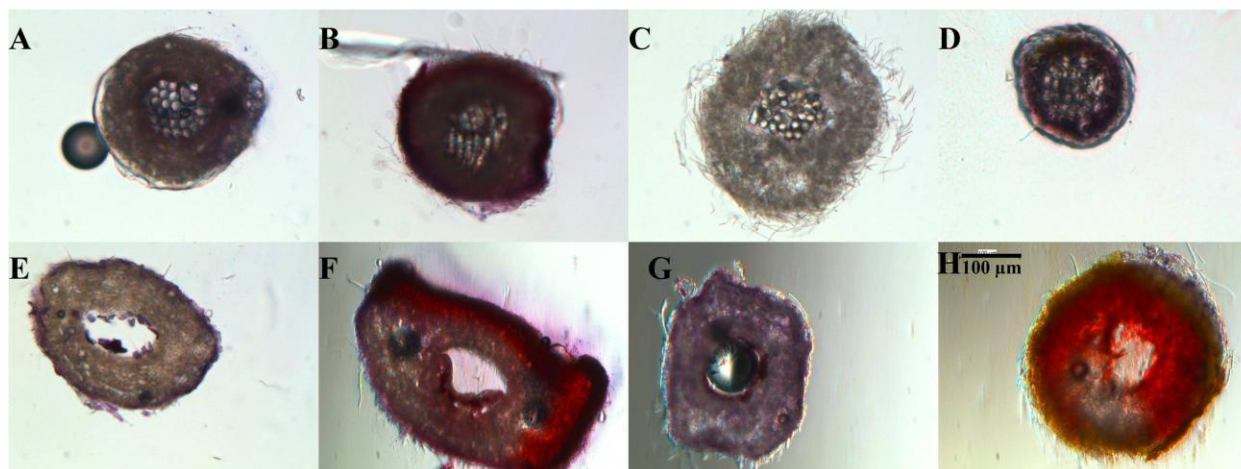


Figure 4.10. Alizarin red stains of scaffolds: PLLA (A, E), PLLA_MIN (B, F), 10% gel/PLLA (C, G), and 10% gel/PLLA_MIN (D, H) after 7 (A-D) and 28 (E-H) days of cell culture. Scale bar 100 μ m.

4.5. DISCUSSION

In this study, we have designed and fabricated nanofibrous PLLA and gelatin/PLLA scaffolds that mimic structural organization of osteons, the building units of cortical bone. We successfully built rotating stage for PGA fibers (Figure 4.1) and utilized it for collecting electrospun nanofibers and creating scaffolds. The resulting scaffolds, seen in Figures 4.2 and 4.5, consisted of concentric layers of electrospun PLLA or gelatin/PLLA nanofibers wrapped around PGA microfiber core, with diameters that ranged from 200-600 μ m.

Scaffolds were mineralized by incubation in 10X SBF. The amount of mineral precipitated was quantified as mineral ash weight and mineralization percentages were calculated and reported in Table 4.1. Scaffolds electrospun from 10% gel/PLLA mixture were found to have the highest average mineral ash weights (13.50 ± 1.85), significantly higher than PLLA alone (2.65 ± 2.23) and 5% gel/PLLA (6.08 ± 2.02). Gelatin, a denatured collagen, provided exposed carboxyl groups which increased mineral percent deposition with increased gelatin concentration. A similar trend can also be seen on the surface ESEM and EDS maps of the scaffolds in Figure 4.3, where the highest amount of calcium phosphate can be seen on the surface of 10% gel/PLLA scaffolds. Similar findings were also previously reported by our group for electrospun 10% gel/PLLA electrospun sheets [25]. Mineral precipitated on the scaffolds was identified using EDS and X-ray diffraction as brushite and

hydroxyapatite. Similar results were also reported previously with mineralization by incubation in 10X SBF [26-28]. It has been reported that brushite can be potential starting material for bone substitutes, and can be converted to hydroxyapatite [27, 29].

A four week degradation study was performed with an attempt to degrade out the PGA core fibers and create canals that would mimic haversian canals found in osteons. The average weight loss recorded ranged from 14 to 21 wt%, however there was no significant differences in weight loss between groups. Two groups, PLLA and PLLA_MIN, showed significant wt % loss. No significant weight loss was seen for 10%gel/PLLA and 10%gel/PLLA_MIN groups because of large standard deviations due to the low scaffold weights. The most important aspect of the degradation study was to degrade PGA core fibers, but SEM pictures of the cross-sections after 28 days revealed the presence of the PGA inside the scaffolds (Figure 4.5). When the degradation study was performed with PGA fibers alone, fibers degraded within a 4 week period (data not shown). We suspect that the layers of wrapped PLLA fibers around PGA core prevented the degradation of the PGA fibers. PLLA is more hydrophobic and has slower degradation time that can be up two years [17, 19]. Alternative methods will be utilized to create hollow core scaffolds, either changing core polymer or increasing degradation times.

Scaffolds were evaluated for cellular attachment and proliferation using a MC3T3_E1 cell line over period of 4 weeks. All the scaffolds supported cellular attachment, as all the values were significantly higher than negative controls or cells seeded on Ultra-low attachment plates. Also, over the period of 28 days, values for every group of scaffolds increased significantly indicating cellular proliferation. There were no significant differences between PLLA and gelatin/PLLA groups after the day 7 point. The differences were not seen, as the water soluble gelatin the scaffolds was not cross-linked and probably dissolved. Gelatin has been reported to increase cell proliferation, but mostly in the cross-liked state [26]. Also higher absorbances were observed on nonmineralized PLLA scaffolds over mineralized PLLA scaffolds for all time points. Similar effect was also observed on gelatin/PLLA mineralized scaffolds until day 28 point when the absorbances were no different from PLLA and gelatin/PLLA. Cells can also be seen on the surfaces of the scaffolds where actin filaments are stained green and nuclei stained blue (Figure 4.9).

Alkaline phosphatase activity was measured as an early marker of an osteoblastic phenotype activity. On day 14, mineralized gelatin/PLLA scaffolds had significantly higher levels of ALP than PLLA scaffolds. However, at later time points there was no difference in ALP levels between any of the scaffolds. Mavis et al. have also investigated ALP activity on electrospun PCL scaffolds mineralized using a similar procedure, using a modified 10X SBF recipe [30]. They were able to see significant increase in absorbance values for ALP for scaffolds mineralized for 2 and 4 hours using their modified recipe for “less phosphate-rich” 10X SBF, however their results were not normalized for total cell protein or cell number, so it is difficult to compare to our data [30].

Scaffolds were also stained with Alizarin red stains to visualize presence and distribution across the scaffolds over the period of cell study. On day 7 no mineral can be seen on the nonmineralized scaffolds, but by day 28 a thin layer of mineral produced by the cells can be seen on the surface. Intense mineral stains can be seen across the cross-section of the mineralized scaffolds, PLLA and gelatin/PLLA. In addition, the staining runs through the entire cross-section of the scaffolds. So the scaffolds not only supported cell attachment and proliferation, but also provided an environment that allowed cell to produce calcium phosphate and further mineralized the scaffolds.

4.6. CONCLUSION

In this study, we have designed and fabricated electrospun PLLA and gelatin/PLLA scaffolds that mimic structural organization of osteons, building units of cortical bone. We successfully built rotating stage for PGA fibers and utilized it for collecting electrospun nanofibers and creating scaffolds. The resulting scaffolds consisted of concentric layers of electrospun PLLA or gelatin/PLLA nanofibers wrapped around PGA microfiber core, with diameters that ranged from 200-600 μ m. Scaffolds were successfully mineralized utilizing incubation in 10X SBF solution for two hours. Scaffolds supported cellular attachment and proliferation of MC3T3 cells and also provided an environment that allowed cells to produce calcium phosphate, increasing scaffold mineralization. Creating scaffolds that mimic structural organization of an osteon is a first step in creating scaffolds that resemble structural organization and mechanical properties of the cortical bone. Recently our group developed and applied heat sintering technique to create 3D electrospun scaffolds to evaluate for tissue engineering

applications [23]. Similar technique will be utilized to sinter multiple osteon-like scaffolds together.

4.7. ACKNOWLEDGEMENT

The authors would like to thank National Science Foundation, grant No. 0926970 for funding this study.

4.8. REFERENCES

1. Hing, K.A., *Bone repair in the twenty-first century: biology, chemistry or engineering?* Philos Transact A Math Phys Eng Sci, 2004. **362**(1825): p. 2821-50.
2. Giannoudis, P.V., H. Dinopoulos, and E. Tsiridis, *Bone substitutes: an update*. Injury, 2005. **36 Suppl 3**: p. S20-7.
3. Chen, J., B. Chu, and B.S. Hsiao, *Mineralization of hydroxyapatite in electrospun nanofibrous poly(L-lactic acid) scaffolds*. J Biomed Mater Res A, 2006. **79**(2): p. 307-17.
4. An, Y.H. and R.A. Draughn, *Mechanical testing of bone and the bone-implant interface*. 2000, Boca Raton, Fla.: CRC Press. 624 p.
5. Wang, X. and S. Puram, *The toughness of cortical bone and its relationship with age*. Ann Biomed Eng, 2004. **32**(1): p. 123-35.
6. Ritchie, R.O., *How does human bone resist fracture?* Ann N Y Acad Sci. **1192**(1): p. 72-80.
7. Rho, J.Y., L. Kuhn-Spearing, and P. Zioupos, *Mechanical properties and the hierarchical structure of bone*. Med Eng Phys, 1998. **20**(2): p. 92-102.
8. Beniash, E., *Biominerals-hierarchical nanocomposites: the example of bone*. Wiley Interdiscip Rev Nanomed Nanobiotechnol.
9. Cowin, S.C. and S.B. Doty, *Tissue mechanics*. 2007, New York, NY: Springer. xvi, 682 p.
10. Borden, M., et al., *Structural and human cellular assessment of a novel microsphere-based tissue engineered scaffold for bone repair*. Biomaterials, 2003. **24**(4): p. 597-609.
11. Borden, M., et al., *Tissue engineered microsphere-based matrices for bone repair: design and evaluation*. Biomaterials, 2002. **23**(2): p. 551-9.
12. Wei, G. and P.X. Ma, *Structure and properties of nano-hydroxyapatite/polymer composite scaffolds for bone tissue engineering*. Biomaterials, 2004. **25**(19): p. 4749-57.
13. Wang, X., G. Song, and T. Lou, *Fabrication and characterization of nano composite scaffold of poly(L-lactic acid)/hydroxyapatite*. J Mater Sci Mater Med. **21**(1): p. 183-8.
14. Ma, P.X. and R. Zhang, *Microtubular architecture of biodegradable polymer scaffolds*. J Biomed Mater Res, 2001. **56**(4): p. 469-77.
15. Lu, L., et al., *In vitro and in vivo degradation of porous poly(DL-lactic-co-glycolic acid) foams*. Biomaterials, 2000. **21**(18): p. 1837-45.
16. Chen, V.J. and P.X. Ma, *Nano-fibrous poly(L-lactic acid) scaffolds with interconnected spherical macropores*. Biomaterials, 2004. **25**(11): p. 2065-73.
17. Yang, S., et al., *The design of scaffolds for use in tissue engineering. Part I. Traditional factors*. Tissue Eng, 2001. **7**(6): p. 679-89.
18. Stevens, B., et al., *A review of materials, fabrication methods, and strategies used to enhance bone regeneration in engineered bone tissues*. J Biomed Mater Res B Appl Biomater, 2008. **85**(2): p. 573-82.
19. Rezwani, K., et al., *Biodegradable and bioactive porous polymer/inorganic composite scaffolds for bone tissue engineering*. Biomaterials, 2006. **27**(18): p. 3413-31.
20. Liu, X. and P.X. Ma, *Polymeric scaffolds for bone tissue engineering*. Ann Biomed Eng, 2004. **32**(3): p. 477-86.
21. Jang, J.H., O. Castano, and H.W. Kim, *Electrospun materials as potential platforms for bone tissue engineering*. Adv Drug Deliv Rev, 2009. **61**(12): p. 1065-83.

22. Liao, S., et al., *Processing nanoengineered scaffolds through electrospinning and mineralization suitable for biomimetic bone tissue engineering*. J Mech Behav Biomed Mater, 2008. **1**(3): p. 252-60.
23. Wright, L.D., et al., *Fabrication and mechanical characterization of 3D electrospun scaffolds for tissue engineering*. Biomed Mater. **5**(5): p. 055006.
24. Tas, A.C. and S.B. Bhaduri, *Rapid coating of Ti6Al4V at room temperature with a calcium phosphate solution similar to 10x simulated body fluid*. Journal of Materials Research, 2004. **19**(9): p. 2742-2749.
25. Andric, T., L.D. Wright, and J.W. Freeman, *Rapid Mineralization of Electrospun Scaffolds for Bone Tissue Engineering*. J Biomater Sci Polym Ed.
26. Li, X., et al., *Coating electrospun poly(epsilon-caprolactone) fibers with gelatin and calcium phosphate and their use as biomimetic scaffolds for bone tissue engineering*. Langmuir, 2008. **24**(24): p. 14145-50.
27. Yang, F., J.G.C. Wolke, and J.A. Jansen, *Biomimetic calcium phosphate coating on electrospun poly (epsilon-caprolactone) scaffolds for bone tissue engineering*. Chemical Engineering Journal, 2008. **137**(1): p. 154-161.
28. Zhao, J., et al., *Preparation and mineralization of PLGA/Gt electrospun fiber mats*. Chinese Science Bulletin, 2009. **54**(8): p. 1328-1333.
29. Tas, A.C. and S.B. Bhaduri, *Chemical processing of CaHPO₄(.)2H₂O: Its conversion to hydroxyapatite*. Journal of the American Ceramic Society, 2004. **87**(12): p. 2195-2200.
30. Mavis, B., et al., *Synthesis, characterization and osteoblastic activity of polycaprolactone nanofibers coated with biomimetic calcium phosphate*. Acta Biomater, 2009. **5**(8): p. 3098-111.

Chapter 5

Fabrication and Characterization of Three Dimensional Electrospun Cortical Bone Scaffolds

Tea Andric, Katherine E. Degen, Joseph W. Freeman

5.1. ABSTRACT

Bone is a composite tissue composed of organic matrix, inorganic bone mineral, and water. Structurally, bone is organized into two distinct types: trabecular (or cancellous) and cortical (or compact) bone. Trabecular bone is highly porous and usually found within confines of cortical bone. Cortical bone is highly organized and dense. Cortical bone is composed of tightly packed units or osteons, which consist of concentric layers of mineralized collagen fibers. While many scaffolds fabrication techniques have sought to replicate the structure and organization of trabecular bone, very little attempts have been made to mimic the cortical organization of the bone. In this study we fabricated three dimensional electrospun scaffolds composed of heat sintered individual osteon like scaffolds. The scaffolds also contained a system of channels running parallel to the length of the scaffolds, as found naturally in the haversian systems of bone tissue. Cross-linking of the gelatin prior to the mineralization of the scaffolds has helped keep the channels of the osteons from collapsing during dissolution of PEO fibers. Premineralization before formation of the larger scaffold and mineralization increased mineral deposition between the electrospun layers of the scaffolds. A combination of cross-linking and premineralization significantly increased compressive moduli of the scaffolds.

5.2. INTRODUCTION

Bone is a composite tissue composed of organic matrix (20-30 wt %), inorganic bone mineral (60-70 wt %), and water (10 wt%) [1]. Structurally, bone is organized into two distinct types: trabecular (or cancellous) and cortical (or compact) bone. The two types of bone are distinguished by their organization and degree of porosity. Cortical bone is highly organized, dense and compact. It has a low porosity that ranges from 5 to 30% [2] and is usually found on the outside of the bone. Cortical bone is composed of tightly packed units, called osteons, oriented parallel along to the axis of the bone. Osteons are composed of concentric layers of mineralized collagen fibers around central channel, haversian canal, where vasculature and

nerves are housed [3-5]. Osteons can range from 100 to 300 μm in diameter [3, 4]. The high organization and compact nature provide excellent micro-crack propagation prevention and high tensile and compressive mechanical properties. Trabecular bone is generally found surrounded by cortical bone. Trabecular bone is often referred to as spongy bone, due to extensive interconnected network of pores, with porosity as high as 90% [2, 4, 6].

Many fabrication and polymer processing techniques have been investigated for possible bone tissue engineering scaffolds, including sintered microspheres [7, 8], thermally induced phase separation [9-11], particulate leaching [12, 13], and 3D printing [14-17]. All of the scaffolds are characterized by high porosities, pore interconnectivity, and architectures that mimic the structure of the trabecular bone. No fabrication technique, to the best of our knowledge, has attempted to create scaffolds that replicate the structural organization of the cortical bone.

In our previous study we have successfully fabricated electrospun scaffolds that mimic structural organization of an osteon [18]. The scaffolds were fabricated by electrospinning onto PGA microfibers, which were mounted onto rotating fiber set up. The resulting scaffolds had diameters that fall into physiological range of an osteon; however the PGA core fibers were difficult to dissolve during a 4 week degradation study. In this study, the objective was to electrospun scaffolds onto material that can be dissolved out more easily and create channels inside the osteon scaffolds. Heat sintering techniques for creating three dimensional scaffolds were utilized for combining multiple osteon scaffolds into 3D structures.

5.3. MATERIALS AND METHODS

5.3.1. Scaffold Fabrication by Electrospinning

PLLA (inherent viscosity =2.0 dl/g, Mw = 152,000) was purchased from Sigma Aldrich (St. Louis, MO, USA). Poly (ethylene oxide) (PEO) (Mv = 200,000) was purchased from Sigma Aldrich (St. Louis, MO, USA). Dichloromethane (DCM) and dimethylformaldehyde (DMF) were purchased from Fisher Scientific (Pittsburgh, PA, USA). Gelatin, type A, from porcine skin was purchased from Sigma Aldrich (St. Louis, MO, USA). NaCl, KCl, CaCl 2H₂O, MgCl₂ 6H₂O, NaHCO₃, and NaH₂PO₄ were purchased from Fisher Scientific (Pittsburgh, PA, USA).

PEO was dissolved in 10% of 100% ethanol and 90% of deionized water to 10% w/v solution. The solution was electrospun onto rotating mandrel with 5cm diameter at rate of 5 ml/hr and working distance of 10 cm. Total volume of 3ml was electrospun with voltages +10V and -3V. The electrospun mats were cut into 3mm wide strips and rolled into fibers that were used for the next step.

In the next step, electrospinning solutions were prepared by dissolving PLLA to 7 % w/v in 75% DCM and 25% DMF, and dissolving PDLA to 22 % w/v in 75% THF and 25%DMF. The gelatin/PLLA mixture was made by dissolving gelatin in 1ml deionized (dI) water and adding it to the 7% PLLA solution. The amount of gelatin in solution was equal to 10 %, w/w of the amount of PLLA in the solution. As two solutions are not miscible, they were vortexed for 1 hr to mix before electrospinning.

Individual osteon-like scaffolds were electrospun onto rotating PEO fibers using the set up previously reported [18], and shown in Figure 5.1. The fibers were placed into set up and placed in front of negatively charged target, as shown. PLLA/gelatin mixture was electrospun first to total volume of 1.5 ml, with following parameters: working distance of 5 cm, at extrusion rate of 5 ml/hr, and voltages of + 17V and -9V. This was followed by electrospinning of PDLA solution in total volume of 0.5 ml with following parameters: working distance of 15 cm, extrusion rate of 5 ml/hr, and voltages of +13 V and -8V.

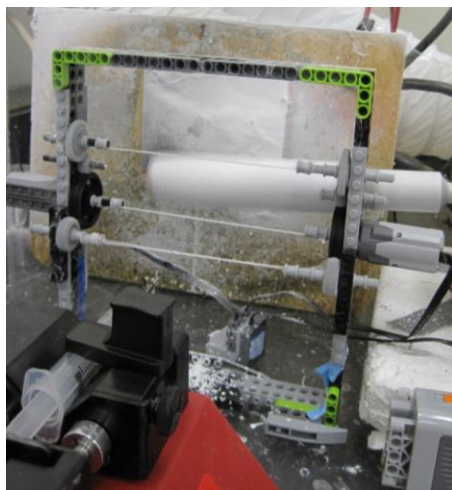


Figure 5.1. Picture of the electrospinning set for rotating PEO fibers

Finally, electrospun mats were also created by electrospinning onto 5 cm diameter rotating mandrel, with total volume of 1ml of PDLA followed by 5ml of PLLA/gelatin solution. The electrospun mats were cut into 1cm wide strips and later used for heat sintering process. All electrospun scaffolds were cross-linked in 2.5% glutaraldehyde vapor for either 2 hours or 17 hours.

5.3.2. *Heat sintering of the Scaffolds*

To fabricate three dimensional electrospun scaffolds, we will be utilizing heat sintering method previously reported by our group [19]. Individual osteons were cut into 1 cm segments, and wrapped with 1cm wide strip of electrospun PLLA/gelatin/PDLA sheet to a diameter of 5 mm. The wrapped scaffolds were then placed in the 5mm diameter with 1 cm height mold and heat sintered at 54°C for 45 minutes.

5.3.3. *Mineralization of the Scaffolds*

All of the scaffolds were mineralized using a previously reported method by incubation in 10X SBF [20, 21]. Briefly, a stock solution was made using NaCl, KCl, CaCl₂·2H₂O, MgCl₂·6H₂O, and NaH₂PO₄, and stored at room temperature. Prior to the mineralization process, NaHCO₃ was added while stirring vigorously, resulting in the following ion concentrations: Ca²⁺ 25 mM, HPO₄²⁻ 10 mM, Na⁺ 1.03 M, K⁺ 5 mM, Mg²⁺ 5mM, Cl⁻ 1.065M, and HCO₃⁻ 10mM. The electrospun scaffolds were incubated in 300 ml of 10XSFBF for various times at room temperature, with mineralizing solution replaced every 2 hours. After being removed from 10X SBF, all the samples were rinsed in dI water to remove mineral not attached to scaffolds, and vacuum dried overnight.

For the scaffolds with premineralization treatment, individual osteons and electrospun sheets were mineralized for 1 hour, and then rinsed in dI water and vacuum dried overnight. The electrospun pieces were then heat sintered as described above and mineralized again as a three dimensional scaffold.

5.3.4. *Alizarin Red Staining*

Mineral deposition and distribution was characterized by the Alizarin red stain. The scaffolds were then fixed in 70% ethanol for 1hr at 4°C, and stained with 40 mM Alizarin red

solution for 10 min. The scaffolds were then washed with dI water five times, placed into cryomolds, imbedded in OCT imbedding medium, and frozen at -20°C. The scaffolds were cut into 200µm section using a Cryostat HM 550 (Thermo Scientific Microm, Walldorf, Germany), and imaged using stereoscope (Vision Engineering, New Milford, CT, USA).

5.3.5. Mechanical Testing

The scaffolds were mechanically tested in compression using an Instron 5869 with Bioplus Bath (Norwood, MA, USA). Scaffolds tested included: Mineralized scaffolds (Min) for 6 hr and 24 hr, cross-linked scaffolds for 2h (CL_2hr) and mineralized for 6hr, scaffolds premineralized for 1 hr without cross-linking (premin1h), and scaffolds cross-linked for 2hr and premineralized (CL_premin1hr) and then mineralized for 6 and 24 hours. For each group we tested six samples (n=6). The tests were performed under simulated physiological conditions in phosphate buffered saline (PBS) (pH= 7.4) at 37°C. The scaffolds were fabricated into 10 mm high cylinders with 5 mm diameter (2:1 height to diameter ratio) and tested in compression until failure with uniform strain rate of 1mm/min (10% stain/min). The data was analyzed to determine yield stress and compressive modulus.

5.3.6. Mineral Ash Weights

After the mechanical testing the samples were vacuum dried overnight and used to determine mineral ash weights. After the initial weight of the samples was recorded, the samples were placed in ceramic crucibles, and then placed into a high temperature furnace (Model No. FD1535M, Fisher Scientific, Pittsburgh, PA, USA) at 700°C for 24 hours. After cooling down, the mineral ash weight was recorded and the average mineral percent deposition calculated as ratio of mineral ash weight to samples original weight. For each group we tested three samples (n=3).

5.3.7. Statistical Analysis

Statistical analysis was performed using JMP 9 software. All the data was analyzed using one way analysis of variance (ANOVA) with Tukey's test to determine statistically significant differences between groups. Statistical significance was tested at $p < 0.05$.

5.4. RESULTS

In this study we electrospun osteon-like scaffolds onto rotating PEO microfibers. The individual electrospun osteon-like scaffolds were successfully heat sintered into 3D scaffolds that mimic the organization of the cortical bone. PEO fibers can then be dissolved out leaving a set of channels running along the length of scaffolds.

5.4.1. *Alizarin Red Staining*

Alizarin red staining was used to stain the mineral deposited on the scaffolds. Majority of the mineral can be seen on the outer most layers of the scaffolds, shown in Figure 5.2. Mineralization process of soaking in 10X SBF has dissolved PEO core fibers out individual osteons, leaving behind a system of channels that run along the length of the scaffolds. Premineralization treatment, without cross-linking of the scaffolds, resulted in the dissolution of PEO cores and collapse of the individual osteon-like scaffolds, as shown in Figure 5.2 B. Cross-linking the osteons prior to the premineralization treatment, helped keep the individual osteons open without collapsing, thus preserving the channels (Figure 5.2 C and D). Keeping the channels open resulted in mineral deposition inside of the channels. However most mineral present after 6hr of mineralization can be seen on scaffolds that have been premineralized and cross-linked (Figure 5.2 D). Similar effects can be seen also after 24 hours of mineralization, where scaffolds that have been premineralized and cross-linked (Figure 5.2 F) have higher mineral deposition than mineralized scaffolds without any treatment (Figure 5.2 E).

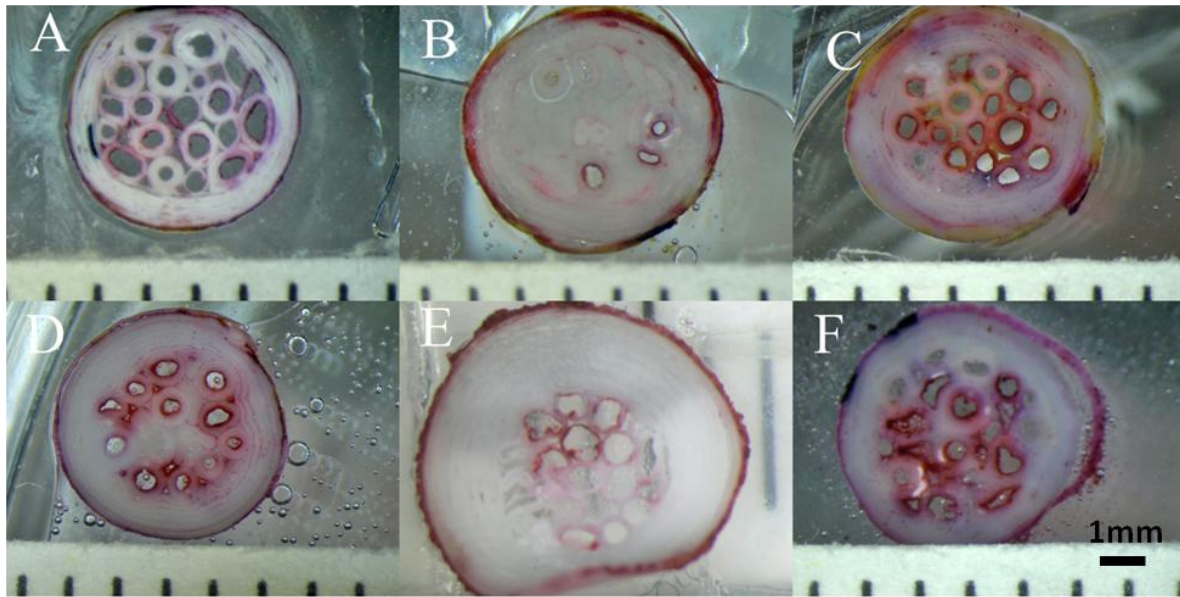


Figure 5.2. Alizarin red stain of cross-sections after 6 hr of mineralization: **A)** Min6h, **B)** Premin1h_Min6h, **C)** CL_Min6h, and **D)** CL_premin1h_Min6h, **E)**Min24h, and **F)**CL_premin1h_Min24h

5.4.2. *Mechanical Testing*

The compressive mechanical properties of the scaffolds were also evaluated. Data for the compressive moduli is shown in Figure 5.3, and the data for the compressive yield stresses is shown in Figure 5.4. After 24 hr of mineralization, scaffolds that were premineralized and cross-linked had significantly higher compressive modulus than just mineralized (6hr and 24hr) scaffolds and premineralized only (6hr) scaffolds. After 6hr of mineralization, scaffolds that were premineralized and cross-linked had significantly higher compressive modulus than premineralized scaffolds only.

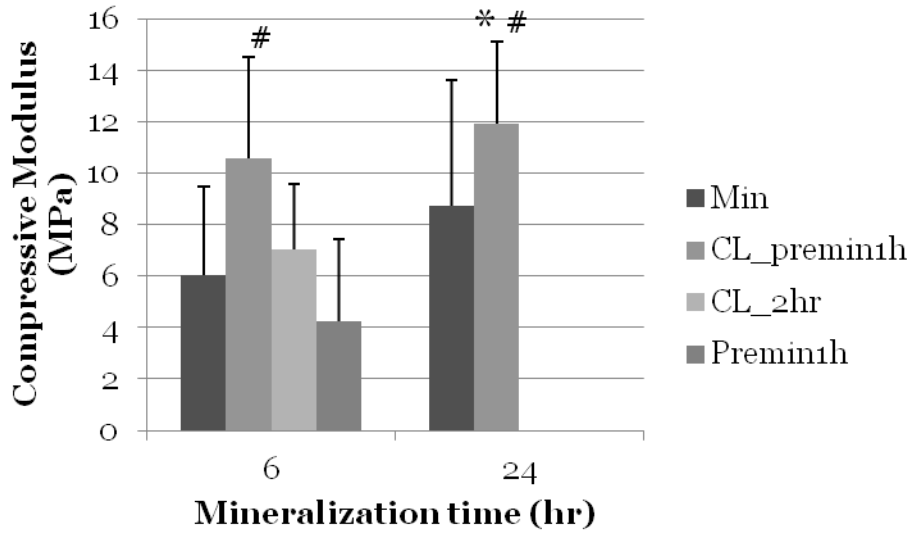


Figure 5.3. Compressive moduli of scaffolds. * - from Min(6hr and 24hr) and Premin1h , # - from Premin1h ($p < 0.05$)

Scaffolds mineralized only (6hr and 24hr) and cross-linked scaffolds (6hr) had significantly higher yield stresses than scaffolds that were premineralized first. Also, scaffolds that were cross-linked only and mineralized only for 6hr had significantly higher yield stress than scaffolds cross-linked and premineralized.

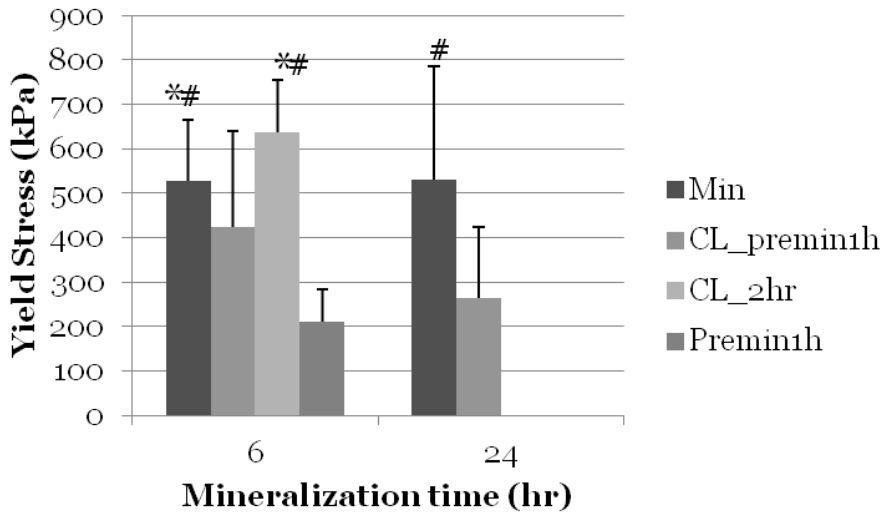


Figure 5.4. Compressive yield stress of scaffolds. * - than CL_Premin1h (6hr) and Premin1hr; # - than Premin1h (p<0.05)

5.4.3. Mineral Ash Weights

Mineral ash weights were determined to quantify the amount of mineral present on the scaffolds. Two groups of scaffolds were analyzed: mineralized only and cross-linked and premineralized scaffolds. Two mineralization times, 6 hr and 24 hr, were investigated. Mineral ash weights of the scaffolds were recorded and shown in Table 5.1. Combination of cross-linking and premineralization treatment resulted in significant increase in mineral deposition both after 6 and 24 hrs of mineralization. Mineral deposition increased with increased mineralization time, as expected.

Table 5.1. Mineral ash weight percentages

Mineralization time	No treatment	CL_Premin1h
6hr	5.51%±3.10%	15.81%±1.87%
24hr	20.55%±2.54%	33.62%±3.69%

5.5. DISCUSSION

In this study we electrospun osteon-like scaffolds onto rotating PEO microfibers. The individual electrospun osteon-like scaffolds were successfully heat sintered into 3D scaffolds that mimic the organization of cortical bone. Mineralization by soaking in 10X SBF dissolved PEO core fibers out individual osteons, leaving behind a system of channels that run along the length of the scaffolds. Cross-linking of the gelatin prior to the mineralization of the scaffolds helped keep the channels of the osteons from collapsing during dissolution of PEO fibers. A premineralization treatment was introduced consisting of mineralizing all individual osteon scaffolds and electrospun mats for 1 hour, prior to heat sintering. The goal was to introduce mineral particles to serve as seeds once the scaffolds are heat sintered into 3D structures. However the premineralization treatment resulted in the dissolution of PEO and collapse of the channels in the scaffolds Figure 5.2 B. Cross-linking the gelatin prior to the premineralization treatment helped keep the channels open and allow mineral deposition on the inside of the channels (Figure 5.2 D and F). Combination of premineralization and cross-linking treatments resulted in better mineral distribution inside the channels of the scaffolds and more mineral overall compared to just mineralization alone, both after 6 hr and 24 hr of mineralization.

Amount of mineral deposited was quantified by determining mineral ash weights of the scaffolds. While increased mineralization time increased mineral deposition, combination of premineralization and cross-linking resulted in significant increase in mineral deposit

We evaluated compressive mechanical properties of the scaffolds and different treatments. Cross-linking of gelatin combined with premineralization significantly increased compressive moduli over mineralization alone after 24 hours and over premineralization alone, after 6 hours of mineralization. Premineralization may affect the mechanics by increasing the overall amount of mineral in the scaffolds and also improving the distribution, as seen in the alizarin red stains. However, presence of the mineral can interfere with binding of the layers during the heat sintering process. Cross-linking of the gelatin may also contribute to the increase in scaffold mechanical strength. Gelatin is water soluble, and without cross-linking process can be dissolved and lost from the scaffolds [22-24]. Electrospun gelatin is commonly cross-linked in glutaraldehyde vapor, which is also a commonly used cross-linking method for electrospun collagen. The cross-linking by glutaraldehyde occurs between the carboxyl groups on the

glutaraldehyde and the amine groups of the gelatin [24]. Gelatin was also found to increase tensile mechanical properties of the electrospun scaffolds, as shown in Chapter 2 [25]. So the cross-linking process is preserving the gelatin and could be contributing to mechanical properties of the scaffolds.

5.6. CONCLUSION

In this study we successfully fabricated three dimensional electrospun scaffolds composed of heat sintered individual osteon like scaffolds. The scaffolds contained a system of channels running parallel to the length of the scaffolds, as found naturally in the haversian systems of bone tissue. Cross-linking of the gelatin prior to the mineralization of the scaffolds has helped keep the channels of the osteons from collapsing during dissolution of PEO fibers. Combination of cross-linking and premineralization significantly increased overall amount of mineral and mineral distribution in the scaffolds, and also improved compressive moduli of the scaffolds. These scaffolds will be investigated further as scaffolds of bone tissue engineering.

5.7. REFERENCES

1. Chen, J., B. Chu, and B.S. Hsiao, *Mineralization of hydroxyapatite in electrospun nanofibrous poly(L-lactic acid) scaffolds*. J Biomed Mater Res A, 2006. **79**(2): p. 307-17.
2. An, Y.H., S.K. Woolf, and R.J. Friedman, *Pre-clinical in vivo evaluation of orthopaedic bioabsorbable devices*. Biomaterials, 2000. **21**(24): p. 2635-52.
3. Ritchie, R.O., *How does human bone resist fracture?* Ann N Y Acad Sci. **1192**(1): p. 72-80.
4. Rho, J.Y., L. Kuhn-Spearing, and P. Zioupos, *Mechanical properties and the hierarchical structure of bone*. Med Eng Phys, 1998. **20**(2): p. 92-102.
5. Beniash, E., *Biomaterials-hierarchical nanocomposites: the example of bone*. Wiley Interdiscip Rev Nanomed Nanobiotechnol.
6. Cowin, S.C. and S.B. Doty, *Tissue mechanics*. 2007, New York, NY: Springer. xvi, 682 p.
7. Borden, M., et al., *Structural and human cellular assessment of a novel microsphere-based tissue engineered scaffold for bone repair*. Biomaterials, 2003. **24**(4): p. 597-609.
8. Borden, M., et al., *Tissue engineered microsphere-based matrices for bone repair: design and evaluation*. Biomaterials, 2002. **23**(2): p. 551-9.
9. Wei, G. and P.X. Ma, *Structure and properties of nano-hydroxyapatite/polymer composite scaffolds for bone tissue engineering*. Biomaterials, 2004. **25**(19): p. 4749-57.
10. Wang, X., G. Song, and T. Lou, *Fabrication and characterization of nano composite scaffold of poly(L-lactic acid)/hydroxyapatite*. J Mater Sci Mater Med. **21**(1): p. 183-8.
11. Ma, P.X. and R. Zhang, *Microtubular architecture of biodegradable polymer scaffolds*. J Biomed Mater Res, 2001. **56**(4): p. 469-77.
12. Lu, L., et al., *In vitro and in vivo degradation of porous poly(DL-lactic-co-glycolic acid) foams*. Biomaterials, 2000. **21**(18): p. 1837-45.
13. Chen, V.J. and P.X. Ma, *Nano-fibrous poly(L-lactic acid) scaffolds with interconnected spherical macropores*. Biomaterials, 2004. **25**(11): p. 2065-73.
14. Yang, S., et al., *The design of scaffolds for use in tissue engineering. Part I. Traditional factors*. Tissue Eng, 2001. **7**(6): p. 679-89.
15. Stevens, B., et al., *A review of materials, fabrication methods, and strategies used to enhance bone regeneration in engineered bone tissues*. J Biomed Mater Res B Appl Biomater, 2008. **85**(2): p. 573-82.
16. Rezwani, K., et al., *Biodegradable and bioactive porous polymer/inorganic composite scaffolds for bone tissue engineering*. Biomaterials, 2006. **27**(18): p. 3413-31.
17. Liu, X. and P.X. Ma, *Polymeric scaffolds for bone tissue engineering*. Ann Biomed Eng, 2004. **32**(3): p. 477-86.
18. Andric, T., A.C. Sampson, and J.W. Freeman, *Fabrication and characterization of electrospun osteon mimicking scaffolds for bone tissue engineering*. Materials Science & Engineering C-Materials for Biological Applications, 2011. **31**(1): p. 2-8.
19. Wright, L.D., et al., *Fabrication and mechanical characterization of 3D electrospun scaffolds for tissue engineering*. Biomed Mater. **5**(5): p. 055006.
20. Andric, T., L.D. Wright, and J.W. Freeman, *Rapid Mineralization of Electrospun Scaffolds for Bone Tissue Engineering*. J Biomater Sci Polym Ed.
21. Tas, A.C. and S.B. Bhaduri, *Rapid coating of Ti6Al4V at room temperature with a calcium phosphate solution similar to 10x simulated body fluid*. Journal of Materials Research, 2004. **19**(9): p. 2742-2749.

22. Heydarkhan-Hagvall, S., et al., *Three-dimensional electrospun ECM-based hybrid scaffolds for cardiovascular tissue engineering*. *Biomaterials*, 2008. **29**(19): p. 2907-14.
23. Sisson, K., et al., *Fiber diameters control osteoblastic cell migration and differentiation in electrospun gelatin*. *J Biomed Mater Res A*. **94**(4): p. 1312-20.
24. Sisson, K., et al., *Evaluation of cross-linking methods for electrospun gelatin on cell growth and viability*. *Biomacromolecules*, 2009. **10**(7): p. 1675-80.
25. Gupta, D., et al., *Nanostructured biocomposite substrates by electrospinning and electrospraying for the mineralization of osteoblasts*. *Biomaterials*, 2009. **30**(11): p. 2085-94.
26. Zhang, Y., et al., *Electrospinning of gelatin fibers and gelatin/PCL composite fibrous scaffolds*. *J Biomed Mater Res B Appl Biomater*, 2005. **72**(1): p. 156-65.

Chapter 6

Fabrication and Characterization of Complete Electrospun Scaffolds for Bone Tissue Engineering

Tea Andric, Abby R. Whittington, Joseph W. Freeman

6.1. ABSTRACT

Skeletal loss and bone deficiencies are major worldwide problem that is only expected to increase due to increase in aging population. As current standards in treatment autografts and allografts are not without drawbacks, there is a need for alternative bone grafts substitutes. A large number of scaffold fabrications techniques are being investigated for applications in tissue engineering of bone, but very few techniques and approaches have focused on creating scaffolds that mimic organization and properties of cortical bone tissue. In this study, we combined two previously fabricated structures, sintered electrospun sheets and individual osteon-like scaffolds, to create scaffolds that mimic dual structural organization of natural bone with cortical and trabecular regions. Scaffolds were successfully mineralized in 10X SBF up to 48 hr with good mineral distribution throughout the scaffolds. Mineralization for 24 hr significantly increased mechanical properties of the scaffolds, both yield stress and compressive modulus. Scaffolds were found to support cellular attachment and proliferation over 28 days in culture, but scaffolds mineralized for 24hr were found to better support osteoblastic differentiation and mineral deposition.

6.2. INTRODUCTION

Skeletal loss and bone deficiencies are major worldwide problem that is only expected to increase due to increase in aging population. It is estimated that over 600,000 procedures are performed in the US alone annually, with market estimated at 2.5 billion annually [1, 2] . Although the current standard in orthopedic reconstructive surgeries, autograft, has high success rates, it is not without drawbacks, namely limited supply and donor site morbidity. Although the use of alternative graft option, allograft, eliminates the potential drawbacks of the autografts, they do have the limitations of their own, such as chance of disease transmission and high failure

rates. As current standards in treatment are not without drawbacks, there is a need for alternative bone grafts substitutes.

Structurally, bone is organized into two distinct types: trabecular (or cancellous) and cortical (or compact) bone. The two types of bone are distinguished by their degree of porosity. Cortical bone is highly organized, dense and compact and is usually found on the outside of the bone. Cortical bone is composed of tightly packed units, called osteons, oriented parallel along to the axis of the bone. Osteons are composed of concentric layers of mineralized collagen fibers around central channel, haversian canal, where vasculature and nerves are housed [3-5]. Osteons can range from 100 to 300 μm in diameter [3, 4]. The high organization and compact nature provide excellent micro-crack propagation prevention and high tensile and compressive mechanical properties. Trabecular bone is generally found surrounded by cortical bone. Trabecular bone is often referred to as spongy bone, due to extensive interconnected network of pores, with porosity as high as 90% [4, 6, 7]. The variation in bone structure results in a wide range of mechanical properties. Cortical bone has compressive and tensile strengths in the range of 167-215 MPa and 107-140 MPa respectively, and the Young's modulus is 10-20 GPa [6]. Trabecular bone has compressive strength in the range of 3- 9 MPa, and Young's modulus of 0.01 – 0.9 GPa [6]

A large number of scaffold fabrications techniques are being investigated for applications in tissue engineering of bone [8-13]. Some important properties of the scaffolds should be noted when comparing different techniques, namely average pore size, porosity, pore interconnectivity and mechanical properties. Porosity and interconnectivity play an important role in tissue regeneration, as it is necessary for migration and proliferation of the cells and tissue formation within the scaffolds. Higher porosities and larger pore sizes enhance bone ingrowth and osteointegration; optimal pores sizes for scaffolds have been reported to range from 100-300 μm [8, 13-16]. While macroporosity is important for tissue integration, microporosity and surface roughness also play a role in cellular attachment, proliferation, and differentiation [8, 13-16]. Some of the techniques currently investigated for scaffold fabrications include thermally induced phase separation, solvent casting/particulate leaching, heat sintering microspheres, and electrospinning.

Thermally induced phase separation (TIPS) is a technique used to create highly porous 3-D scaffolds by dissolving polymer in a solvent at a higher temperature and then inducing liquid-liquid or liquid-solid phase separation by lowering the temperature. Porosity, pore size and pore orientation is controlled by controlling polymer concentration and temperature gradient [9, 17, 18]. Solvent casting/particulate leaching is a scaffold fabrication technique where water soluble particles or paraffin are used as space holders for future pore networks, while polymer solution is cast around them. After the solvent is evaporated and polymer set, the porogens are leached out leaving a pore network behind. Porosity and pore size is controlled by controlling porogen size [19-21]. While the use of porogens provides the control of pore size and porosity, interconnectivity of the pores can still be a problem [9, 10, 19, 20, 22]. Heat sintering is a technique where the polymer microspheres are heated above glass transition (T_g) of polymer and held for certain period of time, and then cooled down to room temperature. During the heating process, the sintering occurs due to the intertwining of polymer chains between adjacent microspheres, forming bonds. By controlling the size of the microspheres and heat sintering time, the pore size and porosity can be controlled [23-25]. Each processing technique has advantages and disadvantages for applications in bone tissue engineering, but all the techniques seek to create scaffolds that have uniform structure and porosity throughout the scaffolds, unlike the natural dual organization in natural bone. Very few techniques and approaches have focused on creating scaffolds that mimic dual structural organization found in natural bone tissue [26, 27].

In this study, we will focus on fabricating scaffolds that mimic both structures of the bone, cortical and trabecular. To do this we will utilize the electrospinning technique, which can create nanofiber scaffolds that mimic natural extracellular matrix. Electrospun scaffolds are characterized by high surface area, high porosities, and interconnected pore networks [28, 29]. However, electrospun scaffolds were limited to two dimensional structures and as a result very little to no characterization has been performed to determine the compressive mechanical properties of these scaffolds. Our group has characterized heat sintering technique for electrospun scaffolds, which has allowed us to us to investigate and tune compressive mechanical properties of these scaffolds. It also allows us to combine different electrospun structures to create unique and more tailored scaffold architectures. We combined two previously

fabricated structures, sintered electrospun sheets and individual osten-like scaffolds [30], to create scaffolds that mimic dual structural organization of natural bone with cortical and trabecular regions. Scaffolds will be mineralized by incubation in 10X SBF and characterized to determine mechanical properties, mineral deposition and distribution, and cellular activity on the scaffolds.

6.3. MATERIALS AND METHODS

6.3.1. *Electrospinning*

Poly (L-lactide) (PLLA) (inherent viscosity =2.0 dl/g, Mw = 152,000) was purchased from Sigma Aldrich (St. Louis, MO, USA). Poly (D, L-lactide) (PDLA) (inherent viscosity 0.6-0.8 dL/g) was purchased from SurModics Pharmaceuticals (Birmingham, AL, USA). Dichloromethane (DCM), tetrahydrofuran (THF), and dimethylformaldehyde (DMF) were purchased from Fisher Scientific (Pittsburgh, PA, USA). Gelatin, type A, from porcine skin was purchased from Sigma Aldrich (St. Louis, MO, USA). NaCl, KCl, CaCl 2H₂O, MgCl₂ 6H₂O, NaHCO₃, and NaH₂PO₄ were purchased from Fisher Scientific (Pittsburgh, PA, USA).

The electrospinning solutions were prepared by dissolving PLLA to 7 % w/v in 75% DCM and 25% DMF, and dissolving PDLA to 22 %w/v in 75% THF and 25%DMF. The PLLA/gelatin mixture was made by dissolving gelatin in 1ml deionized (dI) water and adding it to the 7% PLLA solution. The amount of gelatin in solution is equal to 10 %, w/w of the amount of PLLA in the solution. As two solutions are not miscible, they were vortexed for 1 hr to mix before electrospinning. Polymer solutions were made in 16 ml batches and to make overall volume of gelatin/PLLA and PLLA solutions equal, 1ml of DCM is replaced with 1ml of gelatin.

First, the PDLA solution was loaded into a 5 ml plastic syringe with an 18-gauge needle, and extruded at a rate of 5 mL/h. PDLA was electrospun on a rotating (~ 2000 RPM) 5 cm diameter mandrel for a total volume of 1ml, at a distance of 15cm with voltages of +12kV and -5kV applied. The gelatin/PLLA was then electrospun directly onto the PDLA layer with a working distance of 5 cm. The voltages applied were +18kV and -7kV. An additional layer of 1ml PDLA was electrospun on top of gelatin/PLLA layer.

Poly (ethylene oxide) was dissolved in 10% of 100%ethaonl and 90% of deionized water to 10% w/v solution. The solution was electrospun onto rotating mandrel with 5cm diameter at

rate of 5 ml/hr and working distance of 10 cm. Total volume of 3ml was electrospun with voltages +10V and -3V. The electrospun mats were cut into 3mm wide strips and rolled into fibers that were used for next step.

Individual osteon-like scaffolds were electrospun onto rotating PEO fibers using the set up previously reported [30]. The fibers were placed into set up and placed in front of negatively charged target, as shown. PLLA/gelatin mixture was electrospun first to total volume of 1.5 ml, with following parameters: working distance of 5 cm, at extrusion rate of 5 ml/hr, and voltages of + 17V and -9V. This was followed by electrospinning of PDLA solution in total volume of 0.5 ml with following parameters: working distance of 15 cm, extrusion rate of 5 ml/hr, and voltages of +13 V and -8V.

Gelatin in all the scaffolds was cross-linked in vapor of 2.5% glutaraldehyde for 2 hours.

6.3.2. Heat Sintering of Scaffolds

The complete scaffolds were assembled by heat sintering individual components together at 54°C for 45 min. The final design consisted of “trabecular” core that is 4mm wide which is surrounded by osteon-like segments and wrapped with electrospun sheet to final diameter of 6mm. This provided 2:1 ratio of trabecular to cortical section.

Dual layer PDLA and gelatin/PLLA mats were cut into 1.2 cm strips and rolled to 4mm segments and heat sintered. Osteon-like scaffolds were cut into small segments and placed around the core and everything was wrapped with electrospun sheet. The complete scaffolds were then heat sintered.

6.3.3. Mineralization of Scaffolds

All the scaffolds were mineralized using a previously reported method by incubation in 10X SBF [31, 32]. Briefly, a stock solution was made using NaCl, KCl, CaCl 2H₂O, MgCl₂ 6H₂O, and NaH₂PO₄, and stored at room temperature. Prior to the mineralization process, NaHCO₃ was added while stirring vigorously, resulting in the following ion concentrations: Ca²⁺ 25 mM, HPO₄²⁻ 10 mM, Na⁺ 1.03 M, K⁺ 5 mM, Mg²⁺ 5mM, Cl⁻ 1.065M, and HCO₃⁻ 10mM . The electrospun scaffolds were incubated in 200 ml of 10XSFBF for 6, 24, and 48 hours at room temperature, with mineralizing solution replaced every 2 hours. After being removed from 10X

SBF , all the samples were rinsed in dI water to remove mineral not attached to scaffolds, and vacuum dried overnight.

For the scaffolds with premineralization treatment, individual osteons and electrospun sheets were mineralized for 1 hour, and then rinsed in dI water and vacuum dried overnight. The electrospun pieces were then heat sintered as described above.

6.3.4. Alizarin Red Staining

Mineral deposition and distribution was characterized by the Alizarin red stain. The scaffolds were stained with 40 mM Alizarin red solution for 10 min. The scaffolds were then washed with dI water five times, placed into cryomolds, imbedded in OCT imbedding medium, and frozen at -20°C. The scaffolds were cut into 200µm section using a Cryostat HM 550 (Thermo Scientific Microm, Walldorf, Germany), and imaged using stereoscope (Vision Engineering, New Milford, CT, USA). Scaffolds from the cell study were fixed in 70% ethanol for 1 hr, rinsed in dI water and the same protocol as above was followed.

6.3.5. Mechanical Properties

The scaffolds were mechanically tested in compression using an Instron 5869 with Bioplus Bath (Norwood, MA, USA). The tests were performed in phosphate buffered saline (PBS) (pH= 7.4) at 37°C. Three mineralization times were investigated 6, 24 and 48 hr, and six samples per each group were tested (n=6). The 12mm X 6mm (2:1 height to diameter ratio) scaffolds were tested in compression until failure with a uniform strain rate of 1.2mm/min (10% strain/min). The data was analyzed to determine yield stress and compressive modulus.

6.3.6. Mineral Ash Weights

After the mechanical testing the samples were vacuum dried overnight and used to determine mineral ash weights. After the initial weight of the samples was recorded, the samples were placed in ceramic crucibles, and then placed into a high temperature furnace (Model No. FD1535M, Fisher Scientific, Pittsburgh, PA, USA) at 700°C for 24 hours. After cooling down, the mineral ash weight was recorded and the average mineral percent deposition calculated as ratio of mineral ash weight to samples original weight. Three samples per group were tested (n=3).

6.3.7. Cell Study

Mouse pre-osteoblastic cells (MC3T3-E1, ATCC) were cultured in Alpha Minimum Essential Medium (α -MEM, Cellgro, Mediatech, Manassas, VA, USA) supplemented with 10% fetal bovine serum (FBS, Cellgro, Mediatech, Manassas, VA, USA) and 1% streptomycin/penicillin (Cellgro, Mediatech, Manassas, VA, USA). The scaffolds were cut into 450 μ m sections Cryostat HM 550 (Thermo Scientific Microm, Walldorf, Germany), soaked in DI water overnight and vacuum dried. The scaffolds were then secured into 24-well Ultra-Low Cluster plates (Costar) using Silastic Medical Adhesive (Dow Corning, Midland, MI, USA) and were sterilized in 70% ethanol for 30 minutes followed by exposure to UV light for 30 minutes. The scaffolds were then washed with PBS and soaked in cell culture medium overnight.

Two groups of scaffolds were used, scaffolds mineralized for 24 hr (Min24) and scaffolds that have not been mineralized (Min0). Approximately 100,000 cells were seeded onto each scaffold and were allowed to attach for one hour before adding culture medium to a final volume of 1 ml. After the cells were seeded the media was supplemented with 3mM β -glycerophosphate and 10 μ g/ml of L-ascorbic acid. The media was changed every other day and the cultures were incubated at 37°C in a humidified atmosphere and 5% CO₂. Cells were cultured for a period of 28 days and data was collected on days 7, 14, 21, and 28.

Cell viability was measured using a Cell Titer 96TM Aqueous Solution Cell Proliferation Assay (MTS Assay) (Promega, Madison, WI, USA) on the following scaffolds Min0 (n=6) and Min24(n=6). At each time point (7, 14, 21, and 28 days) the media was removed, then 300 μ l of fresh media and 60 μ l of the MTS solution were added to each well and incubated at 37°C with 5% CO₂ for three hours. After incubation, 300 μ l of the mixture was transferred to a 48-well plate and diluted with 300 μ l of di water. The plate was read at 490 nm using a plate reader. Calibration curve with known cell numbers was performed on the beginning of the study to correlate MTS absorbance values to cell numbers.

6.3.7.1. Osteocalcin ELISA Assay

Osteocalcin (OCN) is a non-collagenous protein produced by mature osteoblasts during later stages of differentiation. It was measured in the media using an ELISA kit from Biomedical

Technologies, Inc (Stoughton, MA). Media samples (n=4) were collected over the course of 28 days and stored at -80°C until the end of study. The assay was performed according to the manufactures instructions and absorbance was read at 450nm. Osteocalcin content is expresses as ng/cell.

6.3.7.2. Alizarin Red and Fluorescence Stain

Mineral deposition and distribution was characterized by the alizarin red stain. At each time point, the scaffolds were washed with PBS and transferred into new well plates. The scaffolds were then fixed in 70% ethanol for 1hr at 4°C, and stained with 40 mM Alizarin red solution for 10 min. The scaffolds were then washed with dI water five times, placed into cryomolds, imbedded in OCT imbedding medium, and frozen at -20°C. The scaffolds were cut into 50µm section using a Cryostat HM 550 (Thermo Scientific Microm, Walldorf, Germany), and imaged using light microscope (Leica Microsystems LAS AF 6000, Bannockburn, IL, USA).

Cellular attachment on the scaffolds was qualitatively observed by fluorescence staining. Scaffolds were fixed in 3.7% paraformaldehyde and 0.5% Triton X-100 at room temperatures and stained with phalloidin and DAPI. The scaffolds were imaged using a fluorescence microscope (Leica Microsystems, Bannockburn, IL, USA).

6.4. RESULTS

In this study we fabricated complete three dimensional electrospun scaffolds and mineralized then by incubation in 10X SBF. The scaffolds were composed of dual structures, inner core surrounded by osteon-like scaffolds, shown in Figure 6.1. The scaffolds were then further characterized to determine mechanical properties, mineral deposition and distribution, and cellular activity on the scaffolds.

6.4.1. Alizarin Red Staining

Mineral distribution across the scaffolds was observed using the alizarin red staining. Staining of the scaffolds was performed two ways, first the scaffolds were stained with alizarin red and then sectioned and imaged, shown in Figure 6.1 A-C, and then scaffolds were also sectioned and individual sections were stained and imaged, shown in Figure 6.2 D-F. When the

scaffolds were stained and then section (Figure 6.1 A-C) mineral can be seen on the outer edges of the scaffolds with some mineral also found on inside of the osteons channels. No major differences can be seen between mineralization times. When the scaffolds were sectioned then stained much more mineral stain can be seen on the scaffolds. After 6hr of mineralization (Figure 6.1 D) mineral can be seen on the outer edges and on the osteons, but absent from the central core. After 24 and 48 hr (Figure 6.1 E and F) scaffolds are completely covered in mineral and no differences can be seen between two mineralization times.

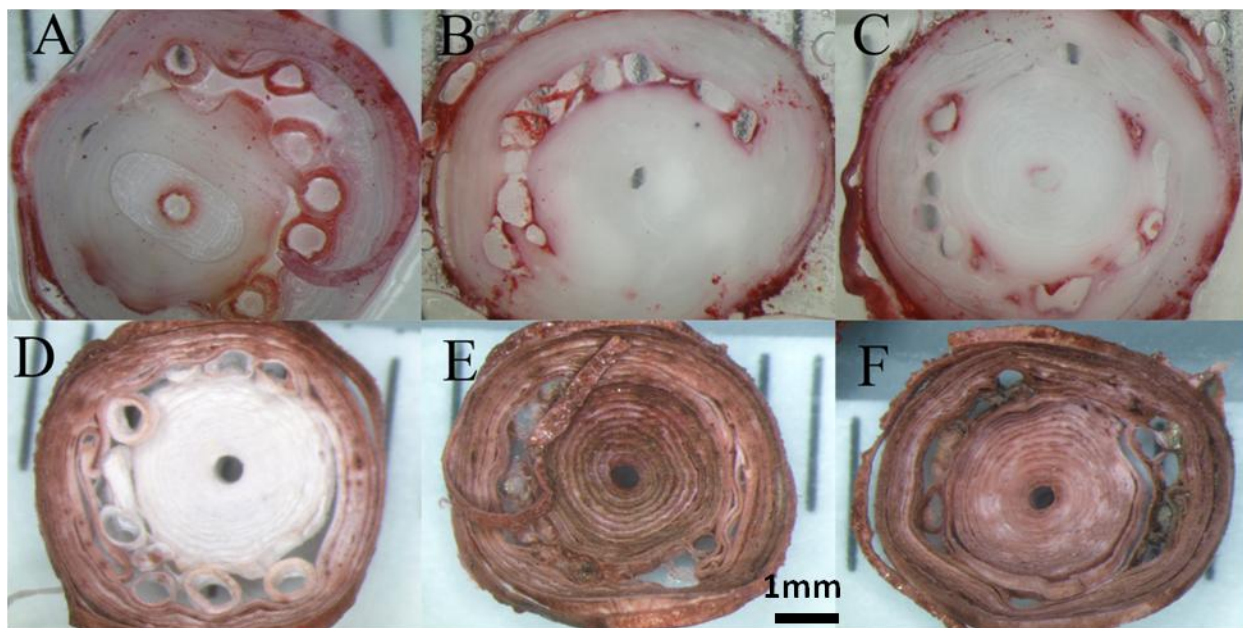


Figure 6.1. Alizarin red staining after 6hr (A, D), 24hr (B, E) and 48 hr(C, F) of mineralization. Scaffolds were stained then sectioned to be imaged (A-C) and also sectioned then stained (D-F)

6.4.2. Mineral Ash Weights

Mineral ash weights were determined to quantify the amount of mineral present on the scaffolds and are shown in table 6.1. Increasing the mineralization time resulted in increase mineral deposition, and each mineralization time point was significantly higher than other two time points.

Table 6.1. Mineral ash weight percentages. Each time point is significantly different from the other two.

Mineralization time (hr)	Mineral Ash Weight
6	6.33%±0.91%
24	17.01%±2.99%
48	26.18%±0.85%

6.4.3. Mechanical Properties

Scaffolds were tested under simulated physiological conditions in compression at 10% strain rate/min. Data was analyzed to determine yield stress and compressive modulus and is shown in Figure 6.2. No significant differences in mechanical properties were seen after 6 hr of mineralization and also between 24 hr and 48 hr of mineralization. Scaffolds mineralized for 24hr and 48hr had significantly higher yield stresses than scaffolds mineralized for 6hr and 0hr. Scaffolds mineralized for 24 hr had significantly higher compressive modulus than non mineralized scaffolds (0hr).

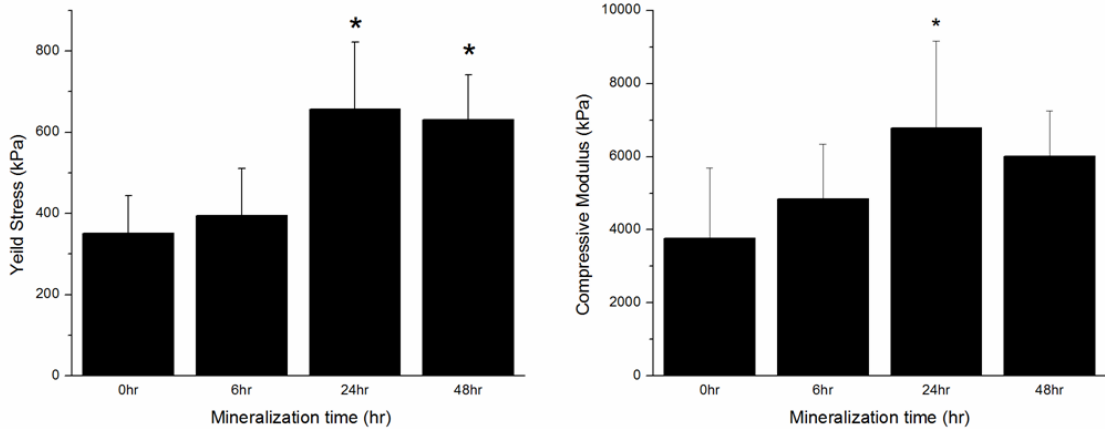


Figure 6.2. Mechanical testing data. * - than 0hr and 6hr mineralization for yield stress, and 0hr mineralization for compressive modulus ($p < 0.05$)

6.4.3. Cell Study

Proliferation of the M3T3-E1 cells on the scaffolds was quantified using MTS assay on days 7, 14, 21, and 28 and the absorbances at 490 nm are shown in Figure 6.3. Over the course of 4 weeks no differences were observed between the groups at any time point. Both groups did experiences significant increase in absorbances over 28 days, Min0 group from day 7 to day 14 to day 21, and Min24 group from day 14 to day 2.

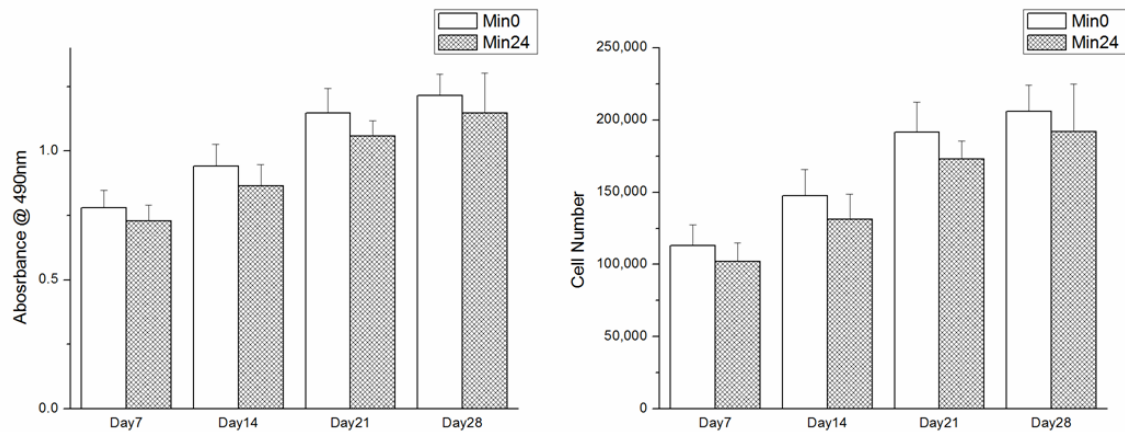


Figure 6.3. MTS absorbances over the 4 week cell study (left) and cell numbers determined from MTS curve (right)

6.4.3.1. Osteocalcin ELISA Assay

Differentiation of osteoblasts was measured by the expression of osteocalcin over the course of the study. Figure 6.4 shows the amount of OCN protein detected in the media as measured by the ELISA kit and normalized by cell numbers. There was an increase in OCN secretion during the last two weeks of the study. Also, there was significant increase in OCN secretion on mineralized scaffolds during days 18-20 and 25-27.

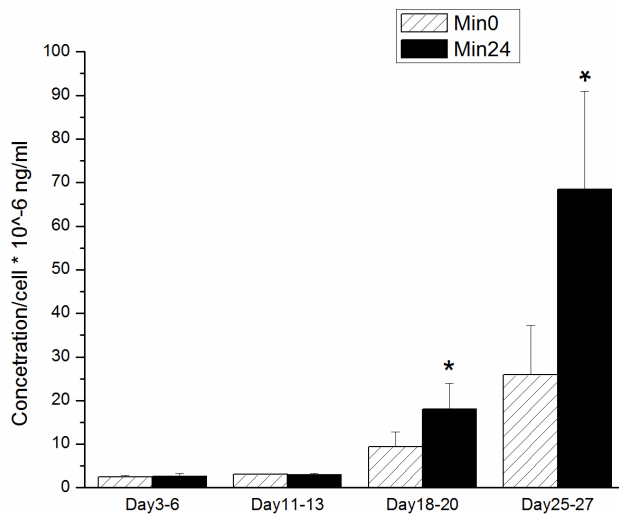


Figure 6.4. Secreted OCN protein in cell culture media. Results normalized by cell numbers determined by MTS assay. * - significantly different than Min0 ($p < 0.05$)

6.4.3.2. Alizarin Red and Fluorescence Stain

At each time point during the cell study, the scaffolds were fixed and stained with alizarin red to visualize mineral deposition and distribution. The pictures are shown in the Figure 6.5. On day 0, prior to the start of the study, small amount of mineral can be seen on Min0 scaffold from the premineralization treatment and much greater amount of mineral can be seen on Min24 scaffolds. Over the course of study increased amount of mineral can be seen both scaffold types, but overall Min24 scaffolds seem to have more mineral present.

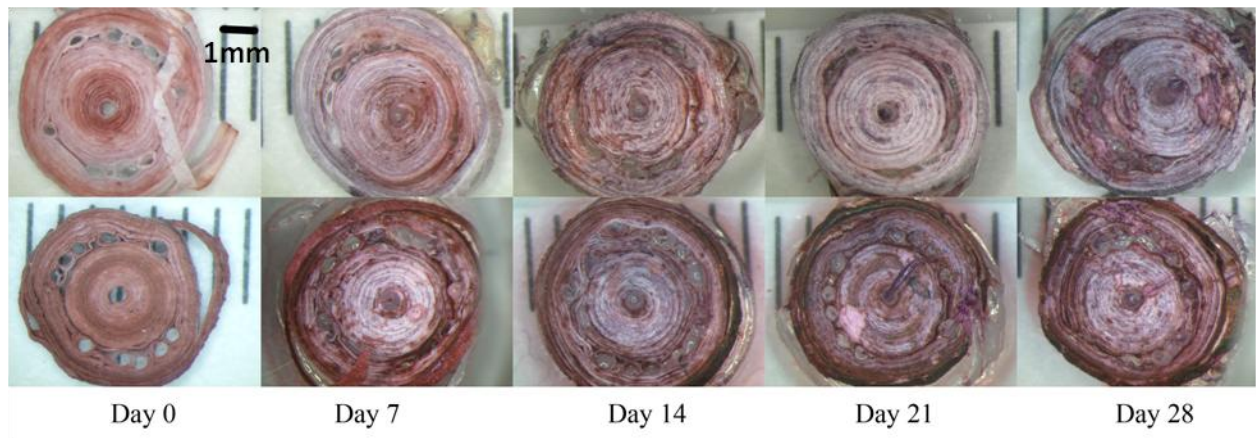


Figure 6.5. Alizarin red stain pictures of scaffolds Min0 (top) and Min24 (bottom) over period of 28 days

Scaffolds were fluorescently stained to visualize cellular attachment and distribution on the scaffolds. Thickness and rough surfaces of the scaffolds it made focusing difficult. Cells can be seen on the edges of the scaffolds and also mostly on the inside of the osteon channels (Figure 6.6).

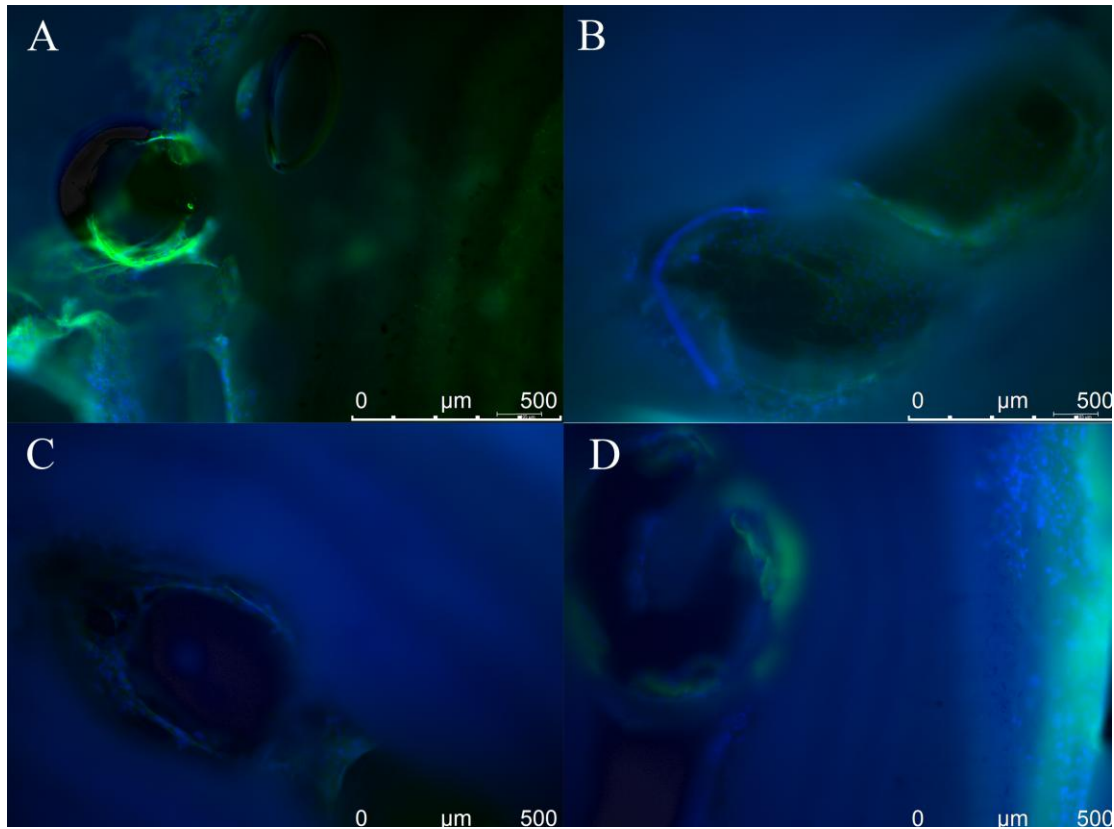


Figure 6.6. Fluorescence stain of actin (green) and nuclei (blue) after 21 days (A, B) and 28 days (C,D) on scaffolds Min0 (A,C) and Min24(B,D)

6.5. DISCUSSION

In this study we have fabricated complete three dimensional electrospun scaffolds and mineralized then by incubation in 10X SBF. The scaffolds were composed of dual structures, inner core composed of wrapped electrospun sheets surrounded by osteon-like scaffolds and which can be seen in Figure 6.1, which mimics natural bone organization. Few attempts have been made to create dual structure scaffolds. One includes biphasic foam scaffolds where degree of porosity varies, with denser scaffolds found in the middle surrounded by outer ring with higher degree of porosity. The scaffolds are made by heat sintering HA particles over porous polymeric sponges at very high temperatures, thus making them not biodegradable [26, 27].

The Figure 6.1 also shows alizarin red stains of mineral on scaffolds that were stained before and after sectioning the scaffolds. When the scaffolds were stained before sectioning, some mineral can be seen on the edges and inside the channels, but overall no major differences

can be observed between mineralization times. When the scaffolds were sectioned and stained, much more mineral can be seen especially on the 24h and 48hr mineralized scaffolds, which are completely covered. When we compared the amount of mineral found on the scaffolds, each mineralization time was significantly higher than the previous one. So while there is a difference in the amount of mineral present between 24hr and 48hr scaffolds, no differences can be seen in the mineral distribution.

Scaffolds were tested under simulated physiological conditions in compression at 10% strain rate/min to determine mechanical properties. Significant increase in mechanical properties was observed after 24 hr of mineralization both in compressive modulus and yield stress. Presence of mineral has significantly increased the mechanical properties. No differences in mechanical properties were seen between 24hr and 48hr mineralization times. While there is a difference in mineral amount, no differences in mechanical properties were observed most likely due to nonuniform mineral distribution throughout the scaffolds. This is commonly seen with scaffolds that are mineralized by static incubation in SBF. Teo et al. utilized a flow chamber to mineralize electrospun scaffolds by alternately immersing them in CaCl_2 and Na_2HPO_4 . This resulted in a more uniform deposition throughout the scaffold, and showed that mineral distribution is more important than overall mineral amount in the scaffolds [33].

Cellular attachment and proliferation was evaluated as mitochondrial activity as measured by the MTS assay over the period of 4 weeks. Over the course of the study both groups of scaffolds supported proliferation of MC3T3-E1 cells, as significant increase in absorbances were observed. Based on the cell numbers as determined by MTS assay, the population of cells doubled after 28 days. However, no differences between mineralized and nonmineralized scaffolds were observed. Similar results were seen in previous work [30, 31] and work published by White et al. [34]. This can be explained by competing processes of proliferation and differentiation in osteoblasts, where one decreases as the other increases [35]. Our results for the expression of OCN protein confirm shown in Figure 6.4 further confirm this. Scaffolds that have been mineralized show significantly higher levels of secreted OCN protein, a most abundant non-collagenous protein found in bone expressed by differentiated osteoblasts. By the end of

study, OCN expression on mineralized scaffolds was almost two-fold higher than non mineralized scaffolds. This finding is consistent by the results previously reported [34, 36].

At the end of each week, scaffolds were fixed and stained with alizarin red to visualize the mineral deposition on the scaffolds (Figure 6.5). Over the course of the cell study, non mineralized scaffolds that starts with very little mineral become much more mineralized, especially around osteon channels. Mineralized scaffolds had much more mineral to start with, but over the course of the study, certain areas seemed to have much more, namely edges and osteon channels. This shows that cells on cite mineralized the matrix, which was previously observed in our work [30] and also published work[34].

Scaffolds were also fluorescently labeled for actin filaments and nuclei to visualize cell attachment and position/distribution. Cells were mostly found on the inside of the osteon channels, as shown in Figure 6.6, and also on the edges of the scaffolds. Lack of cells on the center regions could be explained by the loss of microfiber morphologies due to cryostat sectioning of the scaffolds. As the cutting is performed at -20°C , it can result in plastic deformation of fibers. Loss of microfiber morphology can be seen on SEM of cryostat sectioned scaffolds (Figure 6.7). So the insides of the osteon channels and outside edges could be the only regions there electrospun fiber morphology was preserved. However, we do not foresee this being a problem in the future, as these scaffold were only sectioned for the purposes of this study.

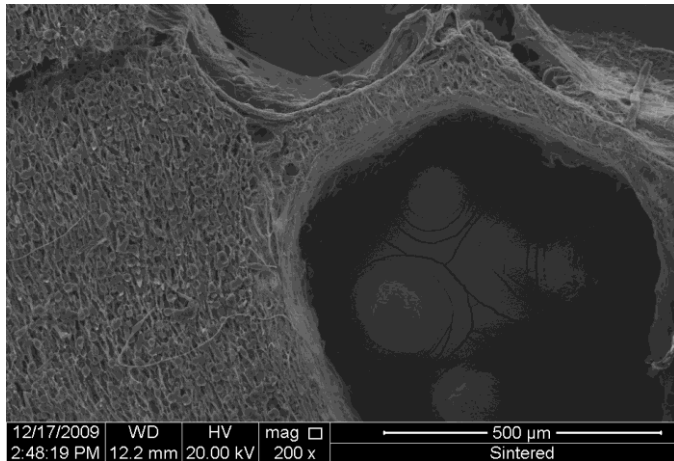


Figure 6.7. SEM image of scaffolds sectioned using cryostat where fiber fusion is visible on the surface.

6.6. CONCLUSION

In this study we have successfully fabricated complete three dimensional electrospun scaffolds that were composed of dual structures, inner core composed of wrapped electrospun sheets surrounded by osteon-like scaffolds. Scaffolds were successfully mineralized in 10X SBF up to 48 hr and showed good mineral distribution throughout the scaffolds. Mineralization for 24 hr significantly increased mechanical properties of the scaffolds, both yield stress and compressive modulus under physiological conditions. Both scaffolds were found to support cellular attachment and proliferation over 28 days in culture, but scaffolds mineralized for 24hr were found to better support osteoblastic differentiation and mineral deposition.

6.7. REFERENCES

1. Hing, K.A., *Bone repair in the twenty-first century: biology, chemistry or engineering?* Philos Transact A Math Phys Eng Sci, 2004. **362**(1825): p. 2821-50.
2. Giannoudis, P.V., H. Dinopoulos, and E. Tsiridis, *Bone substitutes: an update.* Injury, 2005. **36 Suppl 3**: p. S20-7.
3. Ritchie, R.O., *How does human bone resist fracture?* Ann N Y Acad Sci. **1192**(1): p. 72-80.
4. Rho, J.Y., L. Kuhn-Spearing, and P. Zioupos, *Mechanical properties and the hierarchical structure of bone.* Med Eng Phys, 1998. **20**(2): p. 92-102.
5. Beniash, E., *Biomaterials-hierarchical nanocomposites: the example of bone.* Wiley Interdiscip Rev Nanomed Nanobiotechnol.
6. An, Y.H. and R.A. Draughn, *Mechanical testing of bone and the bone-implant interface.* 2000, Boca Raton, Fla.: CRC Press. 624 p.
7. Cowin, S.C. and S.B. Doty, *Tissue mechanics.* 2007, New York, NY: Springer. xvi, 682 p.
8. Khan, Y., et al., *Tissue engineering of bone: material and matrix considerations.* J Bone Joint Surg Am, 2008. **90 Suppl 1**: p. 36-42.
9. Liu, X. and P.X. Ma, *Polymeric scaffolds for bone tissue engineering.* Ann Biomed Eng, 2004. **32**(3): p. 477-86.
10. Rezwani, K., et al., *Biodegradable and bioactive porous polymer/inorganic composite scaffolds for bone tissue engineering.* Biomaterials, 2006. **27**(18): p. 3413-3431.
11. Stevens, B., et al., *A review of materials, fabrication methods, and strategies used to enhance bone regeneration in engineered bone tissues.* J Biomed Mater Res B Appl Biomater, 2008. **85**(2): p. 573-82.
12. Yang, S., et al., *The design of scaffolds for use in tissue engineering. Part I. Traditional factors.* Tissue Eng, 2001. **7**(6): p. 679-89.
13. Yu, N.Y., et al., *Biodegradable poly(alpha-hydroxy acid) polymer scaffolds for bone tissue engineering.* J Biomed Mater Res B Appl Biomater. **93**(1): p. 285-95.
14. Hutmacher, D.W., et al., *State of the art and future directions of scaffold-based bone engineering from a biomaterials perspective.* J Tissue Eng Regen Med, 2007. **1**(4): p. 245-60.
15. Karageorgiou, V. and D. Kaplan, *Porosity of 3D biomaterial scaffolds and osteogenesis.* Biomaterials, 2005. **26**(27): p. 5474-91.
16. Stylios, G., T. Wan, and P. Giannoudis, *Present status and future potential of enhancing bone healing using nanotechnology.* Injury, 2007. **38 Suppl 1**: p. S63-74.
17. Ma, P.X. and R. Zhang, *Microtubular architecture of biodegradable polymer scaffolds.* J Biomed Mater Res, 2001. **56**(4): p. 469-77.
18. Maquet, V., et al., *Porous poly(alpha-hydroxyacid)/Bioglass composite scaffolds for bone tissue engineering. I: Preparation and in vitro characterisation.* Biomaterials, 2004. **25**(18): p. 4185-94.
19. Chen, V.J. and P.X. Ma, *Nano-fibrous poly(L-lactic acid) scaffolds with interconnected spherical macropores.* Biomaterials, 2004. **25**(11): p. 2065-73.
20. Liao, C.J., et al., *Fabrication of porous biodegradable polymer scaffolds using a solvent merging/particulate leaching method.* J Biomed Mater Res, 2002. **59**(4): p. 676-81.

21. Lu, L., et al., *In vitro and in vivo degradation of porous poly(DL-lactic-co-glycolic acid) foams*. *Biomaterials*, 2000. **21**(18): p. 1837-45.
22. An, Y.H., S.K. Woolf, and R.J. Friedman, *Pre-clinical in vivo evaluation of orthopaedic bioabsorbable devices*. *Biomaterials*, 2000. **21**(24): p. 2635-2652.
23. Borden, M., et al., *Tissue engineered microsphere-based matrices for bone repair: design and evaluation*. *Biomaterials*, 2002. **23**(2): p. 551-9.
24. Borden, M., et al., *Structural and human cellular assessment of a novel microsphere-based tissue engineered scaffold for bone repair*. *Biomaterials*, 2003. **24**(4): p. 597-609.
25. Lv, Q., L. Nair, and C.T. Laurencin, *Fabrication, characterization, and in vitro evaluation of poly(lactic acid glycolic acid)/nano-hydroxyapatite composite microsphere-based scaffolds for bone tissue engineering in rotating bioreactors*. *J Biomed Mater Res A*, 2009. **91**(3): p. 679-91.
26. Shah, A.R., et al., *Migration of Co-cultured Endothelial Cells and Osteoblasts in Composite Hydroxyapatite/Poly(lactic acid) Scaffolds*. *Annals of Biomedical Engineering*, 2011. **39**(10): p. 2501-2509.
27. Son, J.S., et al., *Hydroxyapatite/poly(lactide) biphasic combination scaffold loaded with dexamethasone for bone regeneration*. *Journal of Biomedical Materials Research Part A*, 2011. **99A**(4): p. 638-647.
28. Jang, J.H., O. Castano, and H.W. Kim, *Electrospun materials as potential platforms for bone tissue engineering*. *Adv Drug Deliv Rev*, 2009. **61**(12): p. 1065-83.
29. Liao, S., et al., *Processing nanoengineered scaffolds through electrospinning and mineralization suitable for biomimetic bone tissue engineering*. *J Mech Behav Biomed Mater*, 2008. **1**(3): p. 252-60.
30. Andric, T., A.C. Sampson, and J.W. Freeman, *Fabrication and characterization of electrospun osteon mimicking scaffolds for bone tissue engineering*. *Materials Science & Engineering C-Materials for Biological Applications*, 2011. **31**(1): p. 2-8.
31. Andric, T., L.D. Wright, and J.W. Freeman, *Rapid Mineralization of Electrospun Scaffolds for Bone Tissue Engineering*. *J Biomater Sci Polym Ed*.
32. Tas, A.C. and S.B. Bhaduri, *Rapid coating of Ti6Al4V at room temperature with a calcium phosphate solution similar to 10x simulated body fluid*. *Journal of Materials Research*, 2004. **19**(9): p. 2742-2749.
33. Teo, W.E., et al., *Fabrication and characterization of hierarchically organized nanoparticle-reinforced nanofibrous composite scaffolds*. *Acta Biomater*. **7**(1): p. 193-202.
34. Whited, B.M., et al., *Pre-osteoblast infiltration and differentiation in highly porous apatite-coated PLLA electrospun scaffolds*. *Biomaterials*, 2011. **32**(9): p. 2294-2304.
35. Owen, T.A., et al., *Progressive development of the rat osteoblast phenotype in vitro: reciprocal relationships in expression of genes associated with osteoblast proliferation and differentiation during formation of the bone extracellular matrix*. *J Cell Physiol*, 1990. **143**(3): p. 420-30.
36. Chou, Y.F., J.C. Dunn, and B.M. Wu, *In vitro response of MC3T3-E1 pre-osteoblasts within three-dimensional apatite-coated PLGA scaffolds*. *J Biomed Mater Res B Appl Biomater*, 2005. **75**(1): p. 81-90.

Chapter 7

Conclusions and Future Directions

7.1. PROJECT CONCLUSIONS

The objective of this project was to utilize electrospinning and heat sintering techniques to create biodegradable full thickness three dimensional biomimetic polymeric scaffolds with macro and nano architecture similar to natural bone for bone tissue engineering. This was achieved by completing series of studies which are summarized below.

First we investigated different techniques to enhance calcium phosphate mineral precipitation onto electrospun PLLA scaffolds when incubated in concentrated simulated body fluid (SBF) 10XSBF. The techniques included the use of vacuum, pretreatment with 0.1M NaOH, and electrospinning gelatin/PLLA blends as means to increase overall mineral precipitation and distribution throughout the scaffolds. Two treatment regimen, pretreatment with NaOH and incorporation of 10% gelatin into PLLA solution, both in combination with vacuum, resulted in significantly higher degrees of mineralization (16.79% and 14.9%, respectively) and better mineral distribution on surfaces and through the cross-sections after 2 hours of exposure to SBF. Mineral on the scaffolds was indentified to be mixture of brushite and hydroxyapatite. While both scaffolds had similar mineral content, 10%gelatin/PLLA scaffolds had significantly higher yield stress (1.73 MPa vs. 0.56MPa) and elastic modulus (107MPa vs. 44MPa) than NaOH pretreated scaffolds. Pretreatment of PLLA scaffolds with NaOH resulted in scaffold degradation and decreased mechanical properties. Both scaffolds were found to support cell attachment and proliferation over the period of 4 weeks. But overall, mixture of 10% gelatin and PLLA resulted in the significantly higher degree of mineralization, increased mechanical properties, and scaffolds that supported cellular adhesion and proliferation.

Next, we applied a heat sintering technique to fabricate 3D electrospun scaffolds that were used to evaluate effects of mineralization and fiber orientation on scaffold strength. We electrospun PLLA/gelatin scaffolds with a layer of PDLA, and heat sintered them into three dimensional cylindrical scaffolds. Scaffolds were mineralized by incubation in 10X simulate body fluid for 6h, 24h, and 48 h to evaluate the effect of mineralization on scaffolds mechanical

properties. The effects of heat sintering hydroxyapatite (HA) microparticles directly to the scaffolds on mineral deposition, distribution and mechanical properties of the scaffolds were also evaluated. Fiber orientation can make a slight difference in nanofibrous scaffold compressive mechanical properties, but this difference is not as profound as the difference seen with increased mineralization. On the other hand, the use of HA microparticles can interfere with nanofiber sintering and decrease scaffold strength, but had significant effect on the mineral deposition on PLLA/gelatin scaffolds. In addition, the use of static mineralization techniques limits the depth of mineralization into the scaffold.

The next part of the project was to develop a technique to fabricate scaffolds that mimic the organization of an osteon, the structural unit of cortical bone. We successfully built a rotating stage for PGA fibers and utilized it for collecting electrospun nanofibers and creating scaffolds. Resulting scaffolds consisted of concentric layers of electrospun PLLA or gelatin/PLLA nanofibers wrapped around PGA microfiber core with diameters that ranged from 200-600 μ m. Scaffolds were successfully mineralized utilizing incubation in 10X SBF solution for two hours. Scaffolds supported cellular attachment and proliferation of MC3T3 cells and also provided an environment that allowed cells to produce calcium phosphate, increasing scaffold mineralization. However, the PGA core fibers did not degrade during the 4 week degradation study, so an alternative material needed to be used as the core for the osteon-like scaffolds. We electrospun PEO mats, which were then cut and rolled into fibers that were used as core fibers for electrospinning osteon-like scaffolds. Soaking fibers in an aqueous environment resulted in dissolution of the PEO core fibers. Individual osteon-like scaffolds were heat sintered to fabricate three dimensional scaffolds which were further mineralized and characterized. Resulting scaffolds contained a system of channels running parallel to the length of the scaffolds, as found naturally in the haversian systems of bone tissue. Cross-linking of the gelatin prior to the mineralization of the scaffolds kept the channels of the osteons from collapsing during dissolution of PEO fibers. The combination of cross-linking and premineralization significantly increased the amount of mineral, mineral distribution, and compressive moduli of the scaffolds.

In final study of the project we combined two previously fabricated structures, sintered electrospun sheets and individual osteon-like scaffolds, to create novel scaffolds that mimic the dual structural organization of natural bone with cortical and trabecular regions. Mineralization

for 24 hr significantly increased mechanical properties of the scaffolds, both yield stress and compressive modulus under physiological conditions. Both nonmineralized and mineralized scaffolds were found to support cellular attachment and proliferation over 28 days in culture, but scaffolds mineralized for 24hr were found to better support osteoblastic differentiation and mineral deposition.

7.2. FUTURE DIRECTIONS

7.2.1. Flow Mineralization

Mineralization by incubation in simulated body fluid is considered to be a biomimetic process, as SBF has similar ion concentrations to human body plasma. By using 5X or 10X solutions, the process can be accelerated to achieve mineral precipitation on the order of hours. But one limiting factor with this mineralization method is nonuniform mineral deposition due to static conditions. Use of vacuum for mineralization two dimensions electrospun mats was successful [1] but, these 3D scaffold are too large to achieve uniform mineralization throughout using this method. Recently Teo et al. utilized a flow chamber to mineralize electrospun scaffolds by alternately immersing them in CaCl_2 and Na_2HPO_4 . This resulted in a more uniform deposition throughout the scaffold. And even though scaffolds mineralized in flow chamber had less mineral overall than scaffold mineralized in static condition, they had significantly higher mechanical properties, indicating that mineral distribution is an important factor [2].

7.2.2. Bioreactors

One of the limitations that all the 3D scaffolds for tissue engineering applications face is nutrient transfer within the scaffolds. To overcome this limitation *in vitro* bioreactor systems are used to convectively transport nutrients to the cells. Use of a bioreactor would allow us to better in vitro investigation of complete 3D electrospun scaffolds that we have fabricated. Use of bioreactors has shown to improve cell seeding efficiency, cell proliferation and osteoblastic differentiation. Three types of bioreactors are most often utilized in bone tissue engineering: spinner flasks, rotating wall, and perfusion systems [3]. Spinner flask and rotating wall bioreactor systems effectively create homogenous media solution on the exterior of the scaffolds, but offer limited perfusion of media into the scaffolds. Due to this limited media perfusion matrix production in these scaffolds is limited to the exterior [3]. Perfusion systems actively

perfuse media throughout the scaffolds and expose the cells fluid shear stress. This allows for more uniform matrix production throughout the scaffolds, and cells are exposed to fluid shear stress as in natural bone tissue. However, these systems are complex and expensive to build, and scaffolds need to be highly porous with interconnected pore networks to allow perfusion.

7.2.3. Vascularization of Scaffolds

Bone is highly vascular, metabolically active tissue that is continuously remodeled. In natural bone, vasculature is found within the Haversian channels in individual osteons, ensuring that no point is further than 100 μm from nutrient source. The inability to recreate and vascularize scaffolds *in vitro* has been major limiting factor in tissue engineered constructs. While use of bioreactors improves nutrient delivery *in vitro*, the problem still exists in *in vivo* situations. Novel design of our complete scaffolds that contains channels within the osteon-like scaffolds that run parallel to the scaffold length better mimics the native tissue. Channels within the scaffolds could be seeded with endothelial cells (ECs) to allow co-culture with osteoblastic cells. Literature shows that co-culture of the two cell types had positive effects on both cell types: ECs release higher amount of VEGF than in monoculture and osteoblasts up regulate expression of alkaline phosphatase [4].

Preliminary data, shown in Figure 7.1, was done in collaboration with Dr. Chris Rylander, where individual osteon-like channels were loaded with fluorescent microspheres using hollow microneedle for loading.

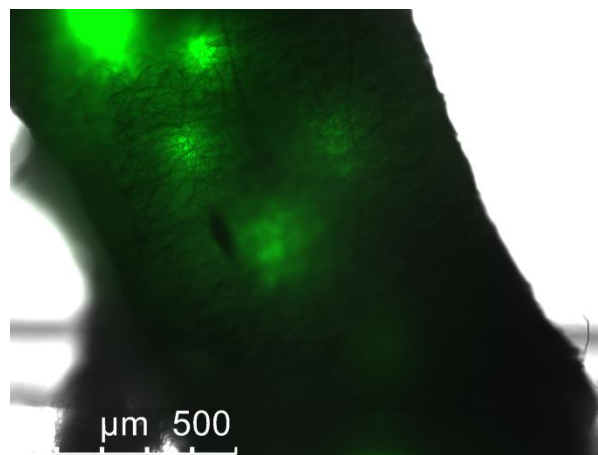


Figure 7.1. Electrospun scaffolds with channels loaded with fluorescent microbeads.

7.2.4. Improving Mechanical Properties

One of the challenges all scaffolds for bone tissue engineering face is matching bone natural mechanical properties. While polymers alone are not strong enough, pure ceramics are too brittle, and composite materials so far have failed to match bone properties. One of the approaches for increasing mechanical properties that is being investigated is use of carbon nanotubes (CNT), which have very high mechanical properties, as reinforcements. Multi-walled carbon nanotubes have been successfully dispersed and electrospun in polymer solution and have shown to increase tensile mechanical properties of scaffolds [5]. They have also shown to improve compressive mechanical properties of calcium phosphate cements. Furthermore, fictionalization of CNT with $-OH$ or $-COOH$ can induce mineral precipitation when incubated in SBF [6]. However, so far effects of addition of CNT to electrospun scaffolds in combination with SBF mineralization on compressive mechanical properties have not been investigated.

7.3. REFERENCES

1. Andric, T., L.D. Wright, and J.W. Freeman, *Rapid Mineralization of Electrospun Scaffolds for Bone Tissue Engineering*. J Biomater Sci Polym Ed.
2. Teo, W.E., et al., *Fabrication and characterization of hierarchically organized nanoparticle-reinforced nanofibrous composite scaffolds*. Acta Biomater. **7**(1): p. 193-202.
3. Yeatts, A.B. and J.P. Fisher, *Bone tissue engineering bioreactors: Dynamic culture and the influence of shear stress*. Bone, 2011. **48**(2): p. 171-181.
4. Santos, M.I. and R.L. Reis, *Vascularization in Bone Tissue Engineering: Physiology, Current Strategies, Major Hurdles and Future Challenges*. Macromolecular Bioscience, 2010. **10**(1): p. 12-27.
5. McKeon-Fischer, K.D., D.H. Flagg, and J.W. Freeman, *Coaxial electrospun poly(epsilon-caprolactone), multiwalled carbon nanotubes, and polyacrylic acid/polyvinyl alcohol scaffold for skeletal muscle tissue engineering*. Journal of Biomedical Materials Research Part A, 2011. **99A**(3): p. 493-499.
6. Low, K.L., et al., *The effect of interfacial bonding of calcium phosphate cements containing bio-mineralized multi-walled carbon nanotube and bovine serum albumin on the mechanical properties of calcium phosphate cements*. Ceramics International, 2011. **37**(7): p. 2429-2435.